Environmental assessment of agro-ecosystems. An integrated approach to manage agri-environmental risks.

Benoit Gabrielle

UNIVERSITE PIERRE ET MARIE CURIE

Paris 6

Habilitation à diriger des recherches

Dossier de candidature

présenté par

Benoît GABRIELLE

ANNEXES

[1] **B. Gabrielle**, S. Menasseri, and S. Houot. Analysis and field-evaluation of the CERES models' water balance component. *Soil Science Society of America Journal 59 :1402-1411*, 1995.

[2] **B. Gabrielle**, P. Denoroy, G. Gosse, E. Justes, and M. N. Andersen. Development and evaluation of a CERES-type model for winter oilseed rape. *Field Crops Research 57 : 95–111*, 1998.

[3] **B. Gabrielle** and S. Bories. Theoretical appraisal of field-capacity based infiltration model and their scale parameters. *Transport in Porous Media 35 : 129–147*, 1999.

[4] **B. Gabrielle**, R. Roche, *P. Angas*, C. Cantero-Martinez, L. Cosentino, *M. Mantineo*, M. Langensiepen, C. Hénault, P. Laville, B. Nicoullaud, and G. Gosse. A priori parameterisation of the CERES soil-crop models and tests against several european data sets. *Agronomie 22 : 119-132*, 2002.

[5] **B. Gabrielle**, *J. Da-Silveira*, S. Houot, and J. Michelin. Field-scale modelling of C-N dynamics in soils amended with municipal waste composts. *Agriculture Ecosysystems and Environment 110 : 289-299*, 2005.

1995

Publication 1

Reprinted from the *Soil Science Society of America Journal*
Volume 59, no. 5, September–October 1995
677 South Segoe Rd., Madison, WI 53711 USA

Analysis and Field Evaluation of the Ceres Models Water Balance Component

Benoît Gabrielle,* Safya Menasseri, and Sabine Houot

ABSTRACT

The soil water status partly determines the N losses from soil–crop systems. With the ultimate objective of estimating N losses, the capacity-based water balance module of the Ceres models was tested against field data collected from various pedoclimatic regimes in France. A process-oriented analysis of initial simulation results for a loamy soil prompted introduction of Darcy's law in the drainage and capillary rise parts of the model. As a result, a more accurate prediction of the soil water storage and surface water content was achieved. This was confirmed by comparing model output against independent data from bare or maize (*Zea mays* L.)-cropped conditions and for silt loam or sandy loam soils. For a 1-yr period, the mean square error between modeled and measured water storages was in the range 1.9 to 3 cm^2 water for the modified model, in contrast with 4 to 12 cm^2 using the original model (which performed best on well-drained soils). A unidimensional sensitivity analysis was conducted with regard to the three new parameters introduced in the revised model: the saturated hydraulic conductivity and two texture-dependent constants used in simple analytical representations of the moisture retention and hydraulic conductivity curves. The sensitivity analysis proved that this more physical approach in capacity-based models required less rigorous parameterization than mechanistic models. Moreover, the accuracy of the simulations performed with the modified model fell within the experimental error in the measurements.

RECENT CONCERN about the environmental impacts of agricultural activities has increased the importance of accurate estimates of N losses from soil–crop systems. The two major processes involved in loss of N from soils are the leaching of NO_3^- and the upward emission of gaseous compounds, which are mainly NH_3 and N_2O. The volatilization of NH_3, which is highly dependent on fertilizer type (Nelson, 1982), will not be considered further. Nitrous oxide, which is involved in the radiative forcing of the Earth's climate, is cyclically produced by nitrification and denitrification in soil (Hutchinson and Davidson, 1993). Both nitrification and denitrification are dependent on soil water status. Loss of soluble N is controlled by percolation below the root zone (van Kessel et al., 1993; Rolston et al., 1984).

The Ceres models provide a coherent framework for the modeling of the N, water, and C cycles in soil–crop systems. They simultaneously simulate (on a daily time step) crop growth, C and N turnovers in soil, and heat and mass transfer in soil. They may therefore be used to estimate N losses in a predictive way, because their operation requires only routine on-site measurements (i.e., weather records and soil pedological characterization). However, the soil water balance submodel is a simplified one, and to this purpose, it seemed prudent to compare output of the model with experimental field data from diverse soil environments. Few such evaluations have been conducted (e.g., Comerma et al., 1985), especially for European conditions. This work compares predictions from the original water transfer model and from a revised water transfer model with measured soil water content on silt loam and sandy loam soils. A sensitivity analysis of both forms of water budget is presented.

MATERIALS AND METHODS

Conceptual Background

The Ceres-Maize soil water balance model, described by Jones and Kiniry (1986), may be termed functional, following the classification proposed by Addiscott and Wagenet (1985). It is unidimensional along a vertical axis and operates on a daily time step. For each time step, surface infiltration, drainage, evapotranspiration, and redistribution fluxes are sequentially computed (Fig. 1). The soil profile is divided into a set of horizontal homogeneous layers (up to 10), each characterized by specific water retention levels: SAT, field capacity (DUL), and wilting point (LL), expressed as volumetric contents.

Surface infiltration is calculated as the difference between water coming into the system (through rain or irrigation) and runoff, which is calculated as a lateral loss term with the USDA-SCS curve number technique.

In the first layer, drainage (downward flux) then occurs if

B. Gabrielle, Institut National de la Recherche Agronomique, Unité de Bioclimatologie, 78850 Thiverval-Grignon, France; and S. Menasseri and S. Houot, Institut National de la Recherche Agronomique, Laboratoire des Sols, 78850 Thiverval-Grignon, France. Received 4 May 1994. *Corresponding author (gabriele@bcgn.inra.grignon.fr).

Published in Soil Sci. Soc. Am. J. 59:1403–1412 (1995).

Abbreviations: SAT, saturation; DUL, drained upper limit; LL, lower limit; PET, potential evapotranspiration rate; ME, mean residual error; MSE, mean squared residual error.

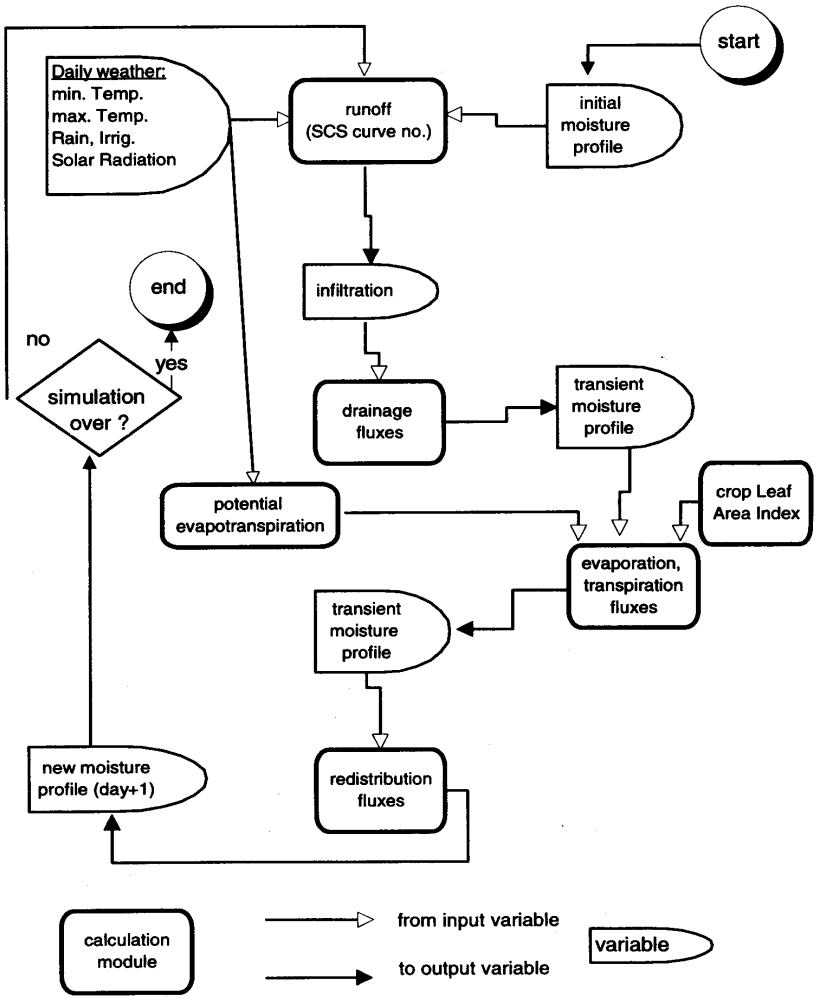

Fig. 1. Flow diagram of the Ceres water balance submodel.

the water level is above the DUL. This drainage is instantly transferred to the second layer, which in turn drains if its resulting water level exceeds the DUL. This downward flow is stopped if the DUL is not reached at some point in the profile. The daily drainage volume from a layer, which corresponds to the water in excess of the DUL, is reduced by a constant coefficient, SWCON. The coefficient SWCON (unitless, ranging from 0 to 1) represents the fraction of the drainage volume that percolates each day and is taken for the whole profile as the value corresponding to the least permeable layer. The daily percolation amount, Dr (cm), from a layer L to the next lower layer $L + 1$ is

$$Dr_{L\to L+1} = SWCON(\theta_L - DUL)z_L \quad [1]$$

where θ_L is the soil water content in layer L ($cm^3\ cm^{-3}$) and z_L the layer's thickness (cm). A PET is computed from daily solar radiation and minimum and maximum air temperatures through a simplified equation (Ritchie, 1972). A two-stage model, proposed by Ritchie (1971), yields the potential soil evaporation rate, and the potential transpiration rate is calculated from the crop leaf area index and PET (Ritchie, 1972). The actual rates are determined by soil water availability, in the top layer for the soil evaporation term and throughout the root zone for the plant transpiration term.

After evapotranspiration has depleted some layers in the profile, the resulting upward fluxes are modeled with a semiempirical equation. It relates the daily amount of capillary water C_f (cm) moving from a layer L to the next higher layer $L - 1$ to their moisture contents θ_L and θ_{L-1}, their thicknesses z_L and z_{L-1}, and the lower limits of water content, and is given by

$$C_{fL\to L-1} = \left[0.88e^{17.7(\theta - LL)_{avg}}\right] \frac{(\theta_L - \theta_{L-1}) + (LL_L - LL_{L-1})}{\Delta z} \quad [2]$$

where $(\theta - LL)_{avg}$ is an average of water content in excess

of LL ($cm^3\ cm^{-3}$), and $\Delta z = (z_L + z_{L-1})/2$. The rightmost term represents a nondifferential form of the gradient in total water in a layer. The term in the square brackets represents an empirical expression for average hydraulic conductivity of the two layers as a function of water content. Equation [2] is then derived from the generalized Darcy's law. Possible capillary rise from the water table is not considered.

A modified model (referred to as Ceres2wf, for Ceres with modified water flow), that is based on different equations for the drainage and capillary fluxes, was also used in this study. Equation [1] was replaced by the expression

$$Dr_{L\to L+1} = \begin{cases} K(\theta_L)(\Delta t = 1\ \text{day}) & \text{if } \theta_L \geq DUL_L \\ 0 & \text{if } \theta_L < DUL_L \end{cases} \quad [3]$$

with the constraints that the upper layer L not be reduced below its DUL and that the lower layer $L + 1$ remain below its SAT, i.e.:

$$\begin{cases} Dr_{L\to L+1} \leq (\theta_L - DUL)\, z_L \\ \text{and} \\ Dr_{L\to L+1} \leq (SAT - \theta_{L+1}) z_{L+1} \end{cases} \quad [4]$$

where K is the hydraulic conductivity ($cm\ d^{-1}$) and t is time. The variable K was related to the moisture content by the following expression:

$$K(\theta) = K_s e^{A(\theta - SAT)} \quad [5]$$

where K_s is the saturated hydraulic conductivity ($cm\ d^{-1}$), and A is a dimensionless parameter that depends on soil texture. Equation [3] is an expression of Darcy's law combined with the common unit gravity gradient assumption for downward water flow.

In this model, infiltration is considered to occur in one time step in the top layer, whose water content may transiently exceed SAT because of a ponding effect.

Eq. [2] was replaced by

$$C_{L\to L-1} = K\left(\frac{\theta_L + \theta_{L-1}}{2}\right) \times \frac{h(\theta_{L-1}) - h(\theta_L) - \Delta z}{\Delta z} (\Delta t = 1\ \text{d}) \quad [6]$$

where h is the matric head (cm), which was related to the soil water content by:

$$h(\theta) = e\sqrt{\frac{\ln\left(\frac{SAT}{\theta}\right)}{\gamma}} \quad [7]$$

where γ is a dimensionless parameter that depends on soil texture (Driessen, 1986). There should rigorously be an air-entry head factor in front of the exponential term in Eq. [7].

The flow diagram of this Ceres2wf model is presented in Fig. 2. The three parameters A, K_s, and γ are assumed constant throughout the soil profile and with respect to time, as their equivalents are in the original Ceres model.

Field Experiments

We used data from field experiments conducted at three locations in France: Grignon (48.9°N, 1.95°E), Laon (49.8°N, 3.6°E), and Grenoble (45.4°N, 5.26°E) with two sites T1 and T8. The texture and classification of the soils are presented in Table 1. The Grignon experiments involved, in 1989–1990, a 1-ha field cropped with maize and a bare control plot, and in 1993, a maize-cropped field. The other locations involved bare soils, in 1990–1991 and 1991–1992, respectively.

As for the physical properties of the soils, the water retention levels (LL, DUL, and SAT) were inferred from laboratory measurements of the soil water-retention curves; the DUL and LL were taken at a −0.033 and −1.6 MPa pressure, respectively, as recommended by Blaize (1988) for loam soils. In Grenoble, the soil water-retention curve was extrapolated from field data obtained through simultaneous measurements of the soil water contents and potentials with a neutron probe and tensiometers (Kengni, 1993). The values of these properties are listed in Table 2, along with bulk density profiles. The latter were measured on undisturbed soil cores in laboratory (Grenoble and Grignon) and a γ densitometer in field (Laon).

In 1989–1990 at Grignon, soil moisture profiles were measured (in layers 0–30, 30–60, 60–90, and 90–120 cm) with both neutron probe and gravimetric techniques. The crop was sown on 15 Apr. 1989, grown without irrigation, and harvested on 8 November, when the N and dry matter contents of the aerial parts were determined. The soil was then left bare and moisture profiles were further monitored until 15 Feb. 1990. A control soil, remaining bare for the entire period, was monitored as well. In summer 1993, on the same site, soil water contents were measured daily in a maize-cropped field, with time domain reflectometry probes horizontally set at 5-, 10-, 20-, and 50-cm depths. The crop leaf area index was measured weekly. At Grenoble, soil moisture contents were measured weekly in 10-cm increments with a neutron probe, from June 1991 to February 1992. At Laon, a gravimetric technique was employed to measure bimonthly moisture content in layers 0–30, 30–60, and 60–90 cm, from July 1990 to April 1991.

In each case, the daily weather data (including incoming solar radiation, minimum and maximum air temperatures, and rainfall amount), required as forcing variables by the models, were recorded on site. Irrigation occurred in Grenoble only and was included in the water input to the site. Weekly averaged PET rates, derived from the Penman formula, were used for the soil evaporation calculations at Grenoble, whereas the Ritchie (1972) formula for daily PET rates was used at Laon and Grignon.

The runoff could be considered negligible in all cases, given the hydrologic and topographic conditions of the field.

Model Evaluation

Water content estimates from the models were evaluated with two statistical properties: the ME and MSE, from Wösten et al. (1990). These expressions are defined as

$$ME = \frac{\sum_{i=1}^{n} (s_i - o_i)}{n} \quad \text{and} \quad MSE = \frac{\sum_{i=1}^{n} (s_i - o_i)^2}{n}$$

where n is the number of observations, and o_i and s_i are the observed and simulated values, respectively. The ME indicates whether there is a systematic bias in the simulation and the MSE determines the scatter around the 1:1 line in the plot of calculated vs. observed values. Such indicators cannot account for the experimental variability, which induces residual errors in the measured values themselves. These deviations were relatively low (standard errors in the range 0.5–1 cm water for soil water storage and 0.01–0.02 $cm^3\ cm^{-3}$ for surface water content) and were of little significance to comparisons between the two models.

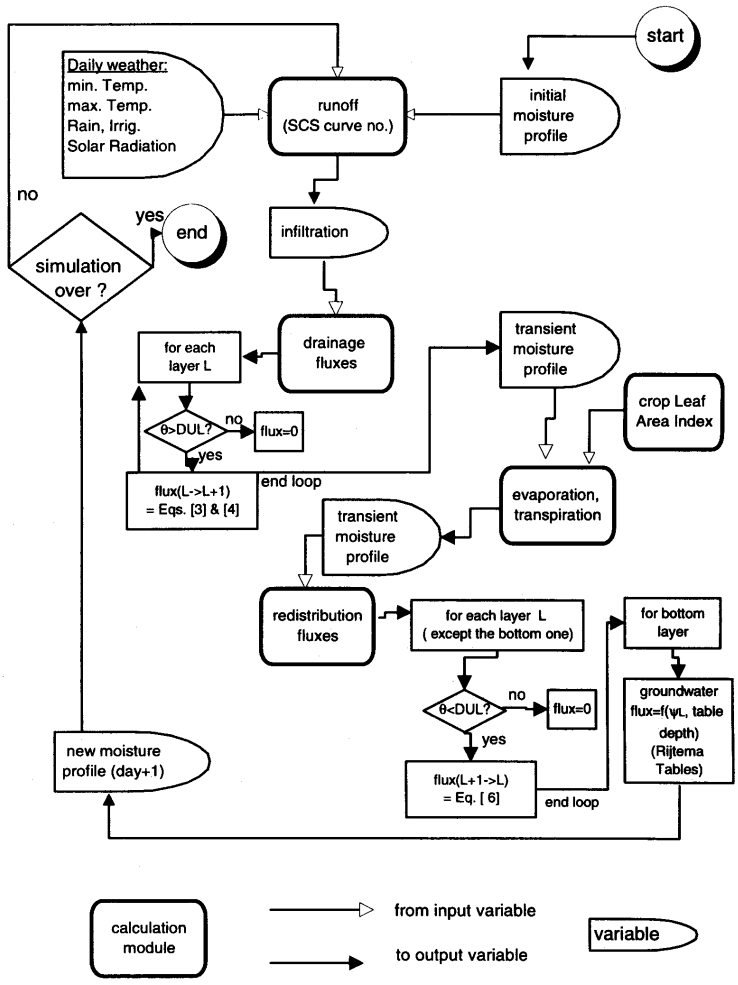

Fig. 2. Flow diagram of Ceres2wf, the modified Ceres water balance submodel.

RESULTS AND DISCUSSION

Process-Oriented Analysis of Model Accuracy

The 1989–1990 Grignon experiment was used for the first test of the simulated drainage, capillary rise, and evapotranspiration. A bare soil situation was selected to remove the uncertainties in water loss contributed by plant transpiration. The simulated evaporation term was assumed correct. In wintertime, evaporation was energy limited and occurred at its potential rate. This Stage 1 evaporation rate (see the classification scheme of Ritchie, 1972) was in good agreement with values obtained with

Table 1. Soils texture characteristics and classification at the three experimental locations.

Location	Texture	Classification (soil taxonomy)
Grignon	0–60 cm: silt loam 60–120 cm: silty clay loam	Typic Eutrochrept
Grenoble (both sites)	0–60 cm: loam 60–90 cm: sandy loam	Typic Ferrudalf with high gravel content (>40% weight)
Laon (both sites)	0–150 cm: loam (Yolo loam type)	Typic Xerorthent

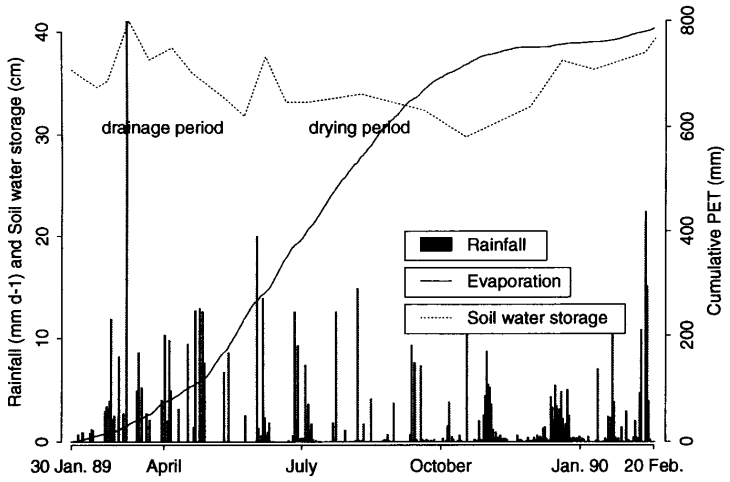

Fig. 3. Time variation of the forcing variables (rain and potential evapotranspiration [PET]) and of the measured soil water storages, in the bare soil case, for the Grignon 1989–1990 experiment.

the Penman formula. Unfortunately, during the summertime when evaporation most frequently occurred in the Stage 2 type of regime, no observations were available to determine its relative accuracy.

Time intervals during which it seemed that either drainage or capillary rise was the predominant process were identified, using the field data shown in Fig. 3. In wintertime (from February to April 1989) in all four of the monitored soil layers, the water contents were above field capacity, which resulted essentially in downward gravity flows. In summertime (June–October), the situation was reversed, which meant that water was mostly moved by capillary suction. Then significant discrepancies between observed and simulated water contents during these two intervals were attributable to the models chosen either for water percolation or capillary rise.

For drainage calculations, the rate parameter SWCON was determined with a procedure based on soil porosity (Jones and Kiniry, 1986). However, the resulting value of 0.37 had to be changed to 0.05 to remove a bias error of 11% in the estimates of total water storages during the drainage period (Fig. 4a). This parameter is a relaxation factor, which incorporates the effect of saturated hydraulic conductivity on limiting flow rate, although the two terms are not theoretically related. Because SWCON was not obtainable a priori, we chose to replace the drainage relationship with one containing hydraulic conductivity as a rate parameter, as expressed in Eq. [3], [4], and [5]. Two additional parameters replace SWCON (see Eq. [5]). The first one, K_s, is the saturated hydraulic conductivity of the soil and should be measured on site. However, it may be estimated by methods available in the literature, for instance through its relation to soil particle-size distribution (Campbell and Campbell, 1982; Driessen, 1986). The second one, A, may be related to soil texture and hydrologic classification (Davidson et al., 1969). In our case, K_s was estimated at 6.5 cm d^{-1} (Driessen, 1986) and A was set to 25 by trial and error on the time period presented in Fig. 4a.

Figure 4b illustrates the water contents predicted by the Ceres model in the drying sequence for the bare soil, using the original calibrated drainage Eq. [1] and [2]. The simulated water contents matched within 10% of observed data for the bottom layers (60–120 cm) but were underestimated by 30% for the 0- to 60-cm layer. It implies that the upward water fluxes were underpredicted in the upper layers. These were computed according to Eq. [2], which is not intended to be calibrated. Rather than trying to fit to the data by arbitrarily modifying Eq. [2], we replaced Eq. [2] with Eq. [6] and [7], which are again based on Darcy's law.

Table 2. Profile characteristics of the four soils involved in the model testing, including the three water retention levels: Saturation (SAT), field capacity (drained upper limit [DUL]), and wilting point (lower limit [LL]).

Horizons	Water retention levels			Bulk density
	LL	DUL	SAT	
cm		$cm^3\ cm^{-3}$		$g\ cm^{-3}$
		Grignon		
0–30	0.133	0.300	0.450	1.33
30–60	0.153	0.320	0.490	1.53
60–90	0.190	0.280	0.450	1.46
90–120	0.195	0.250	0.450	1.50
		Laon		
0–15	0.082	0.247	0.440	1.20
15–30	0.094	0.269	0.440	1.40
30–90	0.100	0.278	0.450	1.45
90–150	0.100	0.278	0.450	1.46
		Grenoble, Site T1		
0–30	0.194	0.254	0.330	1.41
30–60	0.206	0.236	0.320	1.34
60–80	0.100	0.278	0.320	1.27
		Grenoble, Site T8		
0–30	0.167	0.242	0.350	1.41
30–60	0.103	0.208	0.350	1.34
60–80	0.083	0.225	0.350	1.27

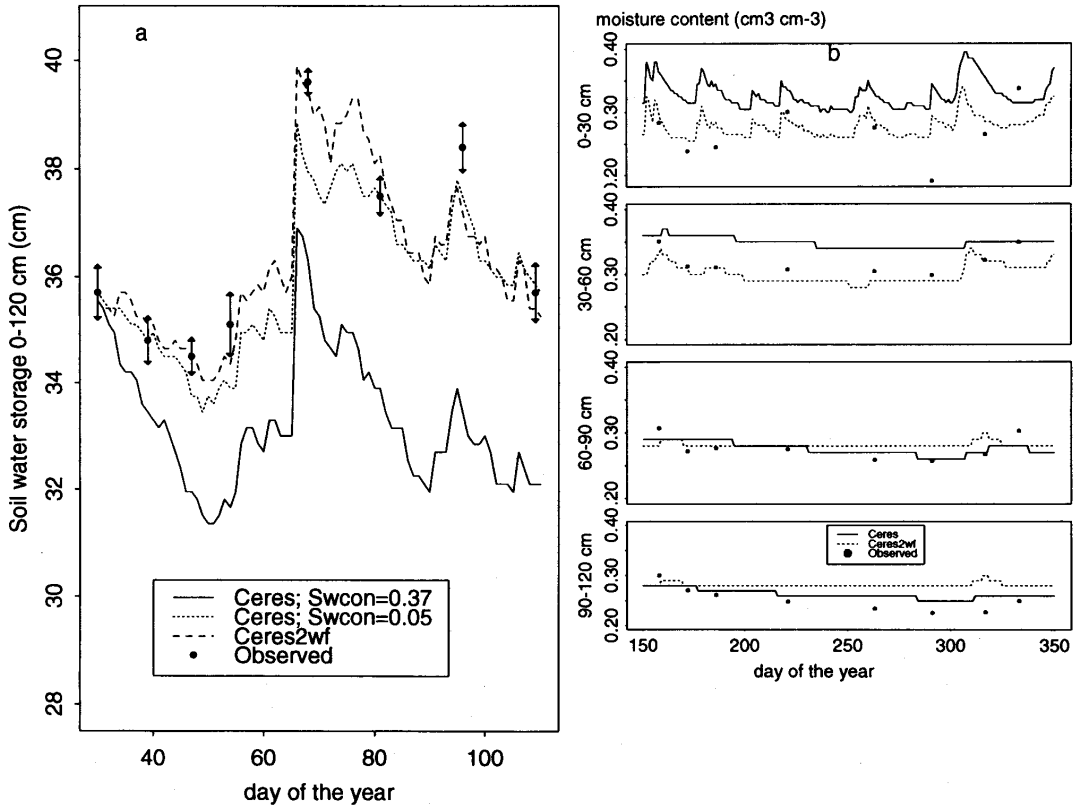

Fig. 4. Experimental and simulated soil water storage and moisture contents, for (a) drainage and (b) drying by capillary rise event, using the original (Ceres) and the modified (Ceres2wf) equations. Results for two values of the Ceres drainage coefficient SWCON (0.05 and 0.37) are shown in (a).

This allowed including water from the water table that flowed into the root zone as a specific item in the water budget. Estimates of the daily volume of water rising from the water table were taken from tables in Driessen (1986). Mean water table depth was estimated at 5 m. Figure 4b also shows the simulated water content of the Ceres2wf model, which matches within 15% of observed data for all layers.

Soil water storage, computed by both Ceres and Ceres2wf, are presented in Fig. 5 for cropped soil. Both forms of the simulation were calibrated with the bare soil observations during the same time periods, so this application constitutes the first validation test. Genetic coefficients were set to values experienced in similar conditions (Ruget, 1993). The simulated dry matter yield and plant N uptake were within 10% of the observed values. Table 3 presents the soil parameters used in the simulations and their sources. The Ceres2wf model performance is fairly good (MSE = 1.9 cm^2 for soil water storage predictions; see Table 4) compared with the Ceres model (MSE = 12.2 cm^2). The main discrepancy between the two simulations stemmed from the groundwater contribution term, but it should also be noted that the Ceres simulation resulted from an unlikely low value of SWCON.

The systematic underprediction of the soil water storage in summer (Fig. 5) by Ceres2wf may indicate that the simulated soil evaporation was overestimated. The two parameters involved (U and $\propto$, see Ritchie, 1972) were not calibrated for lack of data in the literature.

Multilocation Field Evaluation

The Ceres and Ceres2wf models were further tested against independent data from the Laon, Grenoble, and Grignon experiments. The parameters used in the simulations are listed in Table 3. To avoid biases in the Ceres simulations due to an improper choice of SWCON, this parameter was calibrated by trial and error. Two output variables were examined, since they play a critical role in the N losses: the soil surface water content (0–30 cm) and profile water storage. Results are shown in Table 4 and Fig. 6.

In every case, Ceres2wf yielded better MSE and ME than Ceres, but the improvement was less pronounced for well-drained soils. In the Grenoble soil, drainage predominated and ended 1 or 2 d after the rain or irriga-

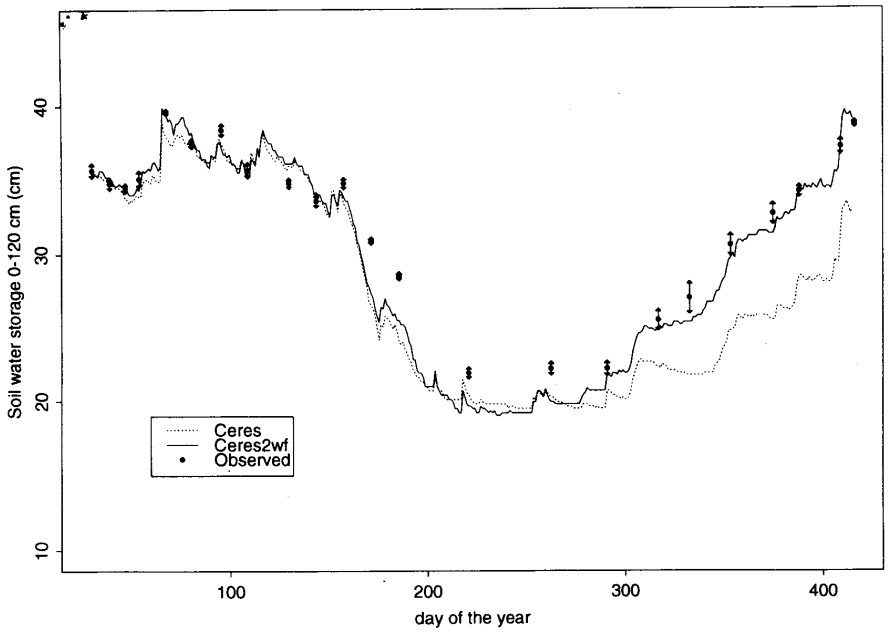

Fig. 5. Experimental and simulated results for the cropped soil in Grignon, 1989-1990, using the original (Ceres) and modified (Ceres2wf) models. The error bars represent the observed standard deviations.

tion event. Equation [1] seems to apply well in this case, because it was developed for such sandy soil regimes. For the other soils, particularly with finer texture, the simulation of drainage was improved by the Darcy's law type of description in Ceres2wf. As noted above, the soil evaporation term seemed to be overestimated, as evidenced by the systematic underestimation of the soil water storage (Fig. 6). This was consistent with comparisons between simulated and actual transpiration and drainage rates (for Grenoble in wintertime conditions) calculated by Kengni (1993) by a zero-flux plane technique. As a result, the total drainage volume was underestimated (by 12% for both models). Furthermore, even by calibrating the corresponding model parameters, the evaporation time series could not be accurately mimicked. Conversely, the 1993 Grignon experimental analysis showed that the drainage and redistribution kinetics were realistically simulated by Ceres2wf (see the low ME and MSE involved). Because of its daily time step, the Ceres2wf model should not be expected to predict average moisture contents for a vertical extent smaller than ≈ 20 cm. Moreover, numerical errors are likely to become significant when low spatial increments are used, which should be kept above 10 or 15 cm, depending on soil types.

The importance of redistribution caused by capillary rise was noted in Grignon, where Ceres2wf produced a better simulation of the surface moisture contents and of the groundwater contribution term.

Sensitivity Analysis

The precision required for the input parameters of a model is important information, particularly when the model use is predictive. We therefore investigated the sensitivity of the original and modified models to the new parameters A, K_s, and γ, as well as to the DUL (top layer) and SWCON. Two situations were considered:

Table 3. Hydrodynamic parameters used in the original Ceres model (the drainage coefficient SWCON) and in the modified Ceres2wf model (the saturated hydraulic conductivity K_s and the constants describing the soil hydraulic conductivity curve, A, and moisture retention curve, γ).

Site and parameter	Value	Obtained from	Method or reference
		silt loam soil	
Grignon			
SWCON	0.05	calibration	trial and error
A, unitless	25	calibration	trial and error
K_s, cm d^{-1}	6.5	literature	Driessen (1986)
γ, cm^{-2}	0.0185	literature	Driessen (1986)
		loam soil	
Laon			
SWCON	0.05	calibration	trial and error
A, unitless	50	literature	Davidson et al. (1969)
K_s, cm d^{-1}	60.5	field measurement	disk infiltrometry
γ, cm^{-2}	0.0185	literature	Driessen (1986)
		gravel with loam over sandy loam (layered)	
Grenoble			
A, unitless	82.5	calibration	Davidson et al. (1969)
K_s†, cm d^{-1}	4.5 (Site T1) 36.0 (Site T8)	field estimation	zero-flux plane
γ, cm^{-2}	0.019	literature	Driessen (1986)

† The value for K_s corresponds to the upper (0-30 cm) layer, which has the least gravel and is the less permeable.

Table 4. Mean residual error (ME) and mean squared residual error (MSE) for the simulations of two output variables of the original (Ceres) and modified (Ceres2wf) models.

Experiment	Number of observations	Soil water storage		Soil moisture content 0–30 cm	
		ME	MSE	ME	MSE
		cm	cm²	% vol.	% vol.²
Grignon, 1989–1990					
(maize-cropped soil)	23			0–120 cm	
Ceres		−2.27	12.2	−2.10	18.43
Ceres2wf		−0.68	1.90	−1.65	8.43
(bare soil)	21				
Ceres		2.51	11.81	5.6	53.11
Ceres2wf		−0.21	1.93	0.25	13.71
Grignon 1993†					
(maize-cropped soil)	92			0–50 cm	
Ceres		−1.87	4.51	−2.54	18.3
Ceres2wf		−0.10	1.83	0.18	12.2
Laon, 1990–1991‡					
(bare soil)	13			0–90 cm	
Ceres		−1.74	5.47	−1.36	8.56
Ceres2wf		−1.50	3.01	−0.07 (1.13)	4.80
Grenoble, 1991–1992‡					
(bare soil)	35			0–80 cm	
Ceres		−2.59	8.00	−3.34	15.15
Ceres2wf		−0.61	2.61	−1.21	18.38

† Top layer: 0–20 cm.
‡ Results are averaged across the two experimental sites.

$$ME = \frac{ME_1 + ME_2}{2},$$

where ME_1 and ME_2 are the ME for each separate site. If $ME_1 \times ME_2 < 0$,

$$|ME| = \frac{|ME_1| + |ME_2|}{2}$$

is indicated in brackets. The number n of observations is the same for both sites.

the 1989 Grignon (moderately well-drained soil) and the 1991–1992 Grenoble (Site T8, well-drained soil) experiments. The standard values chosen for the parameters were those selected in the calibration procedure (Table 3). The output variables examined were total drainage volume and MSE for the surface moisture content. The response to a change in the parameter value, x, was related to the output value change, y, with

$$x = \frac{p - p_{std}}{p_{std}} \quad \text{and} \quad y = \frac{O - O_{std}}{O_{std}}$$

where p is the parameter value, and O the corresponding output value. The std subscript denotes standard values. Parameters were varied one by one, while holding the others to their standard values (even though correlations may be expected between γ and A or γ and the DUL).

The results (Fig. 7) show that the sensitivities of Ceres and Ceres2wf to their rate parameters (SWCON or K_s) are similar, although negligible in the Grenoble case, where drainage was controlled by the DUL. The high slope of the curve of the surface moisture content MSE vs. SWCON for Ceres (100%) implies that SWCON should be determined within a ±15% precision range (which was achieved only through calibration). The same conclusion applies in the case of Ceres2wf for the parameter A, which should be estimated within a ±25% precision range, especially for low values (e.g., A = 25 at

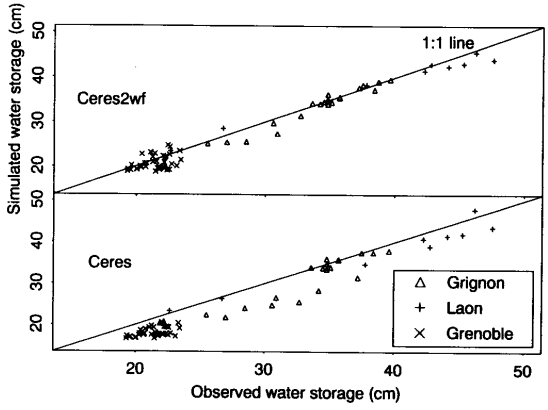

Fig. 6. Comparison between simulated and observed water storages at three sites (Grignon 1989–1990, maize-cropped soil; Laon 1990–1991 and Grenoble 1991–1992, bare soils) using the original (Ceres) and modified (Ceres2wf) models.

Grignon). However, the literature may give sufficient indications of how to accurately estimate A. The parameter γ does not vary as greatly among texture classes as the parameter A does (Driessen, 1986). It was scaled between two extreme values corresponding to the surrounding texture classes and did not have a large influence ($\Delta MSE/\Delta\gamma < 40\%$ for surface moisture content). A texture-related literature value should be satisfactory, even for a stratified soil (Grenoble), if an average value for the profile is used. The simulated surface moisture content was most sensitive to the top-layer DUL. The DUL value was varied within a ±10% range, according to standard deviations cited by Ratliff et al. (1983) for similar textured soils. The high slopes $\Delta MSE/\Delta DUL$ encountered are less pronounced for Ceres2wf, although they still imply a need for a precise determination of the DUL. The standard DUL value for Ceres2wf appeared somewhat below the optimal (see the minimum reached by the water content MSE curve) for both soils. However, the difference in MSE remained below 10%, which proved that the laboratory estimation used to determine the DUL was satisfactory. As an overall result, Ceres2wf seemed less sensitive to variations of the DUL and of the rate water flow parameters than Ceres. Furthermore, it is likely that the literature can provide sufficient data for estimating the new parameters of the revised model. This is not the case for SWCON in Ceres, which is a major problem given its critical role in determining the magnitude of several important output variables.

CONCLUSION

From a formal point of view, the Ceres2wf water balance model may be categorized between standard capacity-based models and predictive mechanistic ones based on the Richards equation. It uses the same type of physical parameters as the latter class, in addition to the water retention levels involved in the former class. Nevertheless, because of its simple, texture-derived rep-

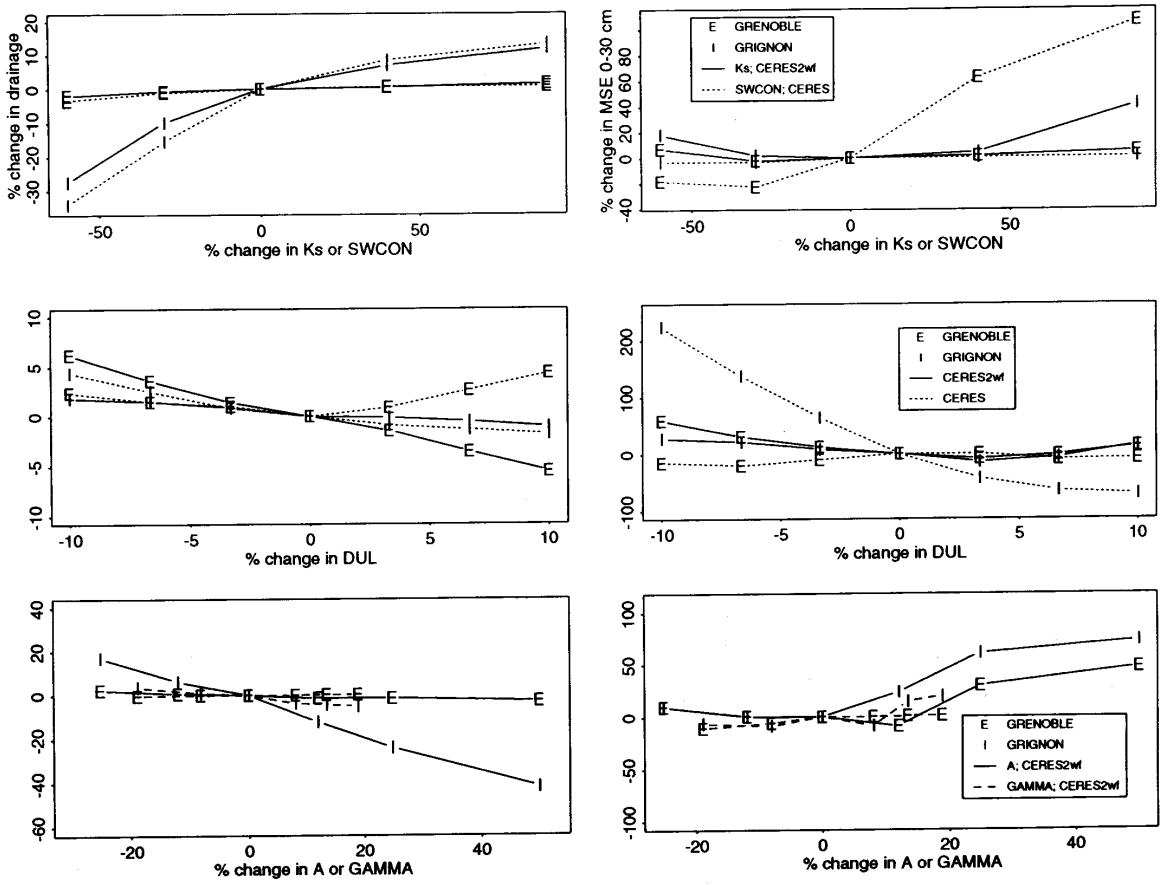

Fig. 7. Variations in the original (Ceres) and modified (Ceres2wf) model outputs (drainage and mean squared residual error [MSE] for the surface moisture content [0–30 cm]), as a function of input parameters variations (expressed as a percentage) for Grenoble (Site T8, Letter E) and Grignon (Year 1989–1990, Letter I). The parameters considered are the drainage coefficient SWCON and the top-layer drained upper limit (DUL) for Ceres and the saturated hydraulic conductivity (K_s), the top DUL, and the constants describing the soil hydraulic conductivity curve (A) and retention curve (γ in text, GAMMA on plot) for Ceres2wf.

resentations of the properties, Ceres2wf does not require on-site measurements in unsaturated conditions, as many predictive mechanistic models do. The extra soil physical properties necessary for operating Ceres2wf, compared with Ceres, are the K_s and two texture-dependent constants used in simple mathematical representations of the moisture retention and hydraulic conductivity curves. The saturated hydraulic conductivity is easier to estimate than the Ceres SWCON parameter, although it can be quite spatially variable across a field. Such spatial variability has not been dealt with in this study, for it is beyond the scope of normal Ceres applications. However, it can be formally addressed by Ceres2wf, for instance by using a scaling factor to produce distribution of the conductivity and retention curves for the field. Although Ceres2wf showed a low sensitivity to K_s, this parameter can take on a wide range of values for different natural soils, even within a textural class (Campbell, 1985).

With regard to the model's validity, Ceres2wf produced fairly accurate simulations. The accuracy was similar to that obtained by Wösten et al. (1990), who cited MSE in the range of 3 to 11 cm^2 when simulating the 0- to 50-cm water storages of sandy soils during 7 yr in the Netherlands using the mechanistic SWATRE model. However, the objectives of the applications of the two types of models are different, especially in regard to their spatial and temporal scales. Ceres yielded good results for well-drained soils (Laon and Grenoble) but only by a calibration of its drainage coefficient SWCON. Ceres performed poorly on the silt loam soil of Grignon, in which redistribution by capillary rise played a more significant role. The method for calculating evapotranspiration, which was developed in other environmental conditions, needs at least a calibration or a field analysis for conditions similar to ours. Although further testing is required (particularly in the case of soils with strong stratification or clayey or sandy texture), the Ceres2wf model developed by this study has the advantage of being based on a more mechanistic parameterization than the

original Ceres water balance submodel. The required input parameters are easily available, and the model achieves an accuracy more consistent with the ultimate objective of evaluating N losses from soil–crop systems.

ACKNOWLEDGMENTS

The authors are indebted to P. Laville (INRA Grignon), B. Mary (INRA Laon), and L. Kengni (LTHE, CNRS, Grenoble) for graciously providing the experimental data that allowed this testing work. Dr. R. Bonhomme and Dr. G. Gosse are also acknowledged for valuable comments on this article.

REFERENCES

Addiscott, T.M., and R.J. Wagenet. 1985. Concepts of solute leaching in soils: A review of modeling approaches. J. Soil Sci. 36:411–424.

Blaize, D. 1988. Guide des analyses courantes en pédologie. Editions INRA, Paris.

Campbell, G.S. 1985. Soil physics with BASIC: Transport models for soil–plant systems. Dev. Soil Sci. 14:51–59.

Campbell, G.S., and M.D. Campbell. 1982. Irrigation scheduling using soil moisture measurements: Theory and practice. Adv. Irrig. 1:25–42.

Comerma, J., L. Guenni, and G. Medina. 1985. Validacion del balance hidrico del modelo Ceres-Maiz en la zona de Maracay, estado Aragua – Venezuela. Agron. Trop. 35:115–132.

Davidson, J.M., L.R. Stone, D.R. Nielsen, and M.E. Larue. 1969. Field measurement and use of soil–water properties. Water Resour. Res. 5:1312–1321.

Driessen, P.M. 1986. The water balance of soil. p. 76–116. *In* H. van Keulen and J. Wolf (ed.) Modelling of agricultural production: Weather, soils and crops. PUDOC, Wageningen, the Netherlands.

Hutchinson, G.L., and E.A. Davidson. 1993. Processes for production and consumption of gaseous N oxides in soil. p. 79–95. *In* D.E. Rolston et al. (ed.) Agricultural ecosystem effects on trace gases and global climate change. ASA Spec. Publ. 55. ASA, CSSA, and SSSA, Madison, WI.

Jones, C.A., and J.R. Kiniry. 1986. Ceres-N Maize: A simulation model of maize growth and development. Texas A&M University Press, College Station.

Kengni, L. 1993. Mesure in-situ des pertes d'eau et d'azote sous culture de maïs irrigué. Application à la plaine de la Biévre (Isère). Ph.D. diss. Université de Grenoble, France.

Nelson, D.W. 1982. Gaseous losses of nitrogen other than through denitrification. p. 327–363. *In* F.J. Stevenson (ed.) Nitrogen in agricultural soils. Agron. Monogr. 22. ASA, CSSA, and SSSA, Madison, WI.

Ratliff, L.F., J.T. Ritchie, and D.K. Cassel. 1983. Field-measured limits of soil water availability as related to laboratory measured properties. Soil Sci. Soc. Am. J. 47:770–775.

Ritchie, J.T. 1971. Dryland evaporative flux in a subhumid climate: I. Micrometeorological influences. Agron. J. 63:51–55.

Ritchie, J.T. 1972. Model for predicting evaporation from a row crop with incomplete cover. Water Resour. Res. 8:1204–1213.

Rolston, D.E., P.S.C. Rao, J.M. Davidson, and R.E. Jessup. 1984. Simulation of denitrification losses of nitrate fertilizer applied to uncropped, cropped, and manure-amended field plots. Soil Sci. 137:270–279.

Ruget, F. 1993. Contribution of storage reserves during grain-filling of maize in Northern European conditions. Maydica 38:51–59.

van Kessel, C., D.J. Pennock, and R.E. Farrell. 1993. Seasonal variations in denitrification and nitrous oxide evolution at the landscape scale. Soil Sci. Soc. Am. J. 57:988–995.

Wösten, J.H.M., C.H.J.E. Schuren, J. Bouma, and A. Stein. 1990. Functional sensitivity analysis of four methods to generate soil hydraulic functions. Soil Sci. Soc. Am. J. 54:832–836.

ELSEVIER

Field Crops Research 57 (1998) 95–111

Field Crops Research

Development and evaluation of a CERES-type model for winter oilseed rape

B. Gabrielle [a,*], P. Denoroy [a], G. Gosse [a], E. Justes [b], M.N. Andersen [c]

[a] *Institut National de la Recherche Agronomique, Unité de Recherche en Bioclimatologie, Thiverval-Grignon, France*
[b] *Institut National de la Recherche Agronomique, Unité d'Agronomie de Châlons-Reims, Reims, France*
[c] *Danish Institute of Plant and Soil Science, Department of Soil Science, Research Centre Foulum, Denmark*

Revised 23 October 1997; accepted 25 October 1997

Abstract

Because of its large N fertiliser requirements and long growth cycle, winter oilseed rape (*Brassica napus* L.) is considered to expose its environment to substantial risks of N losses. Soil–crop models provide unique tools to analyse such impacts, with an accuracy that primarily relies on the simulation of crop C and N budgets. Here, we describe a model simulating the growth and development of oilseed rape that was adapted from CERES-N Maize and a previously existing rape model. In addition to its soil components, the model, called CERES-Rape, has modules for crop phenology, net photosynthesis, leaf area development and grain filling, as influenced by crop N status. A new feature compared to previous rape models is the ability to predict the crop's C and N budgets throughout its growth cycle, including losses from leaves by senescence. It also contains a mechanistic description of N translocation from vegetative parts to pods and grains after the onset of flowering. The model has been calibrated on a one-year experiment with three fertiliser N levels conducted in France, and subsequently tested on a similar experiment from Denmark for which no parameters were adjusted. In the vegetative phase, the time course of biomass and N accumulations in the various plant compartments was well simulated, with predicted values falling within one or two standard deviations from the mean in the measurements, except for the low-N treatments for which the high rates of leaf senescence could not be mimicked. After the onset of flowering, some bias appeared in the simulation of crop N uptake which impaired the predictions of final grain N yields. Simulated grain dry matter yields matched observations within $\pm 15\%$ for the calibration data set, but were over-estimated by a factor of 2 for the other data set. Despite the above shortcomings, the simulation of fertiliser effects on the dynamics of crop N uptake and dry matter was judged sufficiently satisfactory to allow an investigation of N losses from rapeseed–cropped soils with the CERES-Rape model. © 1998 Elsevier Science B.V.

Keywords: Oilseed rape; Soil–crop model; Dry matter; N partitioning

1. Introduction

In temperate regions where its cycle lasts nearly one year, the growth of winter oilseed rape (*Brassica napus* L.) is subjected to climatic hazards that

* Corresponding author. Department of Soil Science (B), Institute of Arable Crops Research, Rothamsted Experimental Station, Harpenden, Herts, AL5 2JQ, UK. E-mail: benoit.gabrielle@bbsrc.ac.uk.

PII S0378-4290(97)00120-2

may exert an important influence on yield, notwithstanding damage by pests. In addition, oilseed rape has high fertiliser requirements, as compared to other winter crops such as winter wheat (*Triticum aestivum* L.), which enhance the risk of N loss from the soil–crop system to the environment, whether by nitrate leaching, ammonia volatilisation or denitrification. In the context of the reformed European Common Agricultural Policy of 1992, which promoted in Europe the cultivation of rape as a bio-fuel crop, it seemed relevant to study the effects of soil and climate variability on both the final yield and the environmental impacts of this crop. As a consequence of their dynamic nature, these effects may only be studied by means of a model simulating the relevant crop processes as related to soil and weather conditions.

A few rapeseed models exist in the literature (Habekotté, 1996; Backx et al., 1984; Petersen et al., 1995), but they are incomplete as regards the above objectives. The first two models do not simulate the autumn and winter phases, whereas the third one (DAISY) accounts neither for the loss of leaves due to senescence, nor for the partitioning of dry matter between pods and vegetative parts after flowering.

On the other hand, the CERES models constitute a coherent, widely used framework for developing and testing soil–crop models embedded in a simulation software shell made available through an international network (IBSNAT, 1990). Here we adapted the CERES-N Maize model (Jones and Kiniry, 1986) to rapeseed by modifying the routines for net canopy photosynthesis, root growth and distribution within the soil profile, N uptake and partitioning of C and N assimilates between crop compartments (roots, leaves, stems, pods, and grain). The resulting model, called CERES-Rape, is described and tested against experimental data in this paper. Its submodel for leaf and pod area indices has, however, already been calibrated and tested in a companion paper (Gabrielle et al., 1998).

The modified routines are based on standard concepts underlying other CERES models (e.g., Villalobos et al., 1996), with attempt to maintain a balance between mechanistic and empirical approaches. A constant radiation-use efficiency (RUE) is used for net canopy photosynthesis in the vegetative phase (Gosse et al., 1986), and is altered in the reproductive phase when pods photosynthesize. The partitioning of dry matter (DM) between stems and leaves depends on development with thermal time, and source–sink relationships are introduced for the translocation of N from vegetative parts to the growing pods after flowering. Effects of N stresses due to low soil availability are taken into account as regards net photosynthesis and leaf or pod elongation.

All the routines mentioned have been calibrated on a data set from a one-year experiment in Northeastern France involving cv. Goéland and three fertiliser N treatments. Using the same parameter set, the model was further evaluated on a 1-yr experiment from Denmark featuring another cultivar (Ceres) and similar N treatments.

2. Materials and methods

2.1. Experimental data

The basic features of the two data sets used in the model tests are summarised in Table 1. The Châlons set was used for the calibration of the model's equations for leaf and pod area (Gabrielle et al., 1998), root growth, N uptake, and assimilate partitioning, whereas the Jyndevad data served for critically evaluating the model predictions of crop DM and N content obtained with the parameter set derived in Châlons. Experimental details are given in Leviel et al. (1998) for Châlons and in Petersen et al. (1995) and Andersen et al. (1996) for Jyndevad.

In all experiments, crops were fully irrigated and weed- and pest-protected, so that associated stresses were negligible. Daily climatic data (global radiation, minimum and maximum air temperatures, precipitation and potential evapotranspiration) were measured at a local weather station located within 1 km from the experimental fields.

In Châlons, three replicate 30 m $\times$ 30 m blocks arranged in a split-plot design with N treatment as main plot and sampling date as subplot were drilled in 0.29-m rows in late summer. At that time, soil inorganic nitrogen storage down to 120 cm was ca. 100 kg N ha^{-1}. Every two weeks (four weeks in winter), in each block, three subsamples of 0.45-m^2 were collected, yielding a surface of 1.3-m^2 per replicate. In Jyndevad, three autumn-sown (0.12-m rows) N treatments were established in 15.2-m^2 plots

Table 1
Selected characteristics of the two experiments used for the calibration and evaluation of the CERES-Rape model

Name and location	Soil	N treatments		Cultivar	Sowing and harvest dates
		Name	Fertiliser N doses (kg N ha^{-1})		
Châlons; 4.1°N, 6.7°E	Grey rendzina on chalk (Typic Udorthent; depth = 40 cm)	N0	0	Goéland	8/9/1994
		N1	135		11/7/1995
		N2	272		
Jyndevad; 54.3°N, 12.3°E	Coarse sand (Orthic Haplohumod; depth = 60 cm)	N0	48	Ceres	20/8/1991
		N1	155		15/7/1992
		N2	261		

arranged in a randomised block design, with four replicates. Every 10 days in spring, 0.5-m^2 samples were taken in each plot.

In all experiments, the collected plants were separated into leaves (with senescent and green fractions), stems, roots (although only the tap root was sampled), and pods. The subsamples were then weighed after drying for 48 h at 80°C, and analysed for carbon and nitrogen content using the Dumas method. To quantify the biomass and N losses from the crop, dead leaves were collected weekly on plastic mesh placed on the soil surface below the canopy.

For the in situ analysis of root growth, 4-m wide and 2.5-m deep trenches were dug once a month perpendicular to the rows, in which a vertical face was prepared using knives, brushes and small bellows to make the roots visible. The presence or absence of roots was then mapped through a 20-mm grid mesh fixed on the face. This yielded the crops' maximum rooting depth for each treatment, but not directly the root length density (RLD, cm roots cm^{-3} soil) which was also of interest in the N uptake part of the model. However, we assumed the distribution of this variable to parallel that of the frequency of occupation we had measured over the profile, with an occupation of 100% corresponding to a maximum RLD value of 5 cm roots cm^{-3} soil, as measured by Petersen et al. (1995) on winter rape.

2.2. Model description

From daily weather data (rain, air temperature, and solar radiation), the CERES-Rape model computes the variables related to crop growth and development and to the soil water and N balances. Its soil components have been tested and adapted for the prediction of soil water flow, nitrate leaching and N mineralisation (Gabrielle et al., 1995; Gabrielle and Kengni, 1996) from the original CERES-N Maize routines, and will not be described here.

The following paragraphs detail the CERES-Rape modules for crop phenology, photosynthesis and leaf and root development, and their interactions with N availability in soil. For these functions, a potential rate linked to air temperature and solar radiation is first calculated and then multiplied by stress factors between zero and unity accounting for possible limitations of N. Lastly, some of the equations and coefficients presented were derived from the Châlons data set.

2.2.1. Crop phenology

Crop emergence occurs after 120 growing degree-days with a base temperature of 0°C (GDD_0) from sowing, as modulated by soil moisture content (Leterme, 1988). The phenology module of CERES-Rape then considers one vegetative stage, from crop emergence to the onset of flowering, and subsequently three reproductive stages:

(i) from the onset of flowering to mid-flowering
(ii) from mid-flowering to the end of flowering
(iii) from the end of flowering to crop maturation.

The four boundary dates associated with the above stages depend on sowing date, on GDD from emergence with a base temperature of 0, and on mean day length until (i) starts. This part of CERES-Rape is

discussed in detail by Husson and Leterme (1998), who found prediction errors of 7 to 9 days for the flowering dates in a cross-validation study involving eight cultivars and over 10 locations in France. Since we focused on the analysis of crop growth processes, we did not deal with the validation of this phenology module, given in addition the limited climatic range of our experimental data. The boundary dates of the reproductive stages were then set to their observed values.

Leaf expansion stops after (ii), when pods become a sink for N and induce translocation of N from leaves and stems. This does not stop photosynthesis in the vegetative parts, but reduces its efficiency and accelerates senescence for lack of N (Sinclair and de Wit, 1975). In addition to the depressive effect of the decreasing leaf N content, the radiation available to the leaves is reduced because of shading by the overlying pods (reflection by flowers is not considered yet). After (i), the N taken up by shoots is partitioned to pods. Pods start elongating after (ii), and progressively increase photosynthesis.

2.2.2. Leaf and pod area

The modelling of the crop leaf and pod area indices (LAI and PAI, respectively) has been described and tested in a companion paper (Gabrielle et al., 1998), and will not be discussed further. In short, the daily increase in LAI or PAI is a function of degree-days with a base temperature of 4.5°C. The potential LAI growth rate is modulated by leaf N content if N is limiting for leaf expansion. Senescence from N deficiencies or mutual shading within the canopy is also included.

2.2.3. Root growth

In the Châlons experiment, the root tip extended downwards with a constant rate in thermal time (base 0°C) of approximately 0.08 cm °C^{-1}, whatever the N treatment (Fig. 1). However, this rate appeared to be reduced by about 40% below the topsoil (0–40 cm layer) in zones of compact chalk that comprised most of the subsoil. In these zones, the potential value of 0.08 cm °C^{-1} still held for the few monitored plants growing over veins where chalk provided mechanical constraint to root elongation (Fig. 1). In the model, the potential rate was diminished

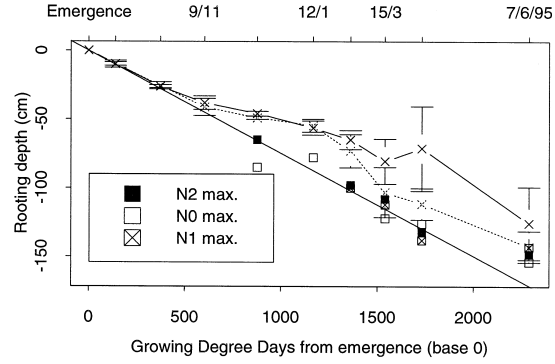

Fig. 1. Dynamics of rooting depth observed in Châlons for the three N treatments. The cross symbols associated with lines represent the average (±1 s.d.) rooting depths for N0 (· · ·) and N2 (———), whereas the square symbols represent the maximum rooting depths observed in veins of altered chalk, where mechanical stresses were negligible. The straight line illustrates the regression of those points against thermal time ($R^2 = 0.98$, $df = 15$), the slope of which is the root maximum penetration rate (see text).

by the empirical coefficient of 40% below the topsoil. The maximum rooting depth observed was 120 cm, so root penetration was not allowed to exceed that depth.

The daily increase in root length density (RLD, cm roots cm^{-3} soil) was considered proportional to the rate of root vertical elongation. In each soil layer L that had been colonised, (with L varying from 1 at the surface to N at the bottom) the variation of RLD was thus:

$$\Delta \mathrm{RLD}(L) = \mathrm{RLD}_{\max} \upsilon_{\mathrm{RLD}}(L) \Delta Z_{\mathrm{r}} \quad (1)$$

where Z_{r} is the rooting depth (cm), $\mathrm{RLD}_{\max}$ is the maximum RLD (set at 5 cm roots cm^{-3} soil, after Petersen et al. (1995)), and υ_{RLD} is the relative lateral extension rate (cm^{-1}).

Such approximation allowed us to derive values of υ_{RLD} for each soil layer, based on the Châlons data for all treatments. Due to the same mechanical stresses as for the root vertical extension, υ_{RLD} was diminished in the chalky layers (varying from 1.33 in the topsoil layer to 0.25 underneath).

2.2.4. Photosynthesis

In the vegetative phase, the daily increase in crop dry matter (ΔDM, t ha^{-1} day^{-1}) resulting from net canopy photosynthesis by the leaves is calculated

from incoming solar photosynthetically active radiation (PAR, MJ m^{-2} day^{-1}) as:

$$\Delta DM = RUE \times PAR(1-a)(1-\exp[-kLAI]) \quad (2)$$

where RUE is the efficiency of the conversion of intercepted PAR (PAR_i) into dry matter (g DM MJ^{-1} m^{-2}). The last two terms in Eq. (2) represent (i) the fraction of PAR that is not reflected by the canopy, calculated as $(1-a)$, where a is the canopy reflectivity for PAR and (ii) the fraction intercepted by the canopy, which is based on a Beer–Lambert attenuation law, with a factor proportional to the leaf area index involving an extinction coefficient k. Canopy reflectivity was taken as 0.05, while k has been shown to be in the range 0.7–1.0 for rape by Andersen et al. (1996), and was here set to 0.75 which is typical for crops with relatively flat leaves, and as derived from Gosse et al. (1983).

Eq. (2) has been successfully used for modeling the dry matter growth of a series of crops, including spring and winter rape (Gosse et al., 1986; Morrison et al., 1995; Andersen et al., 1996), from which studies a median RUE value of 2.4 g DM MJ^{-1} m^{-2} intercepted PAR was selected.

After the start of elongation, pods are said to be autotrophic for C, although translocations from leaves have been reported in their early growth (Leterme, 1985). Pod growth lasts 1000 GDD_0 (Leterme, 1988) with a constant radiation-use efficiency of 2.0 g DM MJ^{-1} PAR during the first 500 GDD_0, linearly decreasing to 0.1 g DM MJ^{-1} PAR because of oil production in grains and pod senescence (Leterme, 1985). The extinction coefficient for pods is set at 0.5 according to measurements by Andersen et al., 1996. The PAI increases from mid-flowering on, and is subject to N stress.

2.2.5. Dry matter partitioning

Throughout the growth cycle, leaf photosynthate is distributed among the root, stem, and leaf compartments. Until stem growth becomes a significant sink in late winter, leaves have priority for dry matter. After a time interval of 1000 GDD_0 from emergence, corresponding to the onset of stem elongation, stems have priority over leaves. New leaves are generated with a specific weight that depends on leaf number (Gabrielle et al., 1998). The fraction of total net photosynthesis (ΔDM, g DM m^{-2} day^{-1}) partitioned to the stems is then dependent on thermal time (base 0°C), and calculated as:

$$\frac{\Delta DM_{stems}}{\Delta DM} = \exp\left[5.85 \times 10^{-3}(GDD_0 - 1500)\right] \quad (3)$$

where ΔDM_{stems} is the dry matter partitioned to the stems. Eq. (3) was established by regression on the data corresponding to the N0 and N2 treatments in Châlons, and its coefficients did not seem to be affected by crop N status (Fig. 2). For $GDD_0 > 1500$, the right-hand side of Eq. (3) is set at 1. Throughout the growth cycle, the photosynthate remaining after partitions to leaves and stems is stored in the roots.

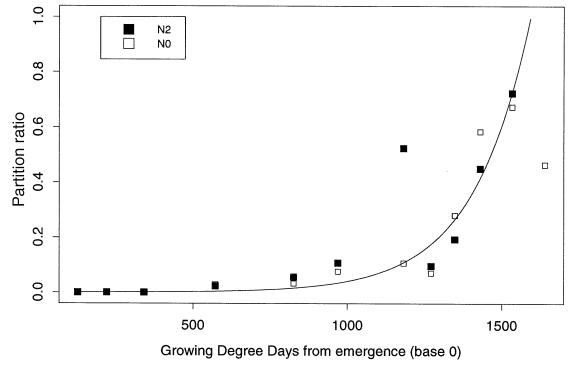

Fig. 2. Fraction of daily dry matter increase that is partitioned to the stems, for two treatments in Châlons (symbols) as a function of thermal time. The solid line is an exponential regression (see text; RMSE = 0.0188, $df = 7$).

In reproductive stage (ii), pod photosynthate is partitioned to pod walls, after which priority is given to the grain. The average size of both pods and grains, as calculated by the phenology module, may limit the intake of dry matter by these compartments on the basis of allometric relationships (Vardon, 1994).

2.2.6. N uptake

N uptake from the soil is based on a supply-and-demand scheme, with the demand being driven only by the vegetative parts (leaves, stems and roots). Crop demand is controlled by a critical N concentration in shoots that represent an optimum for crop biomass production. This concentration decreases

with increasing dry matter, following a relationship relatively similar for all C_3 crops (Greenwood et al., 1990). A particular form of this equation has recently been established for rapeseed by Colnenne et al. (1998), and validated for shoot biomass up to 650 g DM m^{-2}. This critical shoot N concentration is:

$$N_c = 4.48(\mathrm{DM}/100)^{-0.25} \text{ if DM} \geq 90,$$
$$\text{otherwise } N_c = 4.60 \quad (4)$$

where DM is the shoot dry matter (g m^{-2}), and N_c is the critical N concentration (%). Shoots tend to generate new tissue with the critical concentration N_c, and to attain it in the rest of the dry matter where the actual concentration is noted N_a. However, critical N levels may be exceeded by more than 60% for wheat (Justes et al., 1994) and 43% for rapeseed (Colnenne et al., 1998), which corresponds to the maximum shoot N concentrations obtained in field crops. We then allowed an arbitrary 40% margin above N_c for the shoots, which was restricted to the leaves because it appeared that the measured N concentrations in the stems never exceeded the critical shoot concentration. Lastly, the root N demand was taken from CERES-N Maize (Jones and Kiniry, 1986) based on the following N dilution equation:

$$N_{ro} = 4.0(\mathrm{DM}/100)^{-0.3} \text{ if DM} \geq 100,$$
$$\text{otherwise } N_{ro} = 4.00 \quad (5)$$

where DM is the root dry matter (g m^{-2}) and N_{ro} is a N concentration (%) that represents an average level of N in roots for a given level of root biomass under nonstress conditions.

The daily demand (N_{dem}) for each compartment thus reads:

$$\begin{aligned} N_{dem} &= 10^{-2}[\mathrm{DM} \times (1.4N_c - N_a) + \Delta\mathrm{DM} \times 1.4N_c] && \text{for leaves and roots} \\ N_{dem} &= 10^{-2}[\mathrm{DM} \times (N_c - N_a) + \Delta\mathrm{DM} \times N_c] && \text{for stems} \\ N_{dem} &= 10^{-2}[\mathrm{DM} \times (1.4N_{ro} - N_a) + \Delta\mathrm{DM} \times 1.4N_{ro}] && \text{for roots} \end{aligned} \quad (6)$$

with DM referring the compartment of the corresponding dry matter (g m^{-2}), and N_a to the N concentration (%). The unit of N_{dem} is then g N m^{-2}. Because of a systematic underestimation of root N concentration by the model, a 40% margin above the reference level N_{ro} was also allowed for this compartment, as for the leaves.

N supply by the soil depends on the availability of nutrients and on the absorption capacity of the roots in each soil layer. In preliminary tests, when using the original equation of CERES-N Maize for N supply from soil, it appeared that this term was never limiting. Even after calibrating this equation, the simulated dynamics of N supply seemed unlikely, because it was insensitive to low nitrate concentration. Actually, the supply equation was developed for maize undergoing severe water stress, where diffusion of nitrate was limited by dry soil conditions, contrary to our mostly nitrate-limited conditions for winter rape. We then proposed an equation based on a steady-state diffusive transport of NO_3^- to the roots, after Watts and Hanks (1978). The daily supply of N (N_{Sup}, kg N ha^{-1}) from each soil layer in the root zone reads:

$$N_{Sup} = D \times \mathrm{RLD}^{1.5} \frac{([\mathrm{NO_3}] - 0.5)Z}{\theta} \quad (7)$$

where Z is the layer thickness (cm), θ the volumetric moisture content, and $[NO_3]$ is the nitrate concentration in mg N kg^{-1} soil. If $[NO_3] \leq 0.5$ mg N kg^{-1}, there is no absorption, because this residual nitrate is assumed unavailable to the roots. D is analogous to a diffusion coefficient per unit area of root (cm day^{-1}), and was calibrated at 2×10^{-3} cm day^{-1} against absorption data for the N2 treatment. Eq. (7) implies roots are zero-sinks (i.e., the NO_3^- concentration is nil at the root surface), although plants can regulate it by adjusting NO_3^- concentration in xylem (de Willigen and van Nordwijk, 1987). For lack of definite evidence, Eq. (7) does not include the possible effect of the low temperature experienced by the shoots and roots in winter on the absorption of N. Although a temporary depressing effect was exhibited on potted rapeseed plants abruptly subjected to a temperature of 7°C (Laine et al., 1996), this temperature stress was alleviated within a few days as the uptake tended to respond essentially to the crop demand, which had accordingly diminished due to the low temperature (Bigot and Boucaud, 1996). In our model, the indirect effect of low temperatures on crop absorption of N is thus found in the decrease of net photosynthesis; hence, N demand.

2.2.7. N partitioning

In the vegetative parts, the partitioning of N between shoots and roots is in proportion to their respective demands for N. For shoots, N concentration is not identical in leaves and stems, because N demand obeys different equations for either organ.

In the reproductive phase, we modelled the N translocations from roots, stems and leaves to pods after the scheme of Sinclair and Muchow (1995) for maize. Two pools of N available from these organs are calculated at mid-flowering by assuming residual N contents of 0.8 g N m^{-2} for leaves, 0.8 g N g^{-1} DM for stems, and 0.6 g N g^{-1} DM for roots, according to the mean values measured at harvest in Châlons. The N translocation pools are noted TRNLF, TRNST and TRNRO for leaves stems and roots, respectively, and computed (in g N m^{-2}) as:

$$\begin{aligned} \mathrm{TRNLF} &= \mathrm{LAI}(N_a - N_r) && \text{for the leaves} \\ \mathrm{TRNST} &= \mathrm{DM}_{stem}(N_a - N_r) && \text{for the stems} \\ \mathrm{TRNRO} &= \mathrm{DM}_{root}(N_a - N_r) && \text{for the roots} \end{aligned} \quad (8)$$

where a and r denote the actual and residual contents, respectively.

Afterwards, in stages (ii) and (iii), the daily flow of N to the pods from the leaves (or stems) corresponds to the daily GDD (base 0°C) divided by the total duration of pod growth, set at 600 GDD_0, times the pool size. In stage (iii), the N uptake by vegetative components stops. In stage (ii), the translocated N is stored in the pod walls, after which it is partitioned to the growing seeds. In grains and pods, a maximum N concentration of 5% (w/w) is imposed, resulting in either a lower N intake by the pods or a temporary storage in the pod walls if seed demand is limiting.

As a result of translocation, a fraction of leaf area becomes senescent (Gabrielle et al., 1998). Stem biomass is also reduced by assuming that 1 g of translocated N corresponds to 6.25 g of DM.

2.2.8. Water and N stresses

As in CERES-N Maize, environmental stresses are summarised as multiplicative 0–1 factors appearing in the equations for net photosynthesis and leaf and pod elongation.

The water factor is taken here as unity throughout the growing season, since crops were irrigated to prevent water stress. The N stress factors for organ elongation are based on the Nitrogen Nutrition Index (NNI; see e.g., Lemaire et al., 1989), expressed as the ratio of actual to critical N content in a given compartment (leaves or pod walls). NNI is moreover bounded between zero and unity. Eq. (4) was used for calculating critical levels in leaves, whereas a specific curve for N dilution in the pod walls had to be introduced (Gabrielle, 1996).

In CERES-N Maize, a factor similar to the NNI is used to account for N stress on leaf photosynthesis. Here, however, we based this response function on data by Gammelvind et al. (1996), who measured the net CO_2 assimilation rates of winter rape leaves and pods in relation to their specific N content (SLN, g N m^{-2}). A similar relationship was also derived by Sinclair and Amir (1992), both at the leaf and at the canopy level. The 0–1 factor for leaf photosynthesis thus reads:

$$N_{leaf} = (-4.7\mathrm{SLN}^2 + 28.2\mathrm{SLN} - 8.5)/33.8 \quad (9)$$

In addition, N_{leaf} was maintained above 0.2, corresponding to the range of response investigated by Gammelvind et al. (1996). In a similar manner, the N factor for pod photosynthesis reads:

$$N_{pods} = (-1.3\mathrm{SPN}^2 + 8.6\mathrm{SPN} - 2.3)/10.63 \quad (10)$$

where SPN is the specific nitrogen content of pod walls (g N m^{-2}).

2.2.9. Yield components

The yield components (mean number of pods per plant, and of seeds per pod) are calculated at the end of flowering as a function of the amount of radiation intercepted and of the extent of predicted water stress during stage (iii) (Vardon, 1994). From that day onwards, grains start to develop and accumulate C from pod photosynthesis and N from translocation. Oil concentration (O_c, % w/w) in seeds at harvest is calculated from N concentration (N_g, % w/w), and seed weight (SW, g DM $seed^{-1}$) after Andersen et al. (1996):

$$O_c = 63.3 - 7.37N_g + 1.31\mathrm{SW} \quad (11)$$

2.3. Model calibration

In Section 2.2, the equations described were parametrised from the literature or from regressions

on the Châlons data. Thus, as a general rule, these parameter values were not obtained from an adjustment of the CERES-Rape model to observed data. However, systematic discrepancies had to be addressed by such direct curve-fitting in the phenology and N uptake modules. For the former, an underestimate of the grain to pod dry matter ratio led us to increase the potential for DM intake by the grains, as compared to that originally obtained by Leterme (1985) on cv. Jet Neuf.

In Jyndevad, none of the crop parameters obtained in Châlons were calibrated, although the cultivar employed (Ceres) was different. We hypothesized that genotype parameters had little influence, except for the phenological development that was not fully simulated since the actual flowering date was input to the model.

In both sites, the simulated soil water and N dynamics were checked against measurements of soil moisture and N content, and the corresponding parameters were adjusted to provide realistic predictions (Gabrielle, 1996). However, the model was not forced with the observed data of soil water and inorganic N content. Lastly, a freezing event in early January 1995 in Châlons induced losses of green leaf area that were not taken into account by the model; therefore, the simulated values of green LAI, leaf DM and N contents were re-initialised after the freeze.

3. Results and discussion

The major variables relevant to crop growth, as output by CERES-Rape, are compared to field obser-

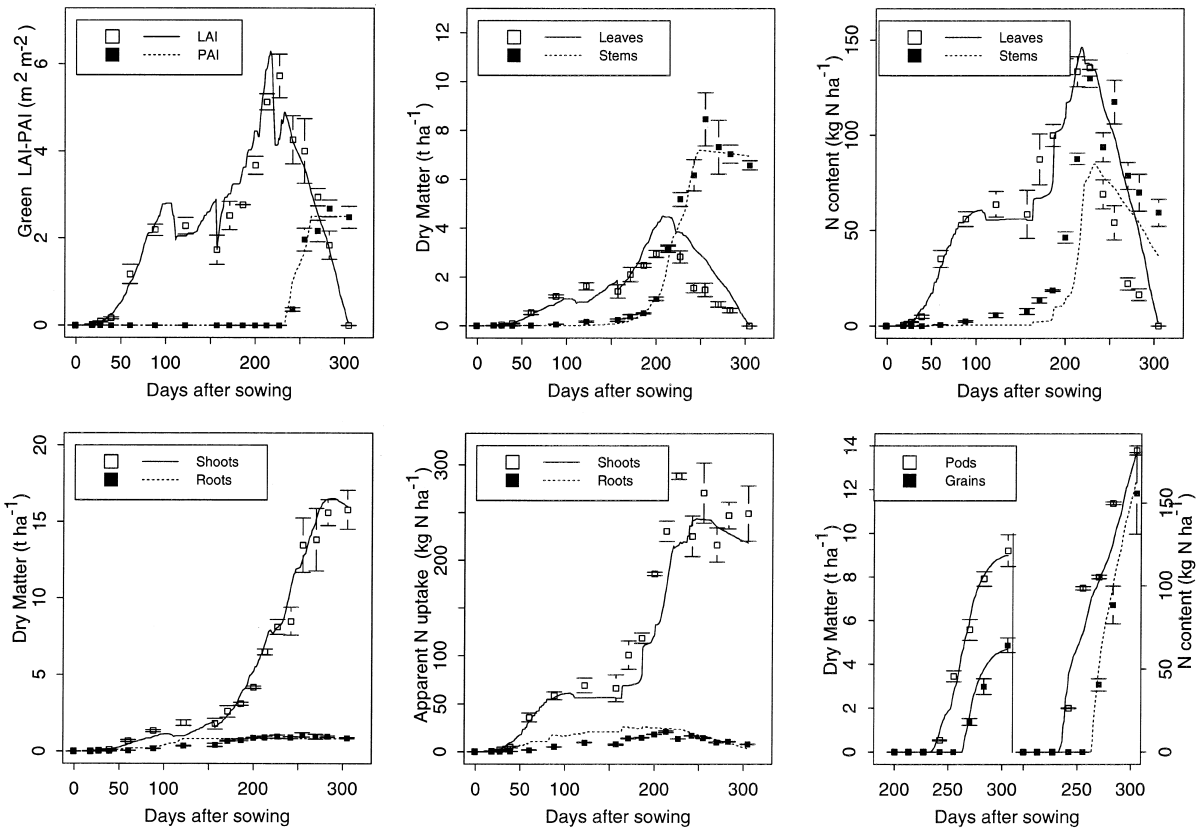

Fig. 3. Selected simulated (lines) and observed (symbols, ±s.d.) variables related to the growth of rapeseed in Châlons, with the CERES-Rape model for the N2 treatment.

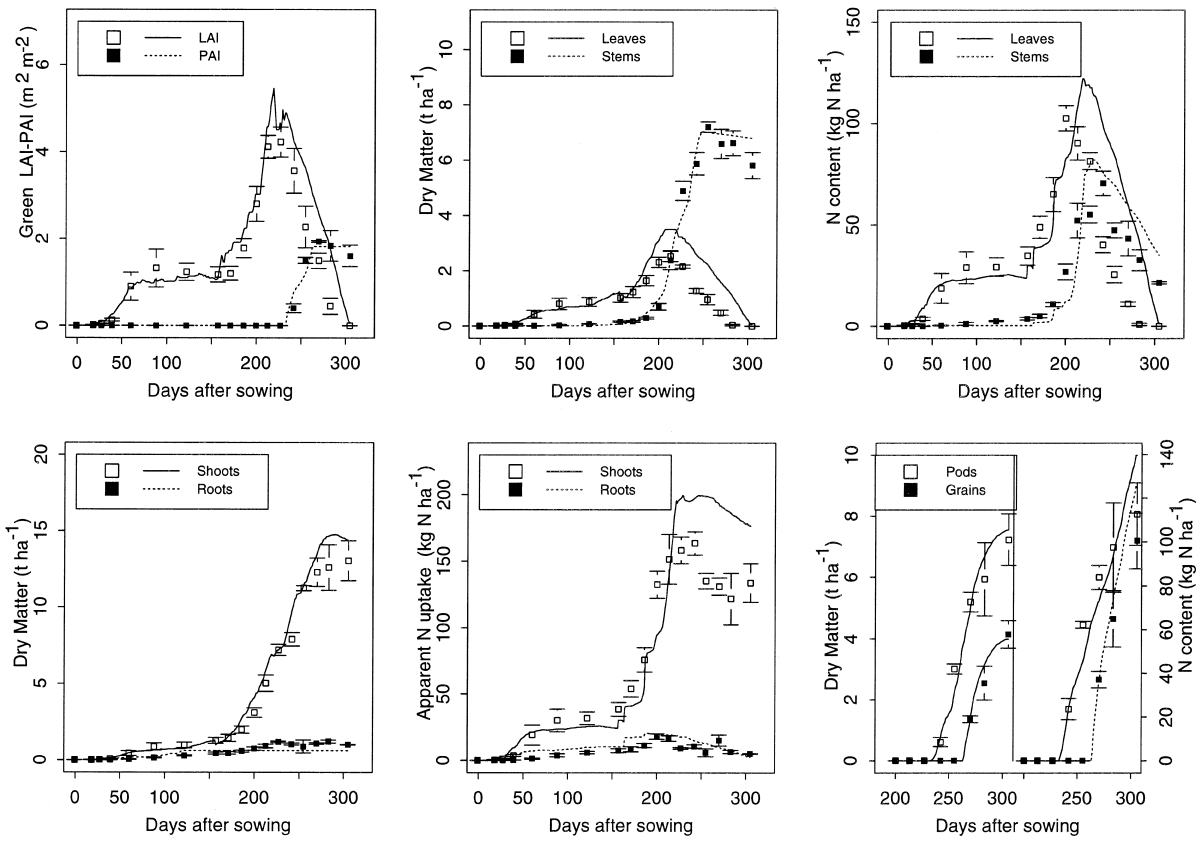

Fig. 4. Selected simulated (lines) and observed (symbols, ±s.d.) variables related to the growth of rapeseed in Châlons, with the CERES-Rape model for the N1 treatment.

vations on Figs. 3–5 for Châlons and on Figs. 6–8 for Jyndevad, for treatments N2, N1 and N0, respectively.

3.1. Vegetative growth

In both locations, the time course of plant total dry matter was well simulated for the high-N treatments (N2 and N1), but tended to be overestimated for the other treatment (N0) from spring onwards. The prediction of potential net photosynthesis was then correct, with the N stress factor being possibly biased. Actually, DM overestimation seemed correlated with an overprediction of green LAI, as was notably the case for the N0 crop in Jyndevad. This emphasizes the sensitivity of DM production to LAI, especially in the low range, as encountered in the N0 treatments. However, since in those cases LAI is limited mostly because of a high turnover of leaves, senescence and green LAI are difficult to predict accurately. As expressed in the model, leaf senescence is driven by threshold parameters, which are relatively sensitive, making it difficult to find the right balance between leaf C–N contents and area at the canopy level.

This difficulty explains why the observed plateau of LAI for the N0 crop in Châlons could not be reproduced by the model from the end of winter onwards, which resulted in an overestimation of crop total DM. In Jyndevad, the model simulated a LAI plateau until spring that must have been too high when compared to actual LAI at its end, and this induced a constant overestimation of crop DM.

Simulation of plant apparent N absorption proved more problematic than dry matter, especially in the spring–summer phases during which different pat-

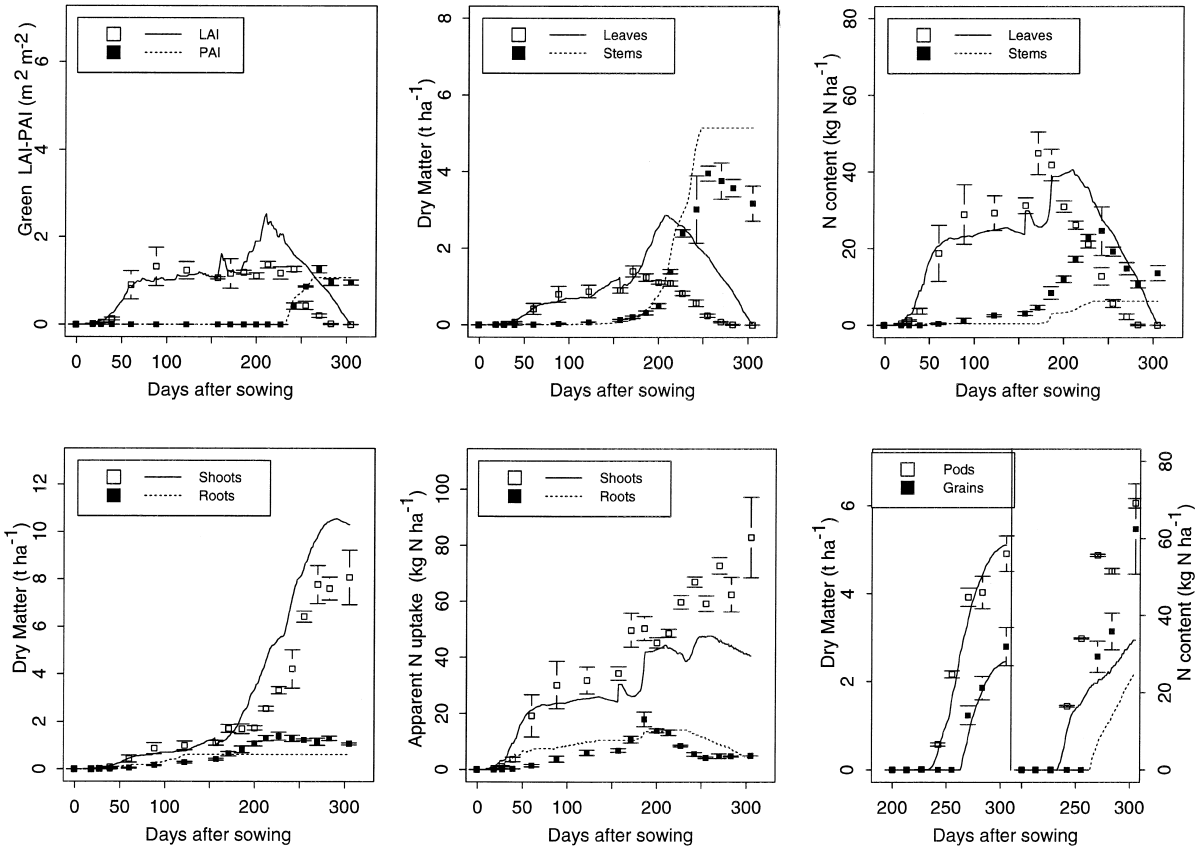

Fig. 5. Selected simulated (lines) and observed (symbols, ±s.d.) variables related to the growth of rapeseed in Châlons, with the CERES-Rape model for the N0 treatment.

terns were observed. Until early spring, crop N was reasonably well simulated, sometimes reflecting small errors in crop DM, with the exception of the N0 treatment in Jyndevad, for which N was markedly underpredicted despite overpredicted DM. This indicates that the N limitation on photosynthesis was not strong enough in the low range of specific leaf N, and also that soil supply may have been underestimated. This is not apparent in the Châlons N0 simulation, but the comparison cannot be made because it involved twofold higher levels of DM.

After flowering, the accumulation of total crop N was strikingly different between the N1–N2 and N0 treatments: crop N stabilised, or even decreased (N1, Châlons) in the former case, whereas it increased by 15–20% in the latter. Such a pattern has also been reported by Schjoerring et al. (1995), but could not be fully explained by CERES-Rape. For the N0 treatments, the model simulated a slight decrease in crop N after flowering because N uptake stopped, and structural N was lost in falling leaves, instead of the observed increase in crop N. This resulted in a marked underestimation of pod N in Châlons. Enabling uptake of N by stems and further translocation to grains after flowering removed this bias (data not shown), but appears to be in disagreement with the hypothesis that stems senesce during that period, as evidenced by their decreasing DM. In addition, this uptake scheme induced an overestimation of crop N for the N1–N2 treatments.

Another factor accounting for bias in Châlons is the strong increase in leaf N concentration observed for all treatments upon regrowth in spring. It corresponded to a storage by the crops of soil N made

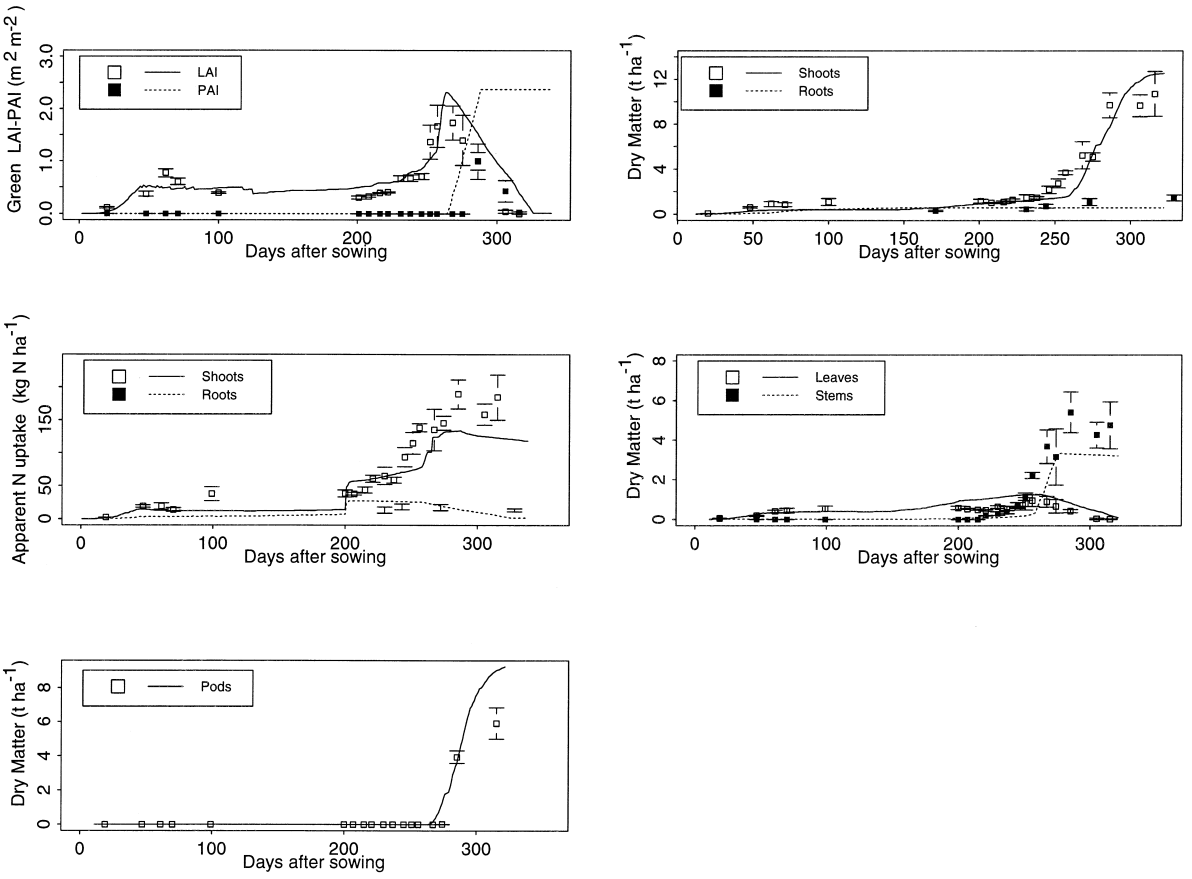

Fig. 6. Selected simulated (lines) and observed (symbols, ±s.d.) variables related to the growth of rapeseed in Jyndevad, with the CERES-Rape model for the N2 treatment.

available through mineralisation and fertiliser application, but could not be explained by the concept of critical N content, since it was also associated with an increasing biomass. This discrepancy underlines a structural weakness of the supply and demand scheme for computing N uptake, relying on the assumption that it is essentially regulated by crop biomass. In cases of high soil N availability, this assumption is indeed likely to be violated, and alternative concepts for N uptake should be worth considering, such as the use of a Michaelis–Menten absorption model with respect to soil NO_3^- concentration that circumvents the use of a plant demand term.

The partitioning of DM between stems and leaves seemed correct for all treatments in Châlons, which would be expected because the regression of Eq. (3) was obtained at the same location. In Jyndevad, except for the N0 treatment for which total DM was biased, the DM of leaves and stems were also correct, which supports the use of a leaf DM demand term to regulate DM allocation in the model. Leaf demand is calculated from the increase in LAI by use of a specific leaf weight (SLW, g DM m^{-2}). SLW was parametrised from measurements on individual leaves in Châlons according to leaf number, and although this parameterisation may vary according to the rape cultivar, it seemed to apply in Jyndevad to some extent. To assume a fixed time course for SLW, regardless of crop N status or cultivar, could be regarded as a weak point in the model. However, this method of driving leaf biomass demand is probably as successful as the common alter-

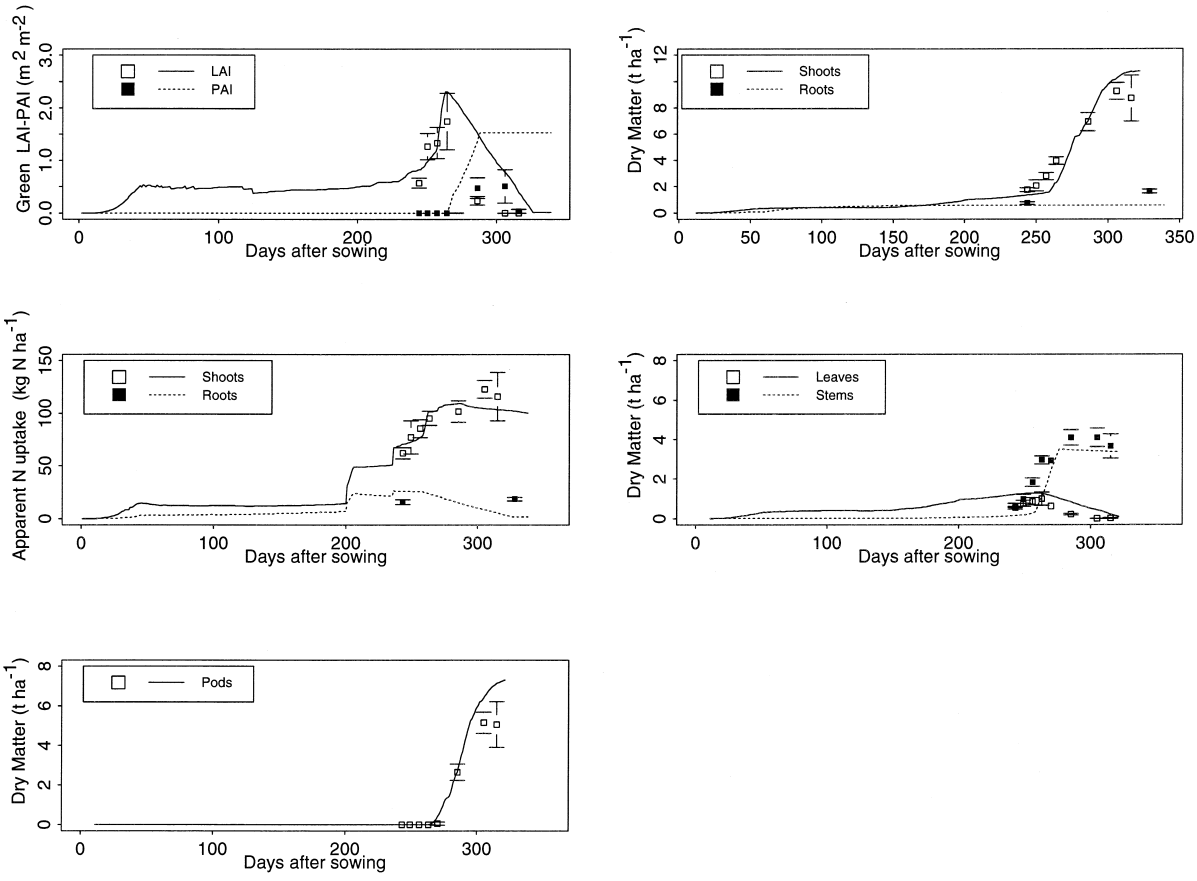

Fig. 7. Selected simulated (lines) and observed (symbols, ±s.d.) variables related to the growth of rapeseed in Jyndevad, with the CERES-Rape model for the N1 treatment.

native consisting in deriving fixed dry matter partitioning factors, as exemplified here for the stem compartment.

Lastly, in the model, DM partition to roots stopped in late winter when stems were becoming a significant sink for photosynthate, whereas in reality the roots accumulated DM for all treatments until late spring. This spring growth is surprising, since at that time rapeseed roots have been found to support the regrowth of shoots rather than to be storing additional reserves (Mendham and Salisbury, 1995). Whatever the particular physiological cause for this, stem DM was overestimated by the model as a result, implying that the partitioning factor for the stems should be reduced to allow more DM into the roots during stem elongation. To maintain agreement with the regression in Fig. 2, this factor could for instance be bounded by 0.9, limiting the strength of stems as a sink for photosynthate.

The results regarding the partitioning of N among the crop compartments are generally similar to those pertaining to DM, except for the previously mentioned underestimation of leaf N in spring in Châlons. Unfortunately, no data were available for Jyndevad.

3.2. Reproductive growth

The timing of the green LAI peak before the decline associated with the onset of pod growth was well simulated, due to the use of the measured date of flowering in the model. However, contrary to the model's hypotheses, the rate of the LAI decline did

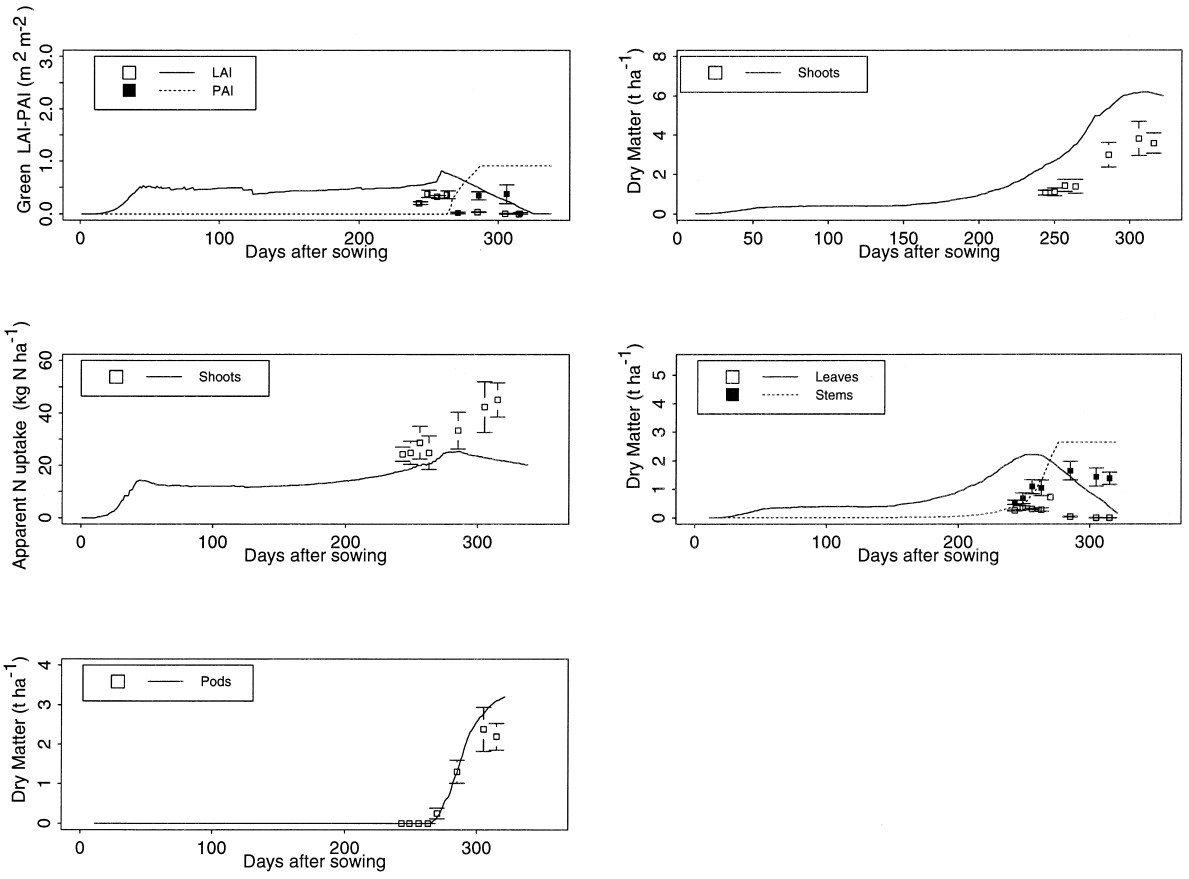

Fig. 8. Selected simulated (lines) and observed (symbols, ±s.d.) variables related to the growth of rapeseed in Jyndevad, with the CERES-Rape model for the N0 treatment.

not appear constant with respect to thermal time, and the simulation was less realistic. The base temperature of 0°C employed here may then be incorrect, although it worked fairly well for the N translocation rate itself in Châlons. The size of the pool of N mobilisable by the pods from the vegetative parts was well predicted only for the N2 crop, but for the other treatments it was strongly affected by the previously mentioned bias in total crop N. The fact that measured N concentration in stems at harvest was also variable caused additional errors in the translocation pools, since the residual contents were fixed in the model.

This resulted in significant discrepancies in the prediction of pod N content at harvest, and to a lesser extent in that of pod DM and pod area index. It appears indeed that the biases in pod N essentially affected the N content of grain, so that pod wall N was realistic enough to reflect the actual N stresses.

In Jyndevad, there were no experimental data available on pod N or grain DM, and the PAI data could not be directly compared to the simulations because these concerned total pod area, whereas the observations pertained to green PAI only. However, it seems that from the beginning of its growth, the PAI tended to be overestimated, which resulted in pod DM being also overestimated. Measured PAI was systematically lower in Jyndevad than in Châlons, implying that the maximum final PAI value, set at 2.5 in Châlons, should be reduced for cv. Ceres used in Jyndevad. Despite the closely controlled irrigation, temporary water stresses cannot also be ruled out on the well-drained sandy soil under the high evaporative demands encountered

Table 2
Measured (± s.d. in brackets) and simulated yield components for the rapeseed crops in Châlons a

Location and treatment	Grain DM yield (t DM ha^{-1})	Grain N yield (kg N ha^{-1})	Oil cont (t oil ha
Châlons N2			
Measured	4.87 (0.33)	155.8 (24.6)	2.43
Simulated	4.69	162.1	1.78
Châlons N1			
Measured	4.13 (0.45)	100.6 (12.7)	2.16
Simulated	3.99	125.9	1.60
Châlons N0			
Measured	2.80 (0.43)	62.5 (11.7)	1.49
Simulated	2.46	25.0	1.37
Jyndevad N2			
Measured	2.40 (0.34)	80.6 (10.8)	1.06 (0.
Simulated	5.06	97.4	2.49
Jyndevad N1			
Measured	2.34 (0.17)	65.2 (4.7)	1.09 (0.
Simulated	4.24	83.4	2.07
Jyndevad N0			
Measured	1.25 (0.16)	33.3 (4.4)	0.60 (0.
Simulated	1.73	14.7	0.99

The straw refers to unharvested parts as a whole (including chaff, roots and pod walls).

during pod growth. Nevertheless, assuming a fixed maximum PAI for an indeterminate plant such as rapeseed remains a crude simplification, because, for instance, the number of pods generated is regulated by the availability of photosynthate from the rest of the plant. A more biological approach to determine the maximum PAI should be considered.

Lastly, for the Châlons data, it is difficult to judge the partitioning of N and DM between pod walls and grains because of the bias in pod N. The relative proportions of N and DM partitioned to grains and pod walls seemed to be reasonably well simulated by the model, despite variations in the observed grain to total pod DM and N ratios.

3.2.1. Yield components

Measured and simulated yield components are presented in Table 2. In Châlons, simulated grain DM yield matched observations within 15%, but grain N content was markedly too low or too high for the N0 or N1 and N2 treatments, respectively. This could be expected from the previously mentioned bias in pod N for N0 and N1, but for N2 it should be ascribed to an incorrect partitioning of N between grain and pod walls at harvest. The model also predicted too much DM in straw, and more specifically in stems, for which the simulated final decrease in biomass was too small. The latter may be ascribed to a mobilisation of photosynthate from stems, along with some respiration in the structural tissues that was not accounted for by the model.

At Jyndevad, DM yield was nearly two-fold overpredicted, whereas N yields were within 30% of observations with a positive bias. These errors are much larger than those pertaining to pods DM and crop total N content, visible as displayed in Figs. 6–8, underlining the model's shortcomings in partitioning pod assimilates between pod walls and grains. The yield discrepancies should however be smaller because (i) an estimated 20% of pods and seeds was lost at harvest and (ii) a short drought period at the beginning of the pod filling phase may have impaired grain yield (Andersen et al., 1996).

As a consequence of the errors on yields, oil contents were overestimated in Jyndevad, although Eq. (11) was partly derived from the Jyndevad data. This relationship was also barely successful in Châlons, where the simulated yields were closer to the observed ones, except for the N0 treatment. The chemical composition of grains strongly depends on their growing and nutrition conditions, thus Eq. (11) applied best to the Châlons N0 treatment because its yields were in the range of those on which the equation was calibrated.

4. Conclusion

This paper presents an attempt at simulating the major processes determining the C and N assimilation of a winter oilseed rape crop throughout its growing season, based on commonly-used principles regarding leaf area development and senescence, net photosynthesis at the canopy level, and translocation of N to reproductive organs, together with the effects of limited soil N availability. Although the equations employed have allowed successful predictions of canopy status for a number of crops (Jones and Kiniry, 1986; Sinclair and Amir, 1992), their application to rape presented additional challenges such as the simulation of a high turnover of leaves or of the mechanisms of pod and grain growth as triggered by an indeterminate flowering. Although few previous modelling exercises have covered the whole growing season or taken N nutrition effects into account, values for most parameters could be assessed from literature or additional data.

In the vegetative phase, the time courses of most of the variables of interest (LAI, dry matter and N contents within the various plant compartments) were well simulated, with the restriction that the model tended to underestimate crop N content, especially for the low N treatments. For the latter, LAI was conversely overestimated, pointing at a tendency to overpredict leaf elongation under N stress, thus overestimating net photosynthesis and ultimately the DM and N loss due to leaf senescence. However, this bias could not be dealt with in the calibration phase, implying that new equations for N stress should be derived from data covering a wider range of conditions than the present set.

In the reproductive phase, despite the use of the observed dates for the onset of flowering, the dynamics of pod and grain growth revealed some shortcom-

ings of the current model. Notable errors occurred in the simulation of pod growth, essentially deriving from previous errors in crop N content, which made it difficult to test the module that partitions pod assimilate to grain. However, the fact that the fluxes of N between vegetative parts and pods and between pod walls and grains were driven by tissue N concentrations interfered with the N stress factors that affect photosynthesis, also determined by N concentrations, making the corresponding parameters very sensitive. An alternative approach, employed for maize and sunflower (Jones and Kiniry, 1986; Villalobos et al., 1996) would consist in calculating a N demand for grains as a driving variable. However, while this scheme is more stable, it cannot account for the variability in grain N content when N is highly available.

While some of its modules, particularly in the reproductive phase, deserve further testing, CERES-Rape provided a sound basis for the modelling of the growth of winter rape, as related to soil N status. Although it might well be outranked by a simple statistical predictor as regards grain yields, it should prove a relevant tool for analysing the time course of C–N balances within the soil–crop system, as already used by Gabrielle (1996) in a study of N losses to the atmosphere and to groundwater under rape.

Along with the identification of varietal parameters, the effects of drought could be included in a later version, as is the case with other models from the CERES family. Further work on the model would be facilitated by its scheduled integration into the DSSAT framework (IBSNAT, 1990).

Acknowledgements

The technical assistance of M. Lauransot and P. Thiébeau in the collection of field data and the contribution of F. Vardon in model programming are acknowledged. The authors are grateful to A.G. Dailey (IACR-Rothamsted) for kindly proofreading the final draft of the manuscript. This work was supported by the French Agency for the Protection of the Environment (ADEME), the Centre Technique Interprofessionnel des Oléagineux Métropolitains (CETIOM), and the AIP Ecofon (INRA). Source code for CERES-Rape is available from the corresponding author.

References

Andersen, M.N., Heidman, T., Plauborg, F., 1996. The effects of drought and N on light interception, growth and yield of winter oilseed rape. Acta Agric. Scand., Sect. B Soil Plant Sci. 46, 55–67.

Backx, M., van Duivenvoorden, J., Goudriaan, J., 1984. Simulation of the production of rapeseed on the basis of a field experiment. Neth. J. Agric. Sci. 32, 247–250.

Bigot, J., Boucaud, J., 1996. Short-term response of *Brassica rapa* plants to low temperature: effects on nitrate uptake and its translocations to the shoot. Physiol. Plant 96, 646–654.

Colnenne, C., Meynard, J.M., Reau, R., Justes, E., Merrien, A., 1998. Determination of a critical N dilution curve for winter oilseed rape. Ann. Bot. (in press).

Gabrielle, B., 1996. Modélisation des cycles des éléments eau–carbone–azote dans un système sol–plante, et application à l'estimation des bilans environnementaux des grandes cultures. PhD Thesis, Ecole Centrale Paris, France, 112 pp.

Gabrielle, B., Kengni, L., 1996. Analysis and field-evaluation of the CERES models' soil components: nitrogen transfer and transformation. Soil Sci. Soc. Am. J. 60, 142–149.

Gabrielle, B., Menasseri, S., Houot, S., 1995. Analysis and field-evaluation of the CERES models' water balance component. Soil Sci. Soc. Am. J. 59, 1402–1411.

Gabrielle, B., Denoroy, P., Gosse, G., Justes, E., Andersen, M.N., 1998. A model of leaf area development and senescence for winter oilseed rape. Field Crops Res. (this issue).

Gammelvind, L.H., Schjoerring, J.K., Mogensen, V.O., Jensen, C.R., Bock, J.G.H., 1996. Photosynthesis in leaves and siliques of winter oilseed rape (*Brassica napus* L.). Plant Soil 186, 227–236.

Gosse, G., Rollier, M., Rode, J., Chartier, M., 1983. Vers une modélisation de la production chez le colza de printemps. Proceedings of the 6th International Rapeseed Congress, Paris, France.

Gosse, G., Varlet-Grancher, C., Bonhomme, R., Chartier, M., Allirand, J., Lemaire, G., 1986. Production maximale de matière sèche et rayonnement intercepté par un couvert végétal. Agronomie 6, 47–56.

Greenwood, D.J., Lemaire, G., Gosse, G., Cruz, P., Draycott, A., Neeteson, J.J., 1990. Decline in percentage N of C3 and C4 crops with increasing plant mass. Ann. Bot. 66, 425–436.

Habekotté, B., 1996. Winter oilseed rape: analysis of yield formation and crop type design for higher yield potential. PhD Thesis, Wageningen Agricultural University, NL, 156 pp.

Husson, F., Leterme, P., 1998. Modélisation et validation de la date de floraison du colza d'hiver, Oléagineux, Corps Gras, Lipides (in press).

IBSNAT, 1990. Network report 1987–1990. Technical Report, University of Hawaii, Honolulu, HI, USA.

Jones, C.A., Kiniry, J.R., 1986. Ceres-N Maize: A Simulation Model of Maize Growth and Development. Texas A&M Univ. Press, College Station, Temple, TX, 194 pp.

Justes, E., Mary, B., Meynard, J., Machet, J., Thelier-Huches, L., 1994. Determination of a critical N dilution curve for winter wheat crops. Ann. Bot. 74, 397–407.

Laine, J., Bigot, J., Ourry, A., Boucaud, J., 1996. Effects of low temperatures on nitrate uptake, and xylem and phloem flows of nitrogen, in *Secale cereale* L. and *Brassica napus* L. New Phytol. 127, 675–683.

Lemaire, G., Gastal, F., Salette, J., 1989. Analysis of the effect of N nutrition on dry matter yield of a sward by reference to potential yield and optimum N content. Proceedings of the XVIth International Grasslands Congress, Nice, France, pp. 179–180.

Leterme, P., 1985. Modélisation de la croissance et de la production des siliques chez le colza d'hiver; application à l'interprétation des résultats de rendements. PhD Thesis, INA Paris-Grignon, France, 112 pp.

Leterme, P., 1988. Croissance et développement du colza: Les principales étapes. In: INRA-CETIOM (Ed.), Colza: Physiologie et Élaboration du Rendement. CETIOM Editions, Paris, pp. 23–33.

Leviel, B., Gabrielle, B., Justes, E., Mary, B., Gosse, G., 1998. Water and nitrate budgets in a rapeseed cropped rendzina soil different amounts of fertiliser. Eur. J. Soil Sci. (in press).

Mendham, N.J., Salisbury, P.A., 1995. Physiology: crop development, growth and yield. In: Kimber, D., McGregor, D.I. (Eds.), Brassica Oilseeds. Production and Utilization. CAB International, Wallingford, UK, pp. 11–64.

Morrison, M.J., Stewart, D.W., McVetty, P.B.E., 1995. Maximum area, expansion rate and duration of summer rape leaves. Can. J. Plant Sci. 72, 117–126.

Petersen, C.T., Jorgensen, U., Svendsen, H., Hansen, S., Jensen, H.E., Nielsen, N.E., 1995. Parameter assessment for simulation of biomass production and N uptake in winter rapeseed. Eur. J. Agron. 4, 77–89.

Schjoerring, J.K., Bock, J.G.H., Gammelvind, L.H., Jensen, C.R., Mogensen, V.O., 1995. N incorporation and remobilization in different shoot components of field-grown winter oilseed rape (*Brassica napus* L.) as affected by rate of N application and irrigation. Plant Soil 177, 255–264.

Sinclair, T.R., Amir, J., 1992. A model to assess nitrogen limitations on the growth and yield of spring wheat. Field Crops Res. 30, 63–78.

Sinclair, T.R., de Wit, C.T., 1975. Photosynthate and N requirements for seed production by various crops. Science (Washington, D.C.) 189, 565–567.

Sinclair, T.R., Muchow, R.C., 1995. Effect of N supply on maize yield: I. Modeling physiological responses. Agron. J. 87, 632–641.

Vardon, F., 1994. Adaptation d'un modèle dynamique de simulation de colza d'hiver (FIL) a un modèle de culture gérant l'eau et l'azote (CERES), validation et analyse de sensibilité. MS Report, ENSA Rennes, France, 55 pp.

Villalobos, F.J., Hall, A.J., Ritchie, J.T., Orgaz, F., 1996. OILCROP-SUN: a development, growth, and yield model of the sunflower crop. Agron. J. 88, 403–415.

Watts, D.G., Hanks, R.J., 1978. A soil–water–nitrogen model for irrigated corn on sandy soils. Soil Sci. Soc. Am. J. 42, 492–499.

de Willigen, P., van Nordwijk, M., 1987. Roots, plant production and nutrient use efficiency. PhD Thesis, Wageningen Agricultural University, NL, 282 pp.

Transport in Porous Media **35:** 129–147, 1999.

Theoretical Appraisal of Field-Capacity Based Infiltration Models and their Scale Parameters

B. GABRIELLE[1] and S. BORIES[2]
[1]*Institut National de la Recherche Agronomique, Unité de Recherche en Bioclimatologie, F-78850 Thiverval-Grignon. e-mail: gabriele@bcgn.grignon.inra.fr*
[2]*Centre National de la Recherche Scientifique, Institut de Mécanique des Fluides de Toulouse, Av. du Prof. C. Soula, F-31400 Toulouse Cédex. e-mail: bories@imft.fr*

(Received: 2 September 1997; in final form: 13 July 1998)

Abstract. In many hydrological applications, the modelling of water infiltration in soil is based either on Richards' equation or on the empirical concept of field-capacity utilized by capacity-type models. These two approaches feature different integration scales, and are often presented as antagonistic, with the former being physically correct and the latter a practical surrogate, however flawed by uncertain parameters. Here, we conducted a theoretical appraisal of a generic capacity model by comparing its predictions of water content in a macroscopic layer subjected to a constant surface infiltration flux with a length-averaged analytical solution of Richards' equation. We show that the choices of the time and spatial scales for the empirical model are not arbitrary, and discuss the cases in which they lead to an agreement with the mechanistic description, for a range of initial and boundary conditions, and for three soil types (sandy, loamy, and clayey). The concept of field-capacity hardly applies for the sandy soil because of its high hydraulic conductivity, but yields good results for finer textured soils. Provided that layer thickness exceeds 15 cm, capacity-type predictions had a 50% probability of being within 20% of mechanistic solutions, without requiring the hydrodynamic characterisation of the soil.

Key words: water infiltration, field-capacity, soil water balance, analytical solutions, Richards' equation.

1. Introduction

The computation of vertical water infiltration and transfer in soil constitutes a long-debated issue in soil physics as well as in less fundamental fields. As Ross (1990) pointed out, there is an acute need in agronomy or hydrology for efficient methods to estimate the water balance of a cultivated field or a watershed. Such demands have been dealt with in a wide body of literature, from which two main classes of infiltration models may be drawn (Addiscott and Wagenet, 1985). A first approach is based on the physics of transport in porous media at a local scale, defined by that of the average representative volume in which transport parameters are no longer subject to irregular pore-scale variations. Since they derive from basic principles of fluid mechanics, the corresponding equations are deemed as exact representations of reality, provided that the medium is homogeneous at the considered spatial scale.

A rather empirical approach to water flow has also developed on the concept of field-capacity, a moisture content at which gravity and capillary forces are supposed to be exactly balanced in a given macroscopic soil volume. Here, the soil profile is divided into a set of macro-layers that accumulate water until the field-capacity content is reached, and transfer extra incoming water to the next layer down. In the following we denote as macroscopic the vertical scale of these models, which is several orders of magnitude larger than that of the local approach (over 10 cm versus a few millimetres).

Both approaches have been extensively used for the prediction of soil moisture at the field scale, and sometimes compared with respect to their accuracy and operating constraints. Vachaud *et al.* (1990) suggested that empirical models require less inputs and are less sensitive to their spatial variability than local models, which contributes to make them an attractive tool in agronomy and hydrology research. On the other hand, cases where their simulations proved biased have been reported (e.g. Comerma *et al.*, 1985). Using the field-capacity model of Ritchie (1985), Gabrielle *et al.* (1995) could remove a systematic discrepancy between observed and simulated soil water storages by adjusting a rate parameter (drainage coefficient) for water transfer between macro-layers. Such fitting appears rather empirical and may have deterred efforts to establish a connection between the two classes of modelling. However, as far as parameterisation is concerned, the macroscopic approach could greatly benefit from a link with the reference local modelling, since the latter relies on measurable soil properties.

From the local viewpoint, water flow is determined by the soil hydraulic conductivity and water retention curves, in addition to boundary and initial conditions. In its empirical counterpart, it is controlled by the sole field-capacity content (noted θ_{fc}, $m^3\,m^{-3}$) and drainage coefficient. This solution is also an implicit function of the a priori arbitrary choice of the macroscopic layers' thickness L (cm) and the integration time step T (days). There is, however, an obvious link between L and T, since the volume of water leaving a macro-layer is dependent on the elapsed time T and the thickness L through the hydraulic gradient, as formulated in Darcy's law. The objective of this study was to draw theoretical relationships between the macroscopic space and time scales of field-capacity based models, for which their predictions converge with the averages of local solutions. The latter are considered as a correct description of the actual infiltration. The determination of the other macroscopic parameters is also discussed through this comparison. It brings some insight as to whether empirical models are intrinsically biased, because of their lumping time and space coordinates in their capacity parameter, or if they may only apply to certain soil types or forcing conditions.

The present study was conducted for three particular soils (sandy, loamy and clayey), and for a variety of initial and boundary conditions. Both analytical and quasi-analytical solutions to the mechanistic equations were used.

2. Methods

2.1. MODELS' COMPARISON

Throughout the study, we consider one-dimensional infiltration of water into an homogeneous soil volume subjected to a constant incoming surface flux q_0 (cm day^{-1}). The soil moisture profile is taken uniform when infiltration starts, with an initial value of θ_0 (m^3 m^{-3}). Discrepancies between the mechanistic and empirical simulations of water flow may be analyzed in terms of predicted mean water content in the top macro-layer and infiltration flux below that layer. Since both types of modelling respect the mass balance, the solutions in moisture content θ or water flux q are equivalent, so we will mostly focus on θ values. Because they are of prime importance in view of environmental aspects, the discrepancies in water fluxes will also be considered.

The soil water content given by the reference local solution at time t and depth z is noted $\theta(z, t)$, and the mean content in the macro-layer predicted by the empirical model after one time step T is noted $\theta_{L,T}$.

The two models converge if

$$\overline{\theta_L}(T) = \theta_{L,T}, \tag{1}$$

where the left-hand side term is the length-average of the local solution at T, over the macro-layer of thickness L ($\overline{\theta_L}(T) = 1/L \int_0^L \theta(z, T)\,\mathrm{d}z$). If we set the macroscopic time step T to a typical value of one day, it amounts to finding an order of magnitude for L, depending on the soil properties and the infiltration regime.

The discrepancy between the variables in Equation (1) was quantified with a first-order moment m_θ, that represents the mean difference between the length-averaged local solution and the macroscopic one.

$$m_\theta = \frac{L}{q_0 T}[\theta_{L,T} - \overline{\theta_L}(T)]. \tag{2}$$

m_θ is scaled with $q_0 T/L$, which corresponds to the maximum mean moisture variation in the macro-layer (for the mass balance implies $\int_0^L (\theta(z, T) - \theta_0)\,\mathrm{d}z \leqslant q_0 T$). A similar indicator for the water fluxes q could be defined as

$$m_q = \frac{1}{q_0}[q_{L,T} - \overline{q_L}(T)]. \tag{3}$$

As $q = q_0 - [\theta_{L,T} - \overline{\theta_L}]L$, it is easily shown that $m_q = m_\theta$, and thus the relative differences in terms of moisture content exactly match those in water flux.

Both solutions to our infiltration problem depend on the initial and boundary conditions (set by the values of θ_0 and q_0), and on the hydrodynamic properties of the medium. We used the forms proposed by van Genuchten (1980), with

$$h(\Theta) = \frac{1}{\alpha}[\Theta^{-1/m} - 1]^{1-m},$$

$$K(\Theta) = K_s \Theta^{1/2}[1 - (1 - \Theta^{1/m})^m]^2 \quad \text{with} \quad \Theta = \frac{\theta - \theta_r}{\theta_s - \theta_r}, \tag{4}$$

Table I. Assumptions made in the four studied cases, with respect to models' parameters and boundary and initial conditions. q_0 is the water flux applied at the soil surface, θ_0 ($m^3\,m^{-3}$) the initial soil moisture content, and θ_{fc} ($m^3\,m^{-3}$) the field-capacity content

Case Number	Assumptions		
	$T = 1$ day	$\theta_0 = f(q_0)$ (Equation (6))	$\theta_{fc} = f$(soil type) (Equation (5))
I	Y[a]	Y	Y
II	Y		Y
III	Y		
IV			Y

[a] Yes

where K is the hydraulic conductivity ($cm\,day^{-1}$), and h the suction head (cm of water). The s subscripts denote saturated properties, θ_r is the residual water content, and m and α are two constants characterising the unsaturated zone.

Given Equation (4), the local solution is determined by 7 parameters (5 for the $K-\theta$ and $h-\theta$ relationships, in addition to θ_0 and q_0). Assuming the 5 hydrodynamic parameters to be a function of soil type, there remains three degrees of freedom (soil type, θ_0 and q_0). The degrees of freedom amount to five for the macroscopic solution: the field-capacityθ_{fc}, the time and length scales (T and L), and the forcing conditions θ_0 and q_0.

On this overall total of 6 parameters influencing our problem, we took four sets of options (cases) summarised in Table I. As a first option, the integration time T was set to its typical value of 1 day in most of the study. Second, the field-capacity was related to the retention curve, as follows:

$$\theta_{fc} = \theta(h_{fc}), \tag{5}$$

with h_{fc} equalling -100, -333 or -1000 cm for the sandy, loamy and clayey soils, respectively (Baize, 1988). Because Ratliff *et al.* (1983) reported significant differences between such retention-based estimates and field-estimates of θ_{fc}, the latter was also varied to a small extent in one of the cases. Finally, we considered a simple

Table II. Class and hydrodynamic parameters of the three simulated soils (sandy, loamy, and clayey), from van Genuchten (1980)

Soil class	K_s $cm\,day^{-1}$	θ_s	θ_{fc} $m^3\,m^{-3}$	θ_r	α cm^{-1}	m
Hygiene sandstone	108.0	0.250	0.243	0.153	0.00790	0.904
Silt Touchet GE3	4.96	0.469	0.281	0.190	0.00423	0.505
Beit Netofa Clay	0.082	0.446	0.387	0.000	0.00152	0.145

case where the empirical model predicts: $\theta_{T,L} = \theta_{fc}$, which yielded a relationship between q_0 and θ_0

$$q_0 T = (\theta_{fc} - \theta_0)L, \quad \text{with} \quad \theta_0 < \theta_{fc}. \tag{6}$$

As for soil types, we chose the three contrasting soils (sandy, loamy and clayey) presented by van Genuchten (1980), whose characteristics are listed in Table II.

2.2. ANALYTICAL SOLUTIONS TO RICHARDS' EQUATION

One-dimensional water flow in soil is modelled at the local scale by combining the generalized Darcy's law with the mass balance equation, yielding the Richards equation

$$\frac{\partial \theta}{\partial t} = \frac{\partial}{\partial z}\left[D(\theta)\frac{\partial \theta}{\partial z} - \frac{\partial K(\theta)}{\partial z}\right], \quad \text{with} \quad q = -K(\theta)\frac{\partial H}{\partial z}, \tag{7}$$

where z and t are the vertical and time coordinates, and H is the hydraulic head resulting from capillary and gravity forces ($H = h - z$, with z positively oriented downwards). D is the capillary diffusivity ($cm^2\ day^{-1}$), with $D(\theta) = K(\theta)\partial h/\partial\theta$, and q is the vertical water flux through a cross-section at z, given by Darcy's law in the right-hand side equation. We will study the case of a constant infiltration flux q_0 at the soil surface starting at $t = 0$, in a soil considered as an homogeneous semi-infinite body with an uniform initial moisture profile. The boundary and initial conditions are

$$\begin{aligned} &q(0, t > 0) = q_0, \qquad \theta(z, 0) = \theta_0, \\ &\theta(\infty, t) = \theta_0, \qquad \frac{\partial \theta}{\partial z}(\infty, t) = 0. \end{aligned} \tag{8}$$

We thus have to solve a diffusion problem with a boundary condition of the second kind. Since D is highly dependent on θ, there is no general analytical solution to it, unless D and K are taken constant during the infiltration (which corresponds to a 'linear' soil). To enable direct analytical comparisons with the empirical model, we made this simplifying hypothesis in most of the study, and eventually checked it against a more realistic solution based on a flux-concentration approximation.

2.2.1. *Analytical Solution (Linear Soil)*

With D and K constant, taking the derivative of (7) in θ yields an ordinary diffusion equation for q

$$\frac{\partial q}{\partial t} = D\frac{\partial^2 q}{\partial z^2}, \tag{9}$$

the integration of which leads to

$$q(z, t) = q_0 - (q_0 - K_0)\,\mathrm{erf}\,(u), \tag{10}$$

where erf is the Gaussian error function, and $u = z/[2(Dt)^{1/2}]$. $K_0 = K(\theta_0)$ is the initial water flux in the soil before infiltration begins. Integrating (10) between z and ∞, with q also given by (7), yields

$$\theta(z,t) = \theta_0 + 2(q_0 - K_0)\left(\frac{t}{D}\right)^{1/2} \text{i erfc}(u), \tag{11}$$

where $\text{i erfc}(u) = \exp(-u^2)/(\pi)^{1/2} - u[1 - \text{erf}(u)]$. Since the study aims at comparing macro-layer based models with this local solution to water flow, the quantity of interest is the length-averaged water content in the macro-layer of thickness L, at time T, noted $\overline{\theta_L}(T)$. Appendix A yields

$$\overline{\theta_L}(T) = \theta_0 + \frac{4T(q_0 - K_0)}{L} I_\theta(u_{L,T}),$$

where $u_{L,T} = L/[2(DT)^{1/2}]$ and with

$$I_\theta(u) = \frac{1}{4}\left[\text{erf}(u)(1 + 2u^2) - 2u^2 + \frac{2}{(\pi)^{1/2}} u \exp(-u^2)\right]. \tag{12}$$

In Equation (12), assuming D constant requires an average value which we take as $D = D[(\theta_0 + \theta_{L,T})/2]$, where $\theta_{L,T}$ is the final water content predicted by the capacity model. This makes the local solution somewhat dependent on the macroscopic one. However, preliminary tests against a solution where the local equations were iteratively solved using the final moisture content given by the previous iteration, in place of the macroscopic prediction $\theta_{L,T}$, showed that this hypothesis had very little influence.

2.2.2. *Flux-Concentration Approximation (Real Soil)*

White (1979) proposed a quasi-analytical solution to the above problem based on the flux-concentration approximation. The latter states that, at any depth, the reduced water flux $F(\theta^*)$ depends only on the reduced water content θ^*, with

$$F(\theta^*) = \frac{q - K_0}{q_0 - K_0}, \qquad \theta^* = \frac{\theta - \theta_0}{\theta(0,t) - \theta_0}, \tag{13}$$

where $K_0 = q(z, t = 0)$, and $\theta(0,t) = \theta(z = 0, t)$. It makes it possible to derive implicit integral equations giving the time course of θ (see Appendix B). These can be solved by imposing an empirical relationship between F and θ^*. White (1979) and Boulier *et al.* (1984) found that simply taking $F = \theta^*$ yielded satisfactory results for sandy soils, and we will thus use this closure equation.

As in the analytical case, we are essentially interested in the average moisture content in the macro-layer of thickness L at time T, noted $\overline{\theta_L^{\text{q.a.}}}(T)$, with the q.a. superscript standing for quasi-analytical. The equivalent of Equation (12) for the

present solution is given in Appendix B as

$$\overline{\theta_L^{\text{q.a.}}}(T) = \theta_0 + \frac{\theta(0,T) - \theta_0}{q_0 - K_0} \times \times \left\{ \int_{\theta(L,T)}^{\theta(0,T)} \frac{D(\theta)}{L} \left[1 + \frac{K(\theta)}{(q_0 - K_0)(\theta^* - \kappa(\theta))} \right] \mathrm{d}\theta - K_0 \right\}, \quad (14)$$

where $\kappa(\theta) = (K(\theta) - K_0)/(q_0 - K_0)$ is the reduced hydraulic conductivity.

2.2.3. *Macroscopic Approach*

In this approach the soil is divided into a set of macro-layers that successively accumulate water and transfer it downwards during the infiltration, like reservoirs. In each layer, drainage sets on if the water content exceeds field-capacity on the preceding time step. We used the model of Ritchie (1985), in which the layer's moisture content at time T ($\theta_{L,T}$) is calculated from that at time 0 ($\theta_{L,0}$) as

$$\begin{aligned} &\theta_{L,T} = \theta_{L,0} + \frac{q_0 T}{L} \qquad \text{if} \quad \left(\theta_{L,0} + \frac{q_0 T}{L} \leqslant \theta_{\text{fc}} \right), \\ &\theta_{L,T} = \theta_{L,0} + \frac{q_0 T}{L} - \left(\theta_{L,T} + \frac{q_0 T}{L} - \theta_{\text{fc}} \right) T \times \text{SWCON otherwise}, \end{aligned} \quad (15)$$

where T is the macroscopic time step, and SWCON (day^{-1}) a drainage coefficient ranging from 0 to 1 that incorporates the effect of hydraulic conductivity on limiting flow rate. It misleadingly stands for Soil Water CONductivity (Ritchie, 1985). SWCON was taken from Ritchie and Crum (1989) as 0.01, 0.10 and 1.00 for the clayey, loamy and sandy soils, respectively. In the last section of the paper, the value of SWCON is, however, discussed in relation to soil hydrodynamic properties.

The following comparisons will be limited to the top surface layer, since it is the elementary volume of the description being tested.

To prevent ponding, which the empirical model cannot simulate, the following constraint was imposed on the surface infiltration rate q_0:

$$q_0 \leqslant \min \left[K_{\text{s}}, \frac{(\theta_{\text{s}} - \theta_0) L}{T} \right]. \quad (16)$$

3. Results and Discussion

In this section we first tested the accuracy of the empirical model against the local analytical solution for the four cases of Table I. The validity of the analytical solution is then discussed with reference to the quasi-analytical one, and lastly the value of the empirical rate parameter SWCON in the macroscopic model is approached under a steady-state regime of infiltration.

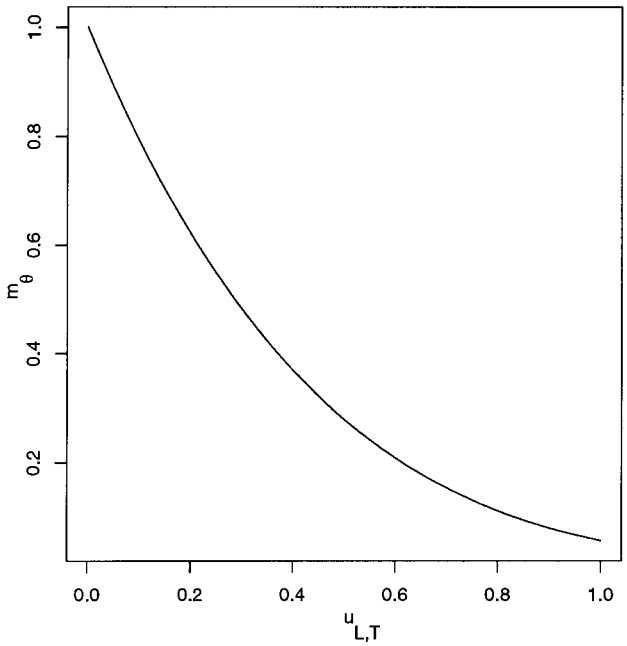

Figure 1. Variations of the empirical model's average error m_θ (unitless) as a function of the dimensionless variable $u_{L,T} = L/(4DT)^{1/2}$, in a simple preliminary case.

3.1. CASE I: INFILTRATION TO FIELD-CAPACITY

In this preliminary case, the combination of Equations (11) and (12), together with the condition on q_0 and θ_0 expressed by Equation (6) yields

$$m_\theta = 1 - 4\left(1 - \frac{K_0}{q_0}\right) I_\theta(u_{L,T}). \tag{17}$$

If $K_0/q_0 \ll 1$ (infi ltration starting in a dry soil for instance),$m_\theta \approx 1 - 4I_\theta(u_{L,T})$, and by fi xing a threshold level form_θ we obtain a simple relationship between L, T and the diffusivity D. If, for example, we want $m_\theta < 0.1$ (i.e. the empirical model yields a relative accuracy of 10%), it can be derived from Figure 1 representing m_θ versus $u_{L,T}$ that L should exceed $1.7 \times (DT)^{1/2}$. With $T = 1$ day, a macroscopic layer of 30 cm would give satisfactory results provided $D \leqslant 800\,\mathrm{cm^2\,day^{-1}}$. This is easily satisfi ed for the clay and loamy soils if we take $D = D(\theta_{\mathrm{fc}})$, with $D(\theta_{\mathrm{fc}})$ equal to 8.13 and 406.3, respectively. For the sandy soil this is not the case as $D(\theta_{\mathrm{fc}})$ equals 1.25×10^5. With such a diffusivity, the above criterion would be satisfi ed for L greater than 600 cm, which is too large a spatial scale for our calculations to hold.

3.2. CASE II: INFILTRATION TO ABOVE FIELD-CAPACITY

For this case, the initial water content θ_0 was set halfway between θ_{fc} and θ_{s}. The contour graphs in Figure 2(a) present the variations of $m_\theta$for L varying between 1

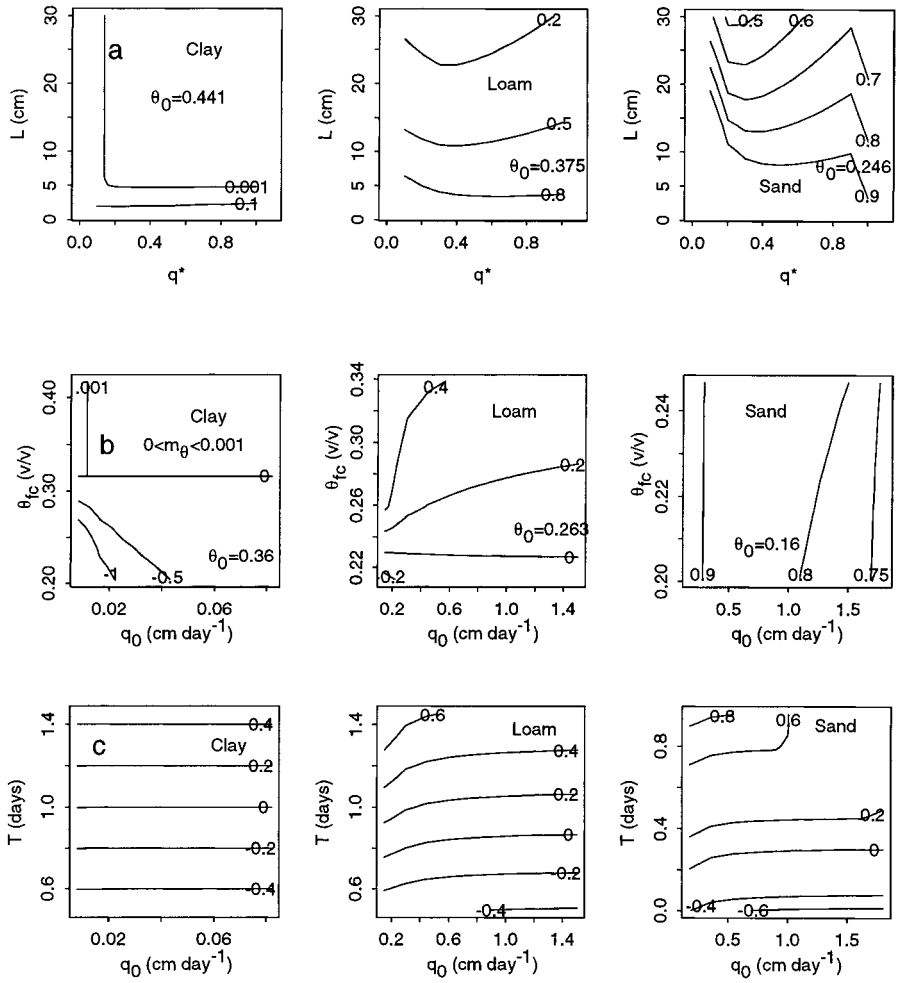

Figure 2. Variations of the macroscopic model's error m_θ (unitless) with the surface infiltration flux q_0 and the macro-layer's thickness L, for the three soil types. Three combinations of initial conditions and macroscopic parameters are used, corresponding to cases II to IV: θ_0 is fixed above the field-capacity content θ_{fc} and q_0 is varied (**a**); θ_{fc} is varied (**b**); the integration time step T is varied (**c**). In case (**c**), θ_0 is the same as in case (**b**).

and 30 cm, and for different infiltrations rates q_0. Those are indicated as reduced values (q^*) relative to the upper boundary for q_0 given by Equation (16) for each L. It is possible to determine regions in the L versus q^* plane in which the results of the empirical model are correct within a 20% margin (i.e. $|m_\theta| \leqslant 0.2$). This 'pass' region is nearly unrestricted for the clay soil, and limited to that where $L \geqslant 25$ cm for the loam. For the sandy soil, the macroscopic approach simply does not seem to apply. Although this is to be further discussed in cases III and IV, it is rather intuitive that in a very well-drained medium it should be delicate to define a field-capacity

content, for the macro-layer has transferred downwards most of the infiltrating water long before the macroscopic time step T has elapsed.

Conversely for the clay soil, two factors contribute to the convergence of macroscopic and microscopic solutions. First, the permitted infiltration rates are very small (0.01 to 0.08 cm day^{-1}) because of the low saturated conductivity of the medium. This induces only small variations in moisture content, although they are scaled by the infiltration rate in m_θ. Second, because the medium has a low diffusivity, water hardly infiltrates below the macro-layer after one day, provided that L exceeds 5 cm, which prevents any discrepancies between the two models.

Overall, the macroscopic model consistently overestimated the actual water content in the macro-layer, which indicates a systematic bias even under drainage conditions ($\theta_0 \geqslant \theta_{fc}$). This positive bias could be expected, and was observed, with $\theta_0 \leqslant \theta_{fc}$ (Case I). In this case, the tipping-bucket scheme keeps accumulating water in the macro-layer, whereas some water actually percolates downwards during the time step T. However, in the reverse drainage mode represented by Case II, the tipping-bucket was rather expected to underestimate the water content because the macro-layer may actually drain to below field-capacity after one day. Instead, the bias persisted and thus the errors of the tipping-bucket model, overall, did not cancel out.

The observed bias should be mitigated because it also depends on the empirical rate parameter SWCON. The end of the study confirmed that it was correctly estimated for the clay and the sand, but underestimated for the loam (which is consistent with a mostly positive m_θ).

Errors tended to decrease with increasing q^*, although they increased again with $q^* \geqslant 0.3$ for the sandy and loamy soils. For the sand, the scaled error m_θ decreased again for $q^* \geqslant 0.9$. The occurrence of these minima and maxima was not associated with particular changes in the infiltration regimes, since the tipping-bucket scheme was in a discharge mode throughout (with $\theta_0 \geqslant \theta_{fc}$). They simply reflect the strong nonlinearity of the diffusion equation with respect to both the infiltration rate and the diffusion coefficient D.

Lastly, m_θ decreased with increasing L, since discrepancies tend to smooth out when averaging over larger scales.

3.3. CASE III: SENSITIVITY TO FIELD-CAPACITY

L was set to 20 cm, and q_0 was varied within the limits of Equation (16) for a fixed θ_0 (Figure 2b). For the clay and loam soils, optimal values for θ_{fc} could be deduced from the 0 iso-contour lines. Since these lines were nearly horizontal, the optimal values for θ_{fc} extended over the whole range of infiltration rates, and may be summarised as $\theta_{fc} \geqslant 0.32$ for the clay and $\theta_{fc} \approx 0.23$ for the loam. The latter value was much lower than that of 0.281 derived from the retention curve (Equation 5). Although the optimal θ_{fc} was also dependent on L (Figure 3), this trend persisted over the whole range of L. The dependence between the true θ_{fc} and L depicted in Figure 3 emphasizes a

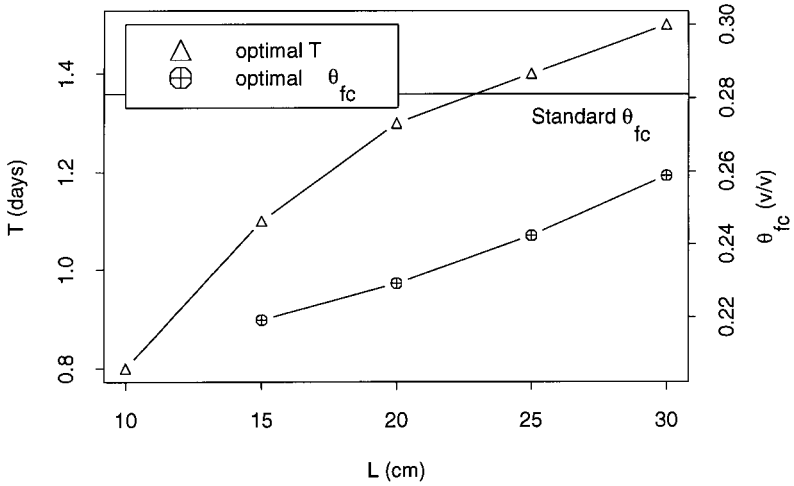

Figure 3. Relationship between two optimal macroscopic parameters (the field-capacity content θ_{fc} and integration time step T) and the macroscopic layer's thickness L, for the loamy soil. They were deduced from the 0 iso-contour lines in m_θ plots similar to those of Figures 2(c) and 2(d). The optimal θ_{fc} corresponds to a T value of 1 day, and the optimal T to the standard value of θ_{fc} given by the horizontal solid line.

conceptual error with the capacity model. According to that description, the larger the reservoir (i.e. the thicker the macro-layer), the greater the amount of water Q that can infiltrate into it before the layer starts draining, with a linear relationship between Q and the layer thickness L. However, in order for this model to be correct it is necessary that the threshold water content above which percolation starts (θ_{fc}) should decrease when L increases, because of the nonlinearity in the actual process of water diffusion in soil with respect to L (see Equation (11)). This dependence should be considered when setting the field-capacity in a macro-layer.

For the sandy soil, the capacity model's bias remained strongly positive ($m_\theta \geqslant 0.6$), and no optimal θ_{fc} was evidenced. As the same applied to the previous cases, it is likely that the daily time step in the calculations was too large for allowing a capacity description.

3.4. CASE IV: INFLUENCE OF THE TIME STEP T

The macroscopic time step T was varied between 0.1 and 1.5 days, with the same initial and boundary conditions as in case III (Figure 2(c)). Optimal values for T were again exhibited for the clay and loam soils, equalling 1.0 and 0.8 day, respectively. The optima in terms of time step were not equivalent to those in terms of θ_{fc}, since the contour lines did not have the same shape. For the clay, the optimal region of Figure 2(a) reduced to a narrow interval. As a general rule, the iso-contour lines also appeared much flatter. Most likely, the sensitivity of m_θ for θ_{fc} was less linear than for T because θ_{fc} is a threshold parameter. The optimal T value also decreased with

decreasing L for the loam (Figure 3), and reached a plateau of about 0.9 day for $L \geqslant 20$ cm. This stresses the diffi culty of predicting infi ltration close to the surface ($L \leqslant 10$ cm) with the capacity scheme. For the sandy soil, an optimum value of 0.3 day could be derived for T at the bottom of the T versus q_0 plane. It means the empirical description would only apply to small time steps, with an order of magnitude close to those employed in the local resolution of mechanistic equations (Ross, 1990). This seems, however, hardly fi t to the purposes of macroscopic models.

3.5. COMPARISON WITH THE QUASI-ANALYTICAL SOLUTION (REAL SOIL)

Using an analytical solution to the infi ltration equations allows a direct comparison between microscopic and macroscopic approaches: for instance, Equation (17) could readily be used to evaluate the goodness of the empirical model, given the scales T and L, and the mean soil diffusivity D. In cases II to IV, the calculation of m_θ was also straightforward. Nevertheless, the dependency of D on θ is highly nonlinear, and this is all the more acute in the saturated region which is of concern to us. Therefore it seemed prudent to compare the analytical solution where D is constant with the more realistic quasi-analytical (q.a.) solution in which D varies during the infi ltration. The average moisture contents in a macro-layer of length L, noted $\overline{\theta_{L,\text{q.a.}}}(T)$ and $\overline{\theta_L}(T)$ for the quasi-analytical and analytical solutions, respectively, were compared in terms of a moment similar to m_θ, $m_\theta^{\text{q.a.}}$, with

$$m_\theta^{\text{q.a.}} = \frac{L}{q_0 T}[\overline{\theta_{L,\text{q.a.}}}(T) - \overline{\theta_L}(T)]. \tag{18}$$

This indicator was calculated for case I with L ranging from 10 to 30 cm.

As illustrated in Figure 4, the discrepancies between the two solutions were negligible for the fi ne-textured soils (loamy and clayey), exceeding 5% in only 5% of the plotting region. On the other hand, they were signifi cant for the sandy soil, with an average rising to more than 10%. This may be ascribed to the strong sensitivity of D to θ in the saturated region, and did not smooth out for large values of L.

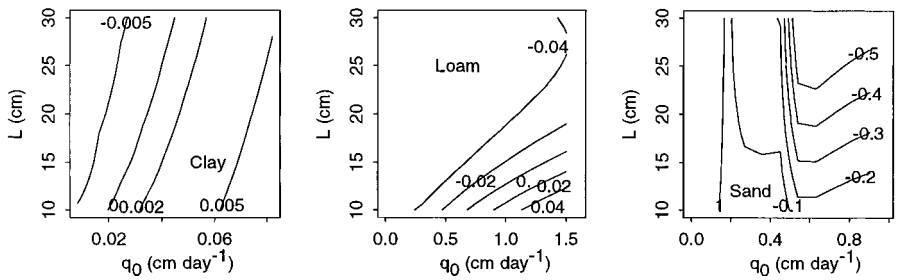

Figure 4. Variations of the mean scaled difference $m_\theta^{\text{q.a.}}$ between the analytical and quasi-analytical solutions of Richards' equation with the macro-layer's thickness L and the infi ltration rateq_0.

However, because of the vertical shape of the iso-contour lines in Figure 4 compared to the rather horizontal iso-contours in Figure 2, the errors that might have arisen from using the analytical solution with the sand had little influence on the trends observed with m_θ (data not shown).

3.6. DETERMINATION OF SWCON IN QUASI-STEADY CONDITIONS

In Equation (15), the values of the rate parameter SWCON were taken a priori from the literature, although it was suggested in the discussion of case II that SWCON should rigorously be estimated from experimental data. In addition this parameter may be related to the soil's saturated hydraulic conductivity K_s, as shown by Emerman (1995).

We examined such a link in a steady-state infiltration regime, when an equilibrium uniform moisture profile has developed within the macro-layer to a depth L, after a sufficient amount of water has infiltrated. Provided that q_0 be smaller than K_s, the quasi-analytical solution gives an expression of the asymptotic moisture content $\theta_{as.}^{q.a.}$ in the macro-layer as being the inverse of the $K(\theta)$ function at q_0, so that (see Appendix B)

$$K(\theta_{as.}^{q.a.}) = q_0. \tag{19}$$

With a quasi steady-state moisture profile, the daily flux draining from the macro-layer predicted by the quasi-analytical solution is q_0, and may be compared to that predicted by the empirical model, noted q_L, and reads

$$q_L = L\left(\theta_{as.}^{q.a.} + \frac{q_0}{LT} - \theta_{fc}\right)\text{SWCON}. \tag{20}$$

Both models converge if $q_L = q_0$, that is if

$$\begin{aligned} q_0 &= L\left(\theta_{as.}^{q.a.} + \frac{q_0}{LT} - \theta_{fc}\right)\text{SWCON} \\ &\Rightarrow \theta_{as.}^{q.a.} = \theta_{fc} + \frac{q_0}{L}\left(\frac{1}{\text{SWCON}} - \frac{1}{T}\right). \end{aligned} \tag{21}$$

Given that SWCON is fixed for any L and q_0, Equation (21) implies that there would be a linear relationship between $\theta_{as.}^{q.a.}$ and q_0. On the other hand, this relationship is given by Equation (19), from which it is clear that Equation (21) is not verified because of the exponential shape of the $K(\theta)$ curve. From Equation (21) we may also draw a relationship between q_0 and the empirical parameters SWCON, θ_{fc}, and L, for a given soil, with

$$\text{SWCON} = \frac{q_0}{L\left(K^{-1}(q_0) + \dfrac{q_0}{LT} - \theta_{fc}\right)}, \tag{22}$$

where K^{-1} is the inverse function of K. The right-hand side term in Equation (22) is depicted in Figure 5 for the three studied soils, with $L = 10$, 20 and 30 cm. This term

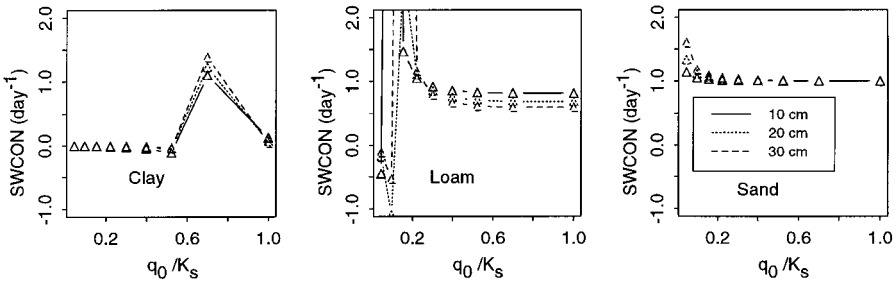

Figure 5. Right-hand side term of Equation (22), which corresponds to the drainage coeffi - cient SWCON, as given by the quasi-analytical solution to infi ltration. Calculations are made for the three soils, and for three values of the macroscopic thickness L (10, 20 and 30 cm).

should be constant were the empirical model correct, but this is obviously not the case, as pointed out by Equation (21). For some infi ltration rates (in the lower range for the loam and the sand, and in the higher range for the clay), SWCON reaches peak values that are outside its physically-plausible range. Except for these peaks, however, the curves in Figure 5 decrease with increasing q_0, and reach a plateau on one of their ends. This stable value of SWCON fi rst indicates that a fi xed value of SWCON (independent of q_0) could give good results in about half of the tested conditions. Second, it gives an order of magnitude for SWCON: around 2.5×10^{-3} for the clay, 0.65 for the loam, and 1.00 for the sand. In the latter case, SWCON is mainly above 1.00, because the water content in the macro-layer drops far below fi eld-capacity after one day, as discussed in case IV. For the other two soils, an inverse relationship appears between SWCON and L when averaging over q_0, which was also mentioned by Emerman (1995) for a tipping bucket model. Its magnitude is influenced by the hydraulic conductivity, being negligible for the soils with high and low hydraulic conductivities, and more marked for the loam.

As a conclusion, SWCON exhibited only weak correlations to the scale parameters, which does not preclude its use in a capacity model with arbitrary time and length steps, as was successfully done by Buttler and Riha (1992) who estimated SWCON directly from soil porosity for an Oxisol. However, the diffi culty in obtaining SWCON a priori for less permeable soils prompted Gabrielle *et al.* (1995) to substitute it for the hydraulic conductivity, yielding a Darcy-like equation for the calculation of the daily flux below the macro-layer that reads

$$q_L(T) = K\left(\theta_{L,0} + \frac{q_0 T}{L}\right) \quad \text{if} \quad \left(\theta_{L,0} + \frac{q_0 T}{L} \geqslant \theta_{\text{fc}}\right).$$

This equation is close to that predicted by the quasi-analytical solution, and is less sensitive to q_0 and L than Equation (21). However, it tends to overestimate q_L, since $K(\theta_{L,t} + q_0 T/L)$ is greater than $K(\theta_{\text{as.}}^{\text{q.a.}})$ in the quasi-steady infi ltration.

4. Conclusion

We analysed the accuracy of an empirical, field-capacity based model of one-dimensional water infiltration in soil, as compared to an analytical solution of Richards' equation, for the prediction of moisture content in a macroscopic layer of thickness L (cm) subjected to a constant infiltration flux q_0 (cm day^{-1}) at its surface during a time step T (days).

Various boundary and initial conditions were simulated for three soils with contrasting hydrodynamic properties, and revealed some biases in a standard application of the empirical model. The deviations were all the more acute as the soil's average capillary diffusivity during infiltration was high, and were maximum around field-capacity. The effect of various empirical parameters was investigated to identify the reasons for these biases. With T fixed at one day, they were dampened with increasing L, and were acceptable (except for the very well-drained sandy medium) for $L \geqslant 15$ cm. As a general rule, the tipping-bucket tended to over-estimate surface water content, and thus to under-rate the infiltration fluxes. This should be kept in mind when using this kind of model to estimate the leaching of solutes such as nitrate or pesticide compounds in the field.

The errors cancelled out for an optimal value of the field-capacity content (θ_{fc}) that varied with L. A relationship between an optimal integration time step T and L was also exhibited. Correlations between T, L, and θ_{fc} could be expected to appear when calibrating a capacity-type model because of its principle: it does not explicitly take the time coordinate into account, given that only θ_{fc}, and to a lesser extent the drainage coefficient SWCON, control the flow out of the reservoir.

The biases observed do not necessarily preclude the applicability of the model. Provided that an order of magnitude of the soil's capillary diffusivity be known, Equation (17) could be used as a first indicator of the model error. For the clay soil studied here, for instance, it showed that no major divergences were likely to be observed, as it proved to be the case. For a soil with higher diffusivity such as the loamy Silt Touchet, taking layers thicker than 15 cm markedly improved the model performance, even if it was not fully unbiased. Reducing the time step could also be a solution, although it proved to be a sensitive variable. As to a highly permeable medium, represented here by the Hygiene Sandstone, it unfortunately seemed to impose a local scale modelling, otherwise strong errors occurred.

If one then chooses to use a capacity model, determining the field-capacity and rate parameters turns out to be the critical point. Because they depend to some extent on the length and time scales chosen, these parameters are not unique. Based on the results of our analysis, Figure 6 provides guidelines as to the estimation of these parameters. The best way to determine θ_{fc} would probably consist in applying its functional definition, as quoted by Baize (1988): it is the water content in a given soil layer after it has drained for one day subsequently to a rainfall event. However, it is often required by model users that it be possible to deduce it a priori from other soil properties, such as the water retention curve, as we did here with Equation (5). As pointed out by Ratliff *et al.* (1983) for a range of soil types, this

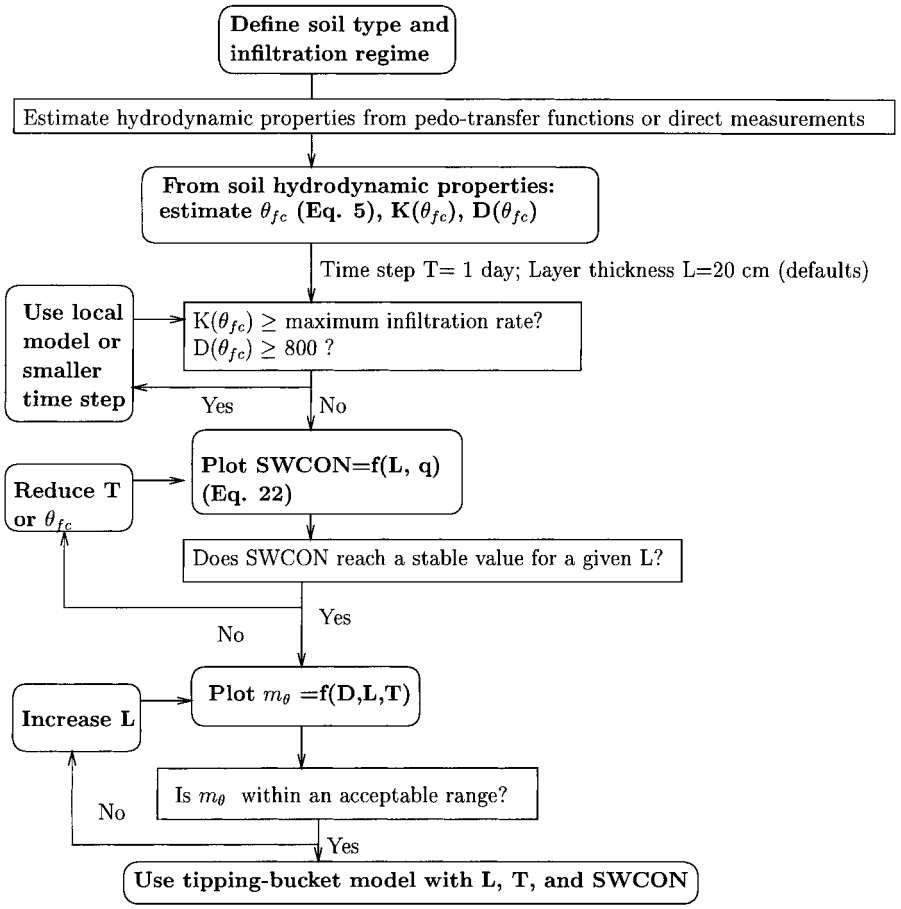

Figure 6. Diagram for setting the time and spatial scales and the capacity and rate parameters of a capacity-based water infiltration model, in a given soil.

does not yield the true θ_{fc}, but here the biases proved acceptable with sufficiently high L ($L \geqslant 15$ cm).

SWCON is perhaps the most empirical macroscopic parameter since its relation to the hydraulic conductivity is not straightforward and involves other parameters (e.g. L and θ_{fc}). The use of more Darcian-based equations such as that of Gabrielle *et al.* (1995), which do not require this parameter, might prove helpful, although slightly more complex.

There is then no theoretical argument for claiming that capacity models are second-rate tools dedicated to an approximate and biased simulation of water infiltration. They provide correct estimates for a range of conditions, provided that they be properly parameterised. This parameterisation issue constitutes their major disadvantage, for their accuracy seems to depend on the knowledge of the user (Diekkrüger *et al.*, 1995). In a comprehensive comparison of soil water balance

models, the latter authors put forward that 'expert knowledge' was a key factor behind the goodness of simulation results. On the opposite, we hope that our analysis of functional infi ltration models, with reference to the mechanistic Richards' equation, should help parameterising them without resorting to such subjective methods.

Appendix A: Averaging the Analytical Solution Over the Macro-Layer

Calculation of $\overline{\theta_L}(T) = 1/L \int_0^L \theta(z, T)\,\mathrm{d}z$, where L is the macro-layer's thickness, with $\theta(z, T)$ given by Equation (11):

$$\overline{\theta_L}(T) = \theta_0 + 2(q_0 - K_0)\left(\frac{T}{D}\right)^{1/2} \int_0^L \mathrm{i\,erfc}(z/[4DT]^{1/2})\,\mathrm{d}z.$$

With $u = z/(4DT)^{1/2}$ and $u_{L,T} = L/(4DT)^{1/2}$, the integral can be computed as

$$(4DT)^{1/2} \int_0^{u_{L,T}} \mathrm{i\,erfc}(u)\,\mathrm{d}u = \frac{u_{L,T}}{L}\left[\int_0^{\infty} \mathrm{i\,erfc}(u)\,\mathrm{d}u - \int_{u_{L,T}}^{\infty} \mathrm{i\,erfc}(u)\,\mathrm{d}u\right].$$

With

$$\int_0^{\infty} \mathrm{i\,erfc}(u)\,\mathrm{d}u = \mathrm{i}^2\mathrm{erfc}(u) = (1 + 2u^2)\mathrm{erfc}(u) - \\ - \frac{2}{(\pi)^{1/2}} u \exp -u^2$$

(Luikov, 1968, p. 652) one obtains the following integral, from which Equation (11) is derived:

$$\int_0^L \mathrm{i\,erfc}(u)\,\mathrm{d}z = \frac{u_{L,T}}{L}[\mathrm{i}^2\,\mathrm{erfc}(0) - \mathrm{i}^2\,\mathrm{erfc}(u)].$$

Appendix B: Averaging the Quasi-Analytical Solution Over the Macro-Layer

Calculation of $\overline{\theta_L^{\mathrm{q.a.}}}(T) = 1/L \int_0^L \theta^{\mathrm{q.a.}}(z, T)\,\mathrm{d}z$, where L is the macro-layer's thickness: integrating $F(\theta)$ in z in Equation (13) yields

$$(q_0 - K_0)z = \int_0^z \frac{q - K_0}{F(\theta)}\,\mathrm{d}z. \tag{B.1}$$

Changing the integration variable from z to $\theta(z)$ (allowed because $\theta(z)$ is monotonous) then gives

$$(q_0 - K_0)z = \int_{\theta(z,T)}^{\theta(z=0,T)} \left[\frac{q - K_0}{F(\theta)}\frac{\partial z}{\partial \theta}\right] \mathrm{d}\theta.$$

An expression of $\partial\theta/\partial z$ can be drawn from Equation (7) as $\partial\theta/\partial z = [q - K(\theta)]/[-D(\theta)]$, whose introduction in the integral transforms it into

$$\int_{\theta(z,T)}^{\theta(z=0,T)} \frac{q - K_0}{F(\theta)} \frac{D(\theta)}{K(\theta) - q} \, \mathrm{d}\theta$$

$$= \int_{\theta(z,T)}^{\theta(z=0,T)} (q_0 - K_0) \left[\frac{D(\theta)}{K(\theta) - K_0 - F(\theta)(q_0 - K_0)} \right] \mathrm{d}\theta.$$

Introduction in Equation (B.1) gives

$$(q_0 - K_0)z = \int_{\theta(z,T)}^{\theta(z=0,T)} \frac{D(\theta)}{F(\theta) - \kappa(\theta)} \, \mathrm{d}\theta.$$

Furthermore, the mass balance implies

$$(q_0 - K_0)T = \int_0^{\infty} (\theta - \theta_0) \, \mathrm{d}z = \int_{\theta_0}^{\theta(z=0,T)} z \, \mathrm{d}\theta.$$

Integrating the latter yields an implicit equation giving $\theta(z = 0, T)$

$$(q_0 - K_0)^2 T = \int_{\theta_0}^{\theta(z=0,T)} \frac{(\theta - \theta_0) D(\theta)}{F(\theta) - \kappa(\theta)} \, \mathrm{d}\theta, \tag{B.2}$$

which can be solved with the approximation $F = \theta^*$. The latter relationship also allows to derive $\overline{\theta_L^{\text{q.a.}}}(T)$, since

$$\int_0^L \theta^{\text{q.a.}}(z, T) \, \mathrm{d}z = \theta_0 + (\theta(z = 0, T) - \theta_0) \int_0^L F \, \mathrm{d}z$$

with

$$\int_0^L F \mathrm{d}z = \frac{1}{q_0 - K_0} \times$$

$$\times \left(\int_{\theta(z=L,T)}^{\theta(z=0,T)(t)} \frac{D(\theta)}{L} \left[1 + \frac{K(\theta)}{(q_0 - K_0)(\theta^* - \kappa(\theta))} \right] \mathrm{d}\theta - K_0 \right).$$

The combination of the last two equations gives Equation (14).

In quasi steady-state conditions, the left-hand term in Equation (B.2), which is proportional to the infi ltrated volume, tends to be infi nite. It implies that the denominator in the fi nite integral of the right-hand term tends to be nil. One obtains

$$K(\theta_{\text{as.}}^{\text{q.a.}}) - K_0 = q(z) - K_0, \quad \forall z$$

and in particular for $z = 0$ $q_0 = K(\theta_{\text{as.}}^{\text{q.a.}})$, with $\theta_{\text{as.}}^{\text{q.a.}}$ being the asymptotic moisture content. It is uniform in the volume considered because $q(z) = q_0$, $\forall z$ (in steady-state conditions the mass balance equation (7) yields $\partial q/\partial z = 0$).

Acknowledgements

This work was supported by a graduate fellowship from the French Agency for Environment (ADEME) and the INRA to B. Gabrielle. Dr M. Vauclin and anonymous referees are acknowledged for helpful comments on the manuscript.

References

1. Addiscott, T. M. and Wagenet, R. J.: 1985, Concepts of solute leaching in soils: a review of modeling approaches, *J. Soil Sci.* **36**, 411–424.
2. Baize, D.: 1988, *Guide des analyses courantes en pédologie*, INRA, Paris, pp. 121–122.
3. Boulier, J. F., Touma, J. and Vauclin, M.: 1984, Flux-concentration based quasi-analytical solution for constant flux infiltration: I. Non-pre and post-ponding infiltration into non-uniform initial profiles,*Soil Sci. Soc. Am. J.* **48**, 245–251.
4. Buttler, I. W. and Riha, S. J.: 1992, Water fluxes in oxisols: a comparison of approaches, *Water Resour. Res.* **28**, 211–229.
5. Comerma, J., Guenni, L. and Medina, G.: 1985, Validacion del balance hidrico del modelo Ceres-Maiz en la zona de Maracay, estado Aragua – Venezuela, *Agronomia Tropical* **35**, 115–132.
6. Diekkrüger, B., Söngerath, D., Kersebaum, K. C. and McVoy, C. W.: 1995, Validity of agroecosystem models. A comparison of results of different models applied to the same data set, *Ecol. Modelling* **81**, 3–29.
7. Emerman, S. H.: 1995, The tipping bucket equations as a model for macropore flow, *J. Hydrol.* **171**, 23–47.
8. Gabrielle, B., Menasseri, S. and Houot, S.: 1995, Analysis and field-evaluation of the CERES models' water balance component, *Soil Sci. Soc. Am. J.* **59**, 1402–1411.
9. van Genuchten, M. T.: 1980, A closed form equation for predicting the hydraulic conductivity of unsaturated soils, *Soil Sci. Soc. Am. J.* **44**, 892–898.
10. Luikov, A. V.: 1968, *Analytical Heat Diffusion Theory*, Academic Press, New York.
11. Ratliff, L. F., Ritchie, J. T. and Cassel, D. K.: 1983, Field-measured limits of soil water availability as related to laboratory measured properties, *Soil Sci. Soc. Am. J.* **47**, 770–775.
12. Ritchie, J. T.: 1985, A user-oriented model of the soil water balance in wheat, In: W. Day and R. K. Atkin (eds), *Wheat Growth and Modelling*, NATO-ASI Series, Plenum, New York, pp. 293–305.
13. Ritchie, J. T. and Crum, J.: 1989, Converting soil survey characterization data into IBSNAT crop model input, In: J. Bouma and A. K. Bret (eds), *Land Qualities in Space and Time*, Pudoc Wageningen, The Netherlands, pp. 156–167.
14. Ross, P. J.: 1990, Efficient numerical methods for infiltration using Richard's equation,*Water Resour. Res.* **26**, 279–290.
15. Vachaud, G., Vauclin, M. and Addiscott, T. M.: 1990, Solute transport in the Vadose zone: a review of models, *Proc. Int. Symp. on Water Quality Modeling of Agricultural Non-point Sources*, USDA-ARS Publ. 81, vol. 1, pp. 81–104.
16. White, I.: 1979, Measured and approximate flux-concentration relationships for absorption of water by soil, *Soil Sci. Soc. Am. J.* **43**, 1074–1080.

Agronomie 22 (2002) 000–000

DOI: 10.1051/agro: 2002003

Original article

A priori parameterisation of the CERES soil-crop models and tests against several European data sets

Benoit GABRIELLE[a,*], Romain ROCHE[a], P. ANGAS[b], C. CANTERO-MARTINEZ[b], L. COSENTINO[c], M. MANTINEO[c], M. LANGENSIEPEN[d], Catherine HÉNAULT[e], Patricia LAVILLE[a], Bernard NICOULLAUD[f], Ghislain GOSSE[a]

[a] UMR Environnement et Grandes Cultures, Institut National de la Recherche Agronomique, Thiverval-Grignon, France
[b] Dept. of plant production, Univ. of Lleida, Spain
[c] Institute of agronomy, Univ. of Catania, Italy
[d] Department of Agricultural Sciences, Univ. of Kiel, Germany
[e] Laboratoire de Microbiologie des Sols, Institut National de la Recherche Agronomique, Dijon, France
[f] Unité de Science du sol, Institut National de la Recherche Agronomique, Ardon, France

(Received 19 February 2001; revised 30 July 2001; accepted 2 October 2001)

Abstract – Mechanistic soil-crop models have become indispensable tools to investigate the effect of management practices on the productivity or environmental impacts of arable crops. Ideally these models may claim to be universally applicable because they simulate the major processes governing the fate of inputs such as fertiliser nitrogen or pesticides. However, because they deal with complex systems and uncertain phenomena, site-specific calibration is usually a prerequisite to ensure their predictions are realistic. This statement implies that some experimental knowledge on the system to be simulated should be available prior to any modelling attempt, and raises a tremendous limitation to practical applications of models. Because the demand for more general simulation results is high, modellers have nevertheless taken the bold step of extrapolating a model tested within a limited sample of real conditions to a much larger domain. While methodological questions are often disregarded in this extrapolation process, they are specifically addressed in this paper, and in particular the issue of models a priori. We thus implemented and tested a standard procedure to parameterize the soil components of a modified version of the CERES models. The procedure converts routinely-available soil properties into functional characteristics by means of pedo-transfer functions. The resulting predictions of soil water and nitrogen dynamics, as well as crop biomass, nitrogen content and leaf area index were compared to observations from trials conducted in five locations across Europe (southern Italy, northern Spain, northern France and northern Germany). In three cases, the model's performance was judged acceptable when compared to experimental errors on the measurements, based on a test of model's root mean squared error (RMSE). Significant deviations between observations and model outputs were however noted in all sites, and could be ascribed to various model routines. In decreasing importance, these were: water balance, the turnover of soil organic matter, and crop N uptake. A better match to field observations could therefore be achieved by visually adjusting related parameters, such as field-capacity water content or the size of soil microbial biomass. As a result, model predictions fell within the measurement errors in all sites for most variables, and the model's RMSE was within the range of published values for similar tests. We conclude that the proposed a priori method yields acceptable simulations with only a 50% probability, a figure which may be greatly increased through a posteriori calibration. Modellers should thus exercise caution when extrapolating their models to a large sample of pedo-climatic conditions for which they have only limited information.

soil-crop models / water balance / nitrogen dynamics / extrapolation

Communicated by Daniel Wallach (Castanet-Tolosan, France)

Correspondence and reprints
Benoit.Gabrielle@grignon.inra.fr

Résumé – titre en français ? . Les modèles déterministes de simulation des systèmes sol-plante sont un outil puissant et parfois exclusif pour étudier l'effet des pratiques culturales sur la productivité et les impacts environnementaux des cultures. Parce qu'ils simulent les principaux phénomènes en jeu, ces modèles peuvent en principe être appliqués à tous types de situations agronomiques ou pédo-climatiques. Dans la pratique cependant, un calage local des paramètres de fonctionnement du système sol-culture s'avère nécessaire. Cette étape constitue un frein à l'extrapolation des modèles qui est trop souvent négligé par les modélisateurs. Dans cet article nous abordons la question sous-jacente à l'extrapolation de l'estimation a priori des paramètres des modèles en testant une procédure standardisée pour les modèles CERES. La vraisemblance des jeux de paramètres ainsi inférés est évaluée en confrontant des résultats de simulation avec des observations issus d'un réseau d'essais sur 5 sites Européens (sud de l'Italie, nord de l'Espagne, nord de la France, nord de l'Allemagne). Sur trois sites, l'erreur commise par CERES s'est avérée comparable à celle sur les mesures. Des écarts significatifs ont toutefois été notés pour différentes variables de sortie sur tous les sites. Ils ont pu être attribués à la simulation du bilan hydrique, de la matière organique du sol ou de l'absorption d'azote par la culture, et corrigés en partie par un ajustement des paramètres en jeu. Nous concluons que la méthode de paramétrisation proposée a une probabilité de seulement 50 % d'aboutir à des résultats réalistes, et que CERES n'a pas pu s'adapter à toutes les situations testées dans sa forme actuelle. L'extrapolation d'un modèle sur un large domaine de conditions pédo-climatiques nécessite donc beaucoup de précautions.

modèles sol-culture / paramétrisation / bilan hydrique / bilan azoté / cycle de l'azote / extrapolation

1. INTRODUCTION

Deterministic models of soil-crop systems have become indispensable tools to generalise results obtained locally under particular field conditions, whether agronomic or studies. In many instances they even play an exclusive role because direct experimental monitoring is too costly to be carried out under a wide range of pedoclimatic conditions. Examples of model applications on a large scale (whether time or space) include: regional and national inventories [12, 27, 36], the impact of climate change [10, 30], integrative assessment of agricultural practices [28, 41], land-use change scenarios [27, 33], or precision agriculture [32].

Because they simulate the major processes occurring within the bio-geochemical cycles of interest, such models may claim to be universally applicable. However, because they deal with complex systems and uncertain phenomena, site-specific calibration is usually a prerequisite to ensure realistic predictions [7, 15, 16]. This obviously hampers a priori extrapolation of the model to other sites, which is of prime importance in the abovementioned applications.

There are two major reasons for which model extrapolation may fail: (i) the model's structure (i.e. its set of equations) does not apply to the particular soil type, climatic conditions or agricultural practices tested, or (ii) the model is supplied with incorrect values. When faced with a failure of the model, users commonly try the second route (parameter fitting) before taking the 'structural' route. For instance, Quemada and Cabrera [29] modified the crop residues decomposition routine of CERES after realising that, even when provided with laboratory-obtained decay rates for the residues CERES could not mimic them in the field. However, in many instances it is difficult to decide between the effect of wrong values and that of unfit model structure, because both have a similar influence on the outcome of prediction. Previous comparison studies in which several N models were tested against independent data sets showed that models achieved various degrees of success, and that their errors could be attributed to both causes [6, 8, 20]. Thus, the issue of their errors remained to be investigated per se. One problem with isolating the role of supplied values is that different models will use sets of parameters variable in nature and definition. To overcome this, Gabrielle et al. [15] proposed comparing models using the same basic information on soil and crop characteristics. They reached the conclusion that the effect of values was predominant over that of structure for three models of varying complexity, albeit for a single site in France. This paper therefore focuses on the issue of estimating correct values when extrapolating models to sites with contrasting climate and soil characteristics.

Usually, model extrapolation follows a test phase involving only a few sets of management / soil / climate conditions compared to the number of combinations considered in the extrapolation. The sizes of the test and extrapolation samples typically follow a ratio of 1 to 100 [4, 31, 38]. Higher ratios are usually associated with the prediction of more limited sets of s. For instance, the size of the inert organic matter pool in the RothC model was assessed based on 28 different data sets worldwide [11], prior to extrapolation to 275 representative soil profiles occurring in Central Hungary [12].

This trade-off between the size of the test sample and the number of parameters addressed originates from the high number of parameters involved in soil-crop models and the scarcity of data to estimate them. Even though

parameters may be screened a priori through sensitivity analyses [25, 39], the remaining set commonly comprises parameters relevant to various routines within the model (e.g., water balance, N turnover or crop phenology). Several categories are thus seldom dealt with simultaneously. Within a given category of s, it is in addition a general rule that the prediction of parameters is disconnected from model evaluation. This applies to the body of literature on pedo-transfer [2], with the notable exception of the 'functional' approach to water balance simulation in The Netherlands [40].

In this paper, we address the above limitations to model extrapolation by testing an a priori procedure under a wide range of conditions in Europe. The network of trials covers a broad climatic gradient, extending from southern Italy to northern Germany, and a range of soil types. As to the procedure, it converts routinely-available soil properties (particle-size distribution, gravel content, bulk density, total soil carbon and nitrogen content) into functional characteristics involved in the simulation of water movement and soil biological transformations (Gabrielle et al., unpublished data).

Our primary objective was thus to assess the reliability of a soil-crop model in a case where no data are available to calibrate model s. In a second step, the model prediction errors, as revealed by the comparison against field-observations, were analysed and corrected by tuning the parameters associated with the processes responsible for the discrepancies. This adjustment aimed at quantifying the distance between the a priori set and the resulting quasi-optimal set.

2. MATERIALS AND METHODS

The steps involved in testing the procedure a priori in the various sites are diagrammed in Figure 1, and described in the paragraphs below.

2.1. Model description and parameterisation

CERES comprises sub-models for the major processes governing the cycles of water, carbon and nitrogen in soil-crop systems. A physical module simulates the transfer of heat, water and nitrate down the soil profile, as well as soil evaporation, plant water uptake and transpiration in relation to climatic demand. Water infiltrates down the soil profile following a tipping-bucket approach, and may be redistributed upwards after evapotranspiration has dried some soil layers. In both of these equations, the generalised Darcy's law has subsequently been introduced in order to better simulate water dynamics in fine-textured soils [16].

Next, a microbiological module simulates the turnover of organic matter in the plough layer, involving both an immobilisation of inorganic N, along with the

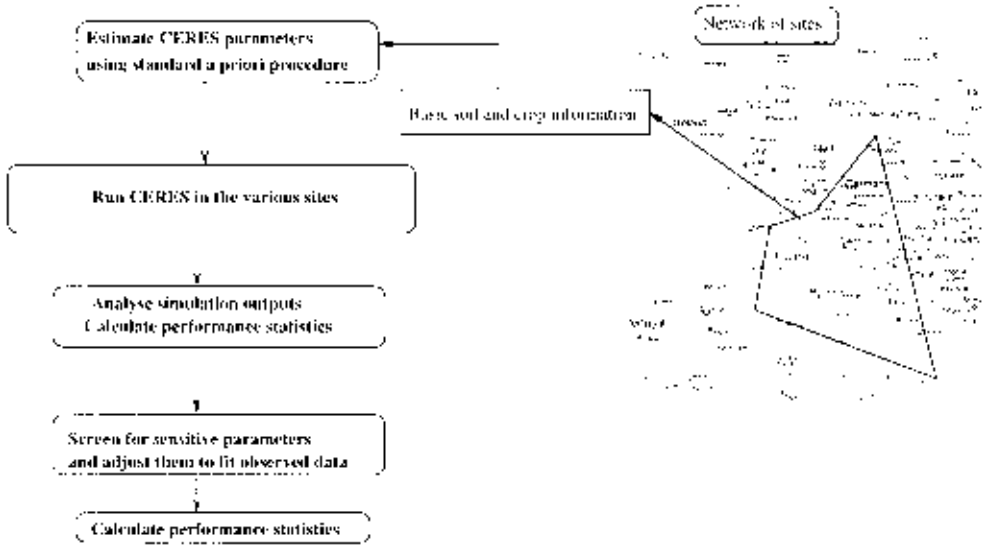

Figure 1. Diagram of the parameterisation and evaluation steps of the CERES model.

transformations of inorganic N (denitrification and nitrification). In this version, the NCSOIL model [26] was substituted for the original module. NCSOIL comprises three OM pools, decomposing at a fixed rate and recycling into the microbial biomass. Nitrification and denitrification follow zero-order kinetics, which are modulated by soil temperature and water content.

Lastly, crop net photosynthesis is a linear function of intercepted radiation according to the Monteith approach, with interception depending on leaf are index based on Beer's law of diffusion in turbid media. Photosynthates are partitioned on a daily basis to currently growing organs (roots, leaves, stems, fruit) according to crop development stage. The latter is driven by the accumulation of growing degree days, as well as cold temperature and day-length for crops sensitive to vernalisation and photoperiod. Lastly, crop N uptake is computed through a supply/demand scheme, with soil supply depending on soil nitrate and ammonium concentrations and root length density. Crop demand is a function of the distance between actual and critical nitrogen content in the aerial and below-ground tissues. Critical nitrogen is defined as the optimum concentration for biomass production, as evidenced from field studies for various crops [5, 23]. It a decreasing power function of crop dry matter.

CERES runs on a daily time step, and requires daily rain, mean air temperature and Penman potential evapotranspiration as forcing variables. The models are available for a large number of crop species, which share the same soil components. Readers may refer to [22] for a more complete description of CERES.

The soil parameters of CERES which were deemed site-specific pertained to either the water balance or biological transformation routines. The former category includes: wilting point, field-capacity and saturation water contents, saturated hydraulic conductivity (layer-wise), and two coefficients describing the water retention and hydraulic conductivity curves. These parameters were calculated from soil properties (namely particle-size distribution, bulk density and organic matter content) by means of several pedo-transfer functions [9, 22, 37].

Soil biological transformation amounts to breaking down the total soil organic matter (SOM) present in the plough layer into several pools featuring distinct decomposition rates and C: N ratios. Within NCSOIL, the SOM sub-model in our version of CERES, the pools comprise: crop residues, microbial biomass, actively decomposing humus and 'passive' humus. Here, we used the breakdown and pool settings proposed by [19], which is dependent on carbon management. More information on the parameters and their calculation may be found on the Internet at *http://www-egc.grignon.inra.fr/ecobilan/cerca/intjavae.htm*, where the estimation procedure has been implemented within an on-line front-end.

As regards the crop growth component of CERES, cultivar-related parameters were either derived from the DSSAT v3 database of varieties [18], calibrated against field observations of phenological development, or based on the dynamics of DM accumulation in the various plant compartments.

2.2. Field data

The trials were conducted in four European countries and included four crop species (Tab. I). Experiments

Table I. Selected data for the field experiments used to test the parameterisation of CERES.

Location	Soil type	Crop management	Year	Reference
Châlons-en-Champagne, France	Hypercalcareous rendosol	Winter rapeseed	1994–95	[17]
Treatments: 3 fertiliser N rates: 0, +135 and +270 kg N·ha^{-1}, and a bare control				
Kiel, Germany	Luvisol	Winter rapeseed	1994–95	[24]
Treatments: 3 fertiliser N rates: 0, +120 and +240 kg N·ha^{-1}				
Villamblain, France	Calcisol	Winter wheat	1998–99	Unpublished
Treatments: 1 fertiliser N rate: +220 kg N·ha^{-1}				
Candasnos, Spain	Calcisol	Winter barley	1996–97	Unpublished
Treatments: 3 fertiliser N rates: 0, +50 and +100 kg N·ha^{-1}				
Barrafranca, Italy	Regosol	Sorghum (Fibre and sweet varieties)	1997	[13]
Treatments: 2 fertiliser N rates: +100 and +120 kg N·ha^{-1}				

were set up in replicate blocks in all sites except at the Kiel site which had no replicates. Soil and crops were sampled every one to three months, and standard weather data as required by CERES were taken from meteorological stations located within 1 km of the experiments. In Candasnos, the solar radiation data were from a station 20 km from the site.

Soil was sampled to a depth of 60 to 120 cm by hand or using automatic augers, in 3 to 8 replicates which were pooled layer-wise in ten to thirty-cm increments. Soil samples were analysed for moisture content and inorganic N using colorimetric methods. In Candasnos, test strips were used for nitrate determination after a comparison with standard colorimetric techniques showed a good agreement between both methods. In Barrafranca, soil nitrate was monitored through its concentration in soil water using suction cups.

Individual plants were sampled in each block over areas of 0.25 to 1.00 m^2, and subsequently separated into leaf, stem, ear (or panicle) and grain compartments. When monitored, leaf area index was measured using an optic area-meter, after which biomass samples were oven-dried for two days for dry matter determination. Lastly, biomass N content was analysed using combustion or digestion techniques except in trials where this variable was not monitored.

2.3. Model evaluation

The simulations of CERES were compared to field observations (means and standard deviations of the replicates) using graphics to capture dynamic trends, and statistical indicators gave an idea of the model's mean error. We used two standard criteria [34]: the mean deviation (MD) and the root mean squared error (*RMSE*). Here, they are defined as: $MD=E\ (Si - Oi)$ and $RMSE=(E\ [(Si - Oi)^2])^{1/2}$, where *Si* and *Oi* are the time series of the simulated and observed data, and *E* denotes the expectancy. *MD* indicates an overall bias with the predicted variable, while *RMSE* quantifies the scatter between observed and predicted data, which is readily comparable with the error on the observed data. The significance level of both statistics was also determined, based on the standard deviations of the observed data [34]. *RMSE* was thus compared with the average measurement error, calculated as: $RMSE_{ERR}=(E\ [\sigma_i^2])^{1/2}$, where σ_i denotes the standard deviation over replicates for sampling date number *i*.

2.4. Model calibration

When discrepancies between model predictions and field-observations occurred, their source was sought stepwise according to heuristic knowledge on the workings of the model. Errors were assumed to propagate from physical to chemical and biological processes. Therefore, we first checked the simulation of soil temperature and water balance, and then soil nitrate movement, crop dry matter accumulation and nitrogen uptake. The parameters associated with the routine appearing to cause the deviations were visually adjusted by trial-and-error, by looking at comparison charts (see Fig. 2 for an example).

Prior to fitting, a large sample of parameters were screened on the basis of the sensitivity of model deviations to their variations. The total set of parameters considered is presented in Appendix 1.

3. RESULTS

3.1. Model performance a priori

When parameterised a priori, CERES achieved an acceptable accuracy in a majority of sites and for most of the variables tested (Tab. II, and Figs. 2 to 6). This may be judged from the fact that in those cases the model's RMSE fell within the experimental error on the measurements with a 95% to 98% probability. At Kiel, observed standard deviations were not available, but the performance indicators were still within the range of published values for other models undergoing similar tests. Cited ranges for model RMSEs include: 0.02–0.08 $cm^3 \cdot cm^{-3}$ for water content, 10–40 kg $N \cdot ha^{-1}$ for topsoil nitrate content [8], for several models in Germany); 0.8 tons of dry $matter \cdot ha^{-1}$ for crop biomass, 0.60 $m^2 \cdot m^{-2}$ for LAI, and 14 kg $N \cdot ha^{-1}$ for crop N uptake [1], with the APSIM model in Australia); 3.4–3.9 $tons \cdot ha^{-1}$ for crop biomass and 1.26–1.7 for LAI [3], with CERES-Maize in Italy). Thus, there was only one site (Candasnos) in which CERES could be rejected with its default parameterisation.

As regards individual variables, there were no consistent patterns across sites for those that CERES failed to predict correctly. Significant deviations occurred for all the variables in at least one of the sites, and no particular routine could be singled out as intrinsically at fault. Crop nitrogen was the most difficult to simulate, with no

Table II. Statistical indicators for the goodness of fit of CERES in the simulation of soil and crop variables in the various European sites. MD and RMSE stand for the model's mean deviation and root mean squared error, respectively, and were calculated for the baseline and calibrated scenarios. The hypothesis that MD is zero was tested using a two-tailed t-Test ($p = 0.95$). RMSE values were compared with the mean standard deviation of the measurements ($RMSE_{ERR}$, see text). The hypothesis that model and experimental errors were equivalent was tested at two levels ($p = 0.95$ and $p = 0.98$).

Statistics	Leaf area index $m^2 \cdot m^{-2}$	Tops dry matter $tons \cdot ha^{-1}$	Tops nitrogen $kg\ N \cdot ha^{-1}$	Soil moisture $m^3 \cdot m^{-3}$	Soil nitrate $kg\ N \cdot ha^{-1}$
Châlons					
N[b]	45	45	45	192	192
RMSE, baseline	0.956	1.42*	30.284	0.036*	5.729**
MD, baseline	0.577	–0.876	7.417	–0.035	1.205
RMSE, calibrated	0.985	1.391*	40.977	0.042	6.968**
MD, calibrated	0.625	–0.779	–6.485	–0.007	1.53
Villamblain					
N	6	6	6	18	18
RMSE, baseline	1.05**	2.415**	27.162**	0.051	10.304**
MD, baseline	1.416	–1.71	25.303	–0.024	–8.876
RMSE, calibrated	0.945**	2.409**	34.725**	0.025	10.82**
MD, calibrated	0.196	–1.702	40.503	0.03	–4.99
Kiel	NA[a]	12	11	18	18
N					
RMSE, baseline	NA	0.517	13.299	0.036	3.959
MD, baseline	NA	0.498	–19.184	–0.035	–2.322
RMSE, calibrated	NA	0.957	54.069	0.032	3.198
MD, calibrated	NA	1.579	–4.998	–0.016	–3.905
Barrafranca					
N	18	18	18	75	66
RMSE, baseline	1.269**	3.756**	21.904**	0.081**	12.68**[c]
MD, baseline	–0.64	–2.973	–14.997	–0.006**	3.433
RMSE, calibrated	1.57**	2.045**	29.156**	0.082**	8.85**
MD, calibrated	0.11	1.15	36.64	–0.002	–2.26
Candasnos					
N	24	24	NA[a]	63	45
RMSE, baseline	0.615	2.368	NA	0.059	10.754**
MD, baseline	0.413	–0.482	NA	0.024	–6.842
RMSE, calibrated	0.873	2.735	NA	0.058	12.971*
MD, calibrated	0.791	0.528	NA	0.022	1.429**

*, **: Significance levels for the tests that MD is zero and that RMSE are not different from mean experimental error (p=0.98 and p=0.95, respectively).
a: Not available.
b: Sample size.
c: In Barrafranca, nitrate is expressed in mg N-per litre of soil solution.

systematic trend of the model to overestimate or underestimate it. The only systematic error was the simulated peak in spring which lead to an overestimation of topsoil nitrate in Châlons, Candasnos and Villamblain (see Figs. 2, 4 and 6).

The extent to which the match against observed data improved through the calibration procedure varied from site to site, as may be seen by comparing the continuous and dashed simulation lines in Figures 2 to 6. Overall, most of the problems associated with the uncalibrated simulations tended to persist. Sorghum biomass was underestimated late in the season, due to a wrong timing of leaf senescence by CERES. In Châlons, although LAI dynamics were correctly simulated throughout the season, CERES underestimated final crop biomass and N content. During the second growing season in Candasnos, CERES over-predicted crop nitrogen and biomass, and the reason for it was unclear since similar discrepancies did not occur for soil water and nitrogen. Despite the change in the nitrification kinetics, CERES could not simulate the nitrate concentration peaks measured after fertiliser application (Fig. 2). It is likely that these discrepancies should be ascribed to a failure in some of the routines rather than to a wrong setting of their parameters. Thus, the statistical indicators of Table II may be considered as representing a structural limit of CERES in its current state, with the exception of Barrafranca where the parameterisation of leaf senescence should definitely be revised based on more thorough experimental work.

3.2. Model calibration for the various sites

In all situations, significant deviations occurred between simulated and observed data for at least one of the state variables monitored (Figs. 2 to 6).

The calibration procedure described in the Materials and Methods section was therefore undertaken to correct these biases. Its results are given in Table III, in terms of processes involved and associated parameters. Soil and crop water balance appeared to be the most critical routine, which is a logical consequence of the postulated error propagation scheme. Related parameters had to be adjusted in most sites, to improve the simulation of either downward water movement (through the field-capacity water content) or root uptake of water and nitrogen. The former process predominated under temperate climates (in the northern sites), whereas the latter prevailed under semi-arid conditions. This distinction illustrates the influence of climate type on model performance, through its effect on model sensitivity to the parameters of its various routines.

Conversely, little could be done to improve the simulation of soil N turnover. Related observed data (measurements of topsoil inorganic N) were either too infrequent over the season (in Kiel or Barrafranca), or the model was not sensitive to the associated parameters (Villamblain). In Châlons, a numerical optimisation of these parameters led to a set of values close to the default set used [14], prompting us to keep the latter. The Spanish site (Candasnos) turned out to be the exception to this rule, with simulations of topsoil nitrate improving when the size of the microbial biomass was increased from 0.9 to 2.3% of total soil carbon. With the default parameterisation, the low C:N ratio of soil organic matter resulted in high levels of simulated immobilisation of inorganic nitrogen and a systematic underestimation of topsoil nitrate.

Apart from those setting the duration of crop development phases whose effect could be readily assessed, crop parameters were deemed too numerous and their structure too complex to be calibrated against our limited sets

Table III. Calibrated parameters for the various experiments simulated with CERES.

Location of experiment	Parameter names	Unit	Fitting variable	Associated routines
Kiel	Field-capacity	$cm^3 \cdot cm^{-3}$	Soil water profile	Water balance
Châlons	Field-capacity	$cm^3 \cdot cm^{-3}$	Soil water profile	Water balance
	Initial size of microbial biomass	mg $C \cdot kg^{-1}$ soil	Topsoil nitrate	Turnover of SOM
Villamblain	Field-capacity	$cm^3 \cdot cm^{-3}$	Soil water profile	Water balance
	Sensitivity to cold temperatures	Unitless	Crop dry matter	Crop phenology
Barrafranca	Sensitivity of root extraction of N to water stress	Unitless	Crop N content	Crop N uptake
Candasnos	Initial size of microbial biomass	mg $C \cdot kg^{-1}$ soil	Topsoil nitrate	Turnover of SOM

of observations. In some instances this conservative option caused important biases. Most notably, simulated leaf senescence began too early at Barrafranca and Villamblain. There might have been some interference of model errors in the simulation of crop growth with the calibration procedure. Indeed, we focused on the sole soil parameters in the calibration and we adjusted them to variables which may have been influenced by crop processes and associated parameters. However, the fact that model errors on crop growth occurred late in the season supports our underlying assumption that they did not impact the calibration of soil parameters.

Lastly, in one site (Villamblain) we decided to alter the nitrification equation by substituting the zero-order kinetics with a first-order scheme. Only through this modification could the dynamics of nitrate and ammonium be simulated within the range of concentrations observed (Fig.?). This choice was in accordance with other similar models [21], but nevertheless goes somewhat beyond the scope of this paper.

3.3. Performance of the calibrated model

It is noteworthy that in the calibrated scenarios the accuracy of CERES did not improve greatly, overall. In many instances, the improvement for one variable resulted in a decreasing accuracy for the other variables. For example, fitting the crop biomass data in Barrafranca caused greater errors in the simulation of crop nitrogen. In Châlons, the visual calibration of microbial biomass against topsoil nitrate data was even associated with a higher RMSE than with the baseline set. This illustrates the limits of such a fitting procedure, although we favoured it because it relates to processes more directly than numerical adjustments do. Another rationale for that

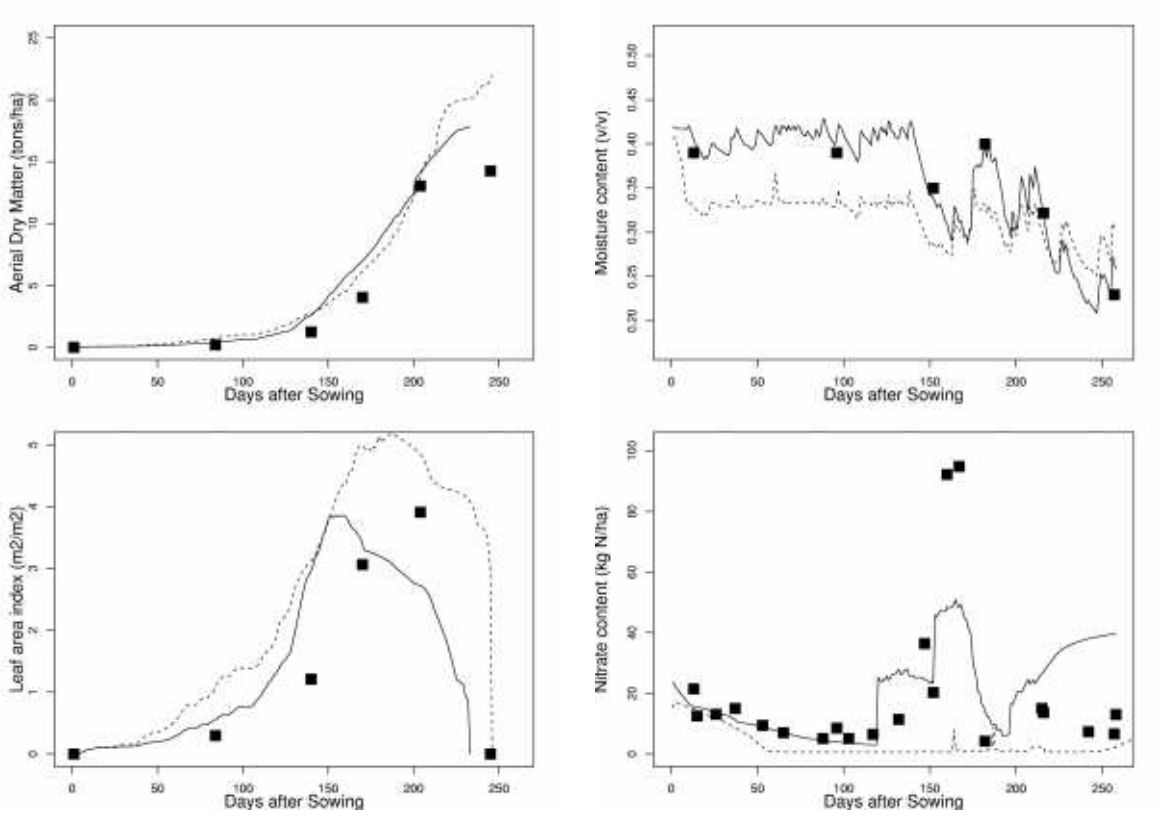

Figure 2. Simulated (lines) and observed (symbols) time course of leaf area index and aerial dry matter (left) and surface (0–30 cm) moisture and nitrate content (right) for the winter wheat crop in Villamblain**.** The simulation lines are dashed for the baseline parameterisation, and solid for the calibrated parameter set.

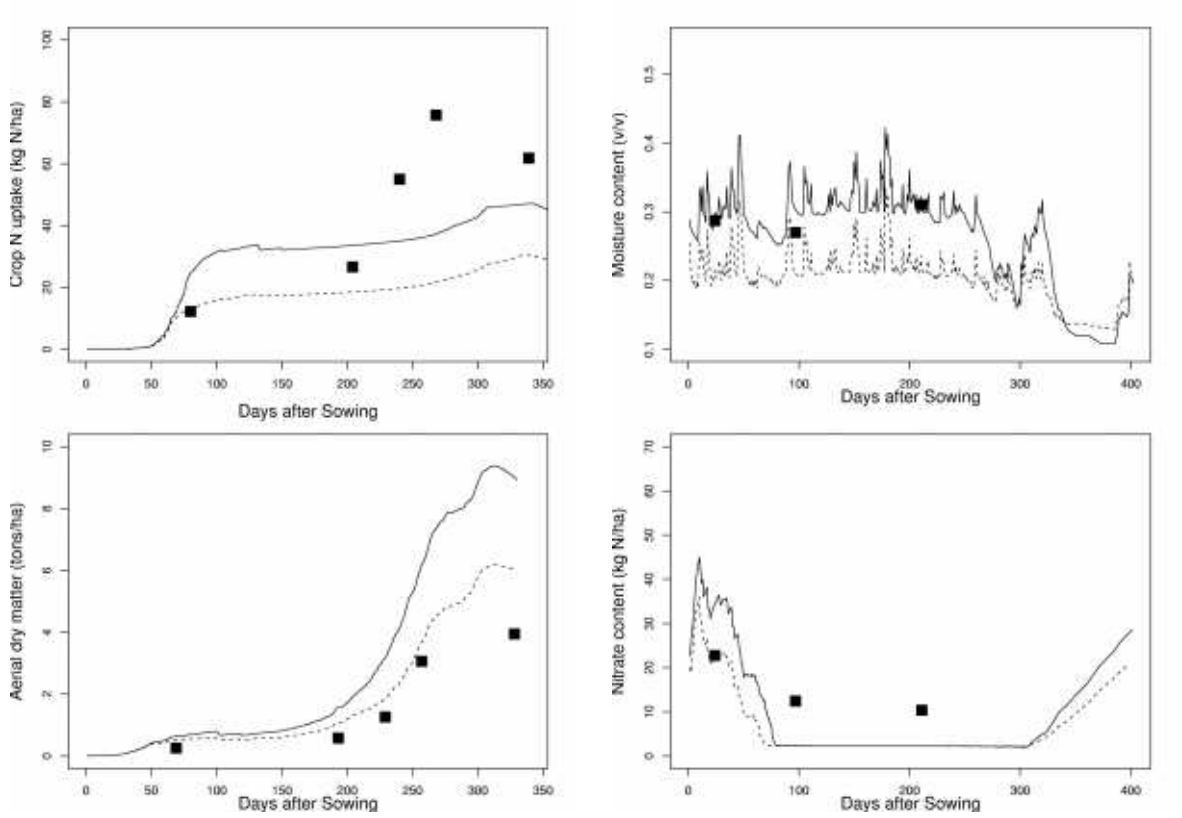

Figure 3. Simulated (lines) and observed (symbols) time course of surface (0–30 cm) soil moisture and nitrate content (right) and crop dry matter and nitrogen uptake (left) for the unfertilised control crop in Kiel**.** The simulation lines are dashed for the baseline parameterisation, and solid for the calibrated parameter set.

is the fact that CERES was poorly sensitive to some of its parameters, probably because it involves too many of them compared to the total number of model outputs. This makes the fitting of one parameter against one variable dependent on a number of other parameters.

4. DISCUSSION

In this extrapolation exercise, a first conclusion may be that a priori parameterisation resulted in a reasonable accuracy of CERES since its error proved acceptable in more than half of the cases tested. Thus, the procedure proposed should be considered as having a 50% probability of yielding acceptable values when employed in a new situation.

For the remaining cases, two routes may be investigated to explain the failure of CERES, as suggested in the introduction. Either the principles and equations within CERES were inadequate for the particular site considered, or the structure applied but model parameters were poorly estimated by the standard procedure. Of the two routes, we only investigated the parameterisation one here, assuming it was responsible for most of the discrepancies observed.

Calibration of the parameters which were detected as causing the discrepancies yielded slightly more acceptable simulations, with model error falling below experimental error for about 70% of tested variables in all sites. However, despite numerous attempts involving a dozen parameters, model calibration could not correct some of the deviations observed, such as the erroneous simulated spring peak in Châlons. One could object that only a thorough, multi-variable search of the minimum model

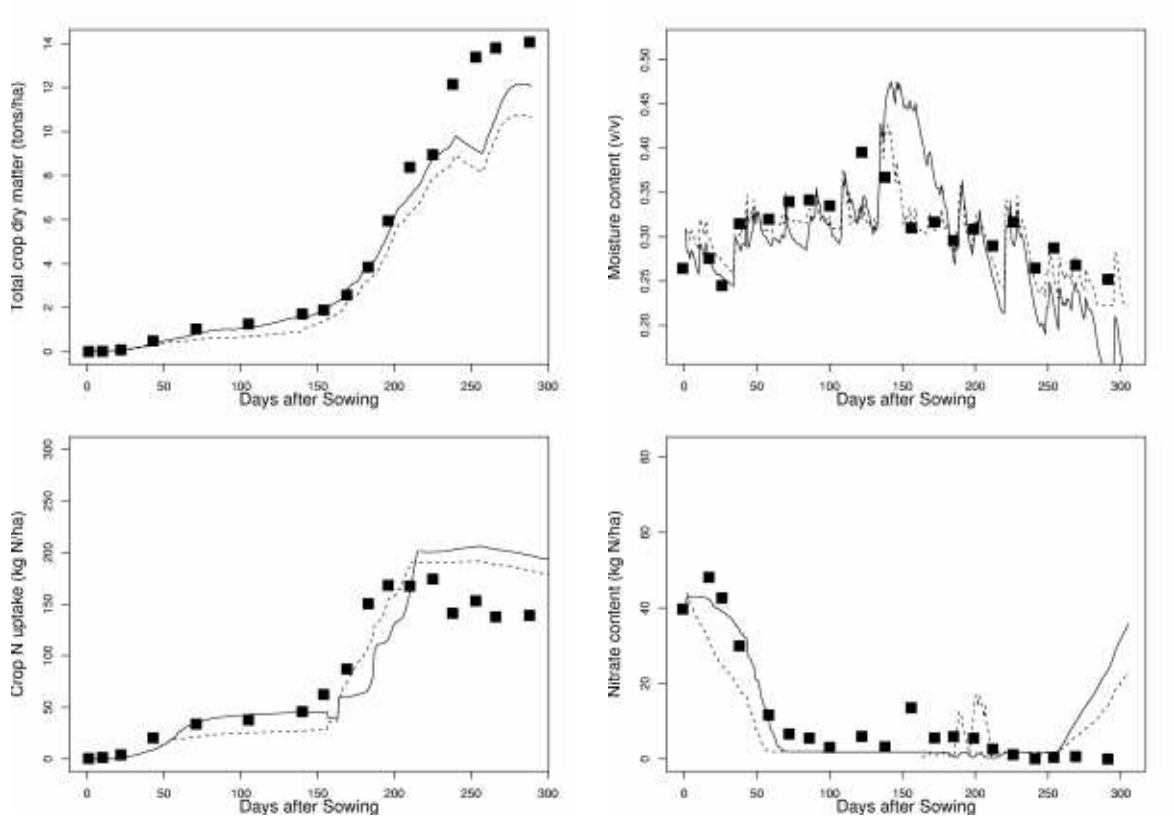

Figure 4. Simulated (lines) and observed (symbols) time course of total crop dry matter and nitrogen uptake (left) and surface (0–30 cm) soil moisture and nitrate content (right) for the moderately-fertilised winter oilseed rape crop in Châlons. The simulation lines are dashed for the baseline parameterisation, and solid for the calibrated parameter set.

error in its parameter space (through numerical optimisation techniques) would have enabled us to rule out parameterisation in the failure of CERES. In this work, however, we did not make use of such rigorous methods since they have proved difficult to apply to soil-crop models. These are indeed complex, highly non-linear and involve too many parameters to allow the automatic search of a global optimum [39]. If we trust that our 'expert-guess' calibration yielded results close to the true statistical optimum of the model, two conclusions arise: (i) the a priori error of CERES is close to its structural (calibrated) error, since the performance indicators of Table II differ by at most 30%; however, (ii) in a minority of cases the structural error is too large and adjustments in model structure are warranted.

In future work on the role of structure vs. parameterisation in determining model accuracy a priori, two lines of work may be pursued. First, the influence of structure may be further investigated by comparing the performances of different models using the same basic information for parameter estimation. Previous work on model comparisons against the same data sets have shown that predictions vary greatly between models, or even between users for a given model, and that all models featured their own domains of validity [8, 35]. However, because they focused on the elusive issue of model validation rather than extrapolation they allowed some degree of site-specific calibration which prevents the identification of pure 'structure'-related effects. Comparison exercises where modellers would be forced to make use of a given set of soil and crop properties should therefore be encouraged. This would also help delineate the respective validity domains of models, which could be made use of by adjusting model structure to soil and

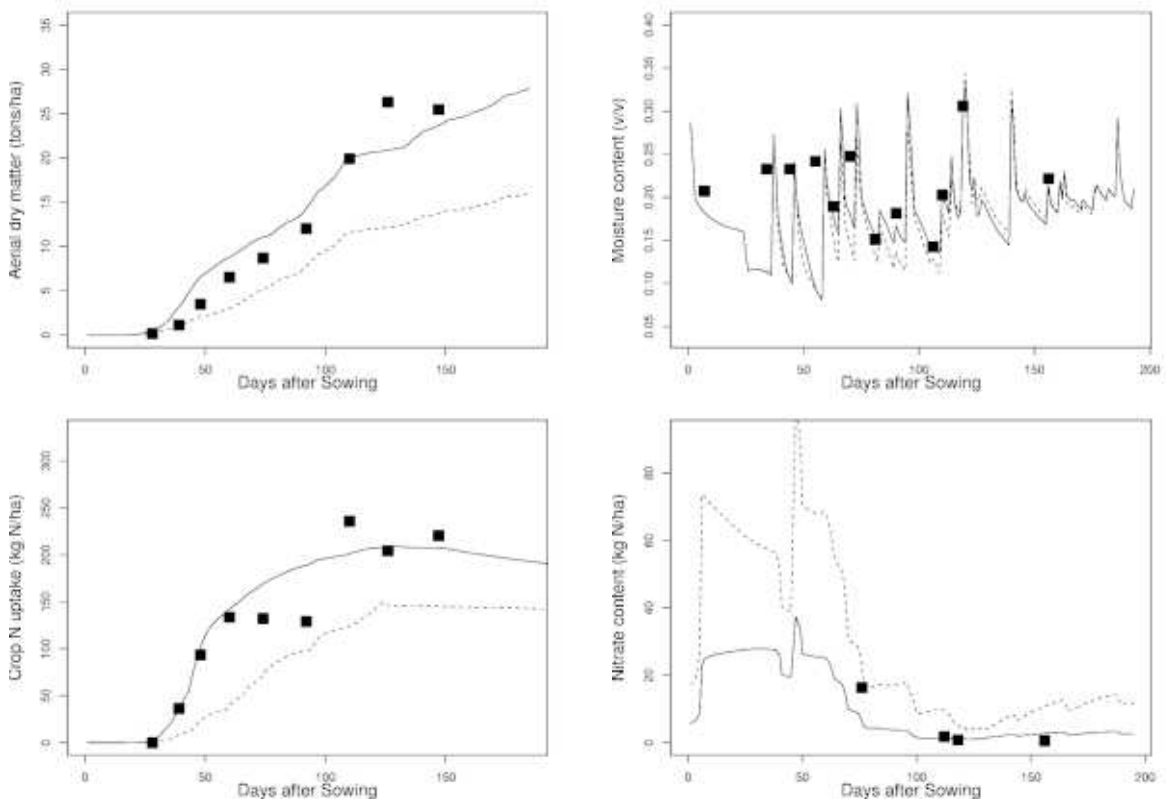

Figure 5. Simulated (lines) and observed (symbols) time course of total crop dry matter and nitrogen uptake (left) and surface (0–30 cm) soil moisture and nitrate content (right) for the moderately-fertilised sweet sorghum crop in Barrafranca. The simulation lines are dashed for the baseline parameterisation, and solid for the calibrated parameter set.

climate types based on a functional classification of the simulated systems.

Secondly, the outcome of various procedures (e.g., pedo-transfer functions) may be compared for a given model. Although it is known that such procedures are all the more relevant as they are applied to pedological conditions similar to those on which they were established [2], it would be interesting to check whether their predictions (input to the model as parameters) may be applied to new conditions.

Whatever the outcome of the above studies, there is a need to extrapolate the test presented in this paper to improve our confidence in large-scale model results. To facilitate the extension of such tests to a wide range of models and soil/crop conditions, we urge the community of model developers and users to organise itself so as to share both models, and data sets to test them.

Acknowledgements: The authors are indebted to the staff who contributed to the collection of the field data presented in this work. Special thanks are expressed to J.C. Germon (INRA, Dijon) who coordinated the research programme in Financial support from Gessol (French Environment Ministry), the EC FAIR project CT-96-1913 and the Comisión Interministerial de Ciencia y Tecnología (CICYT, contract AGF94-019) is acknowledged. We would also like to thank two anonymous reviewers for their valuable comments on the manuscript.

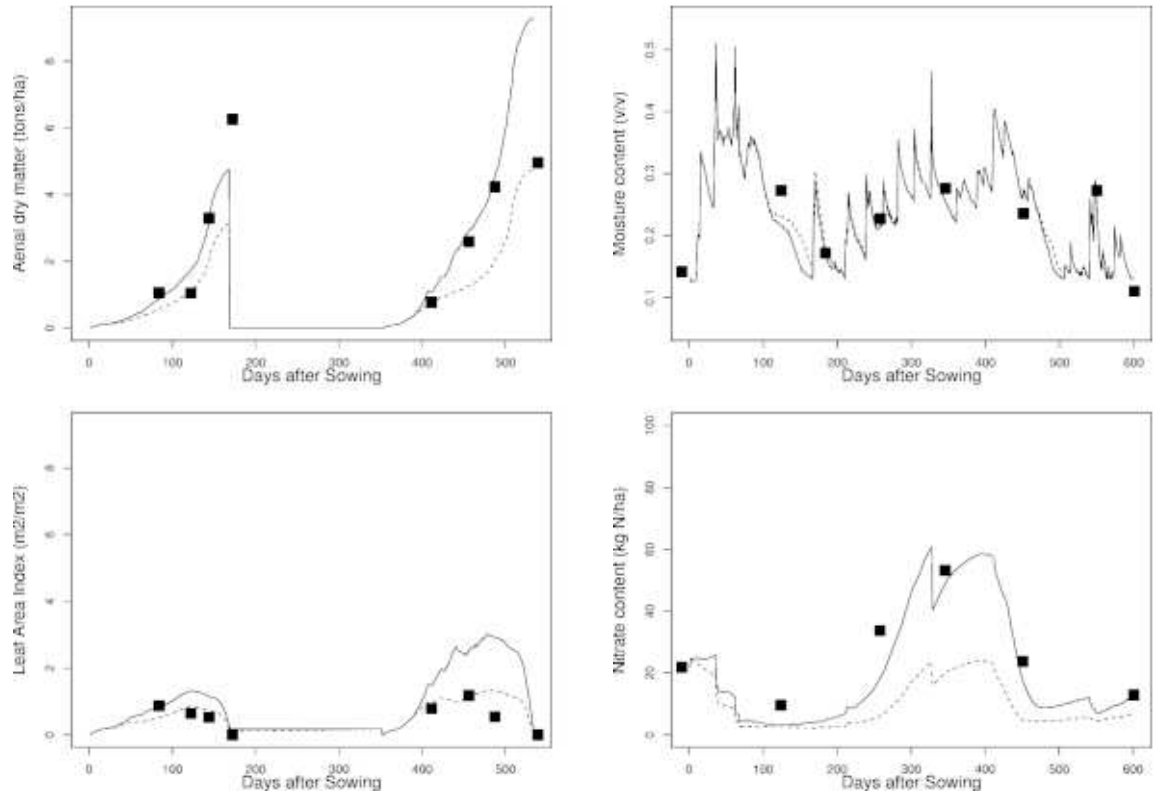

Figure 6. Simulated (lines) and observed (symbols) time course of crop aerial dry matter and nitrogen uptake (left) and surface (0–25 cm) soil moisture and nitrate content (right) for the non-fertilised winter barley crop in Candasnos. The simulation lines are dashed for the baseline parameterisation, and solid for the calibrated parameter set.

REFERENCES

[1] Asseng S., Keating B.A., Fillery I.R.P., Grogory P.J., Bowden J.W., Turner N.C., Palta J.A., Abrecht D.G., Performance of the APSIM-Wheat model in Western Australia, Field Crops Res. 57 (1998) 163–179.

[2] Bastet G., Bruand A., Quétin P., Cousin I., Estimation des propriétés de rétention en eau des sols à l'aide de fonctions de pédotransfert: une analyse bibliographique, Étude et Gestion des Sols 5 (1998) 7–28.

[3] BenNouna B., Katerji N., Mastrorilli M., Using the Ceres-Maize model in a semi-arid mediterranean environment. Evaluation of model performance, Eur. J. Agron. 13 (2000) 309–322.

[4] Chipanshi A.C., Ripley E.A., Lawford R.G., Large-scale simulation of wheat yields in a semi-arid environment using a crop-growth model, Agric. Syst. 59 (1999) 57–66.

[5] Colnenne C., Meynard J.M., Reau R., Merrien A., Determination of a critical N dilution curve for winter oilseed rape, An. Bot. 81 (1997) 311–317.

[6] DeWilligen P., N turnover in the soil-crop system: comparison of fourteen simulation models, Fertil. Res. 27 (1991) 141–149.

[7] Delécolle R., Travasso M.I., Adaptation of the CERES-Wheat model for large-area yield estimations in Argentina, Eur. J. Agron. 4 (1995) 347–353.

[8] Diekkrüger B., Söngerath D., Kersebaum K.C., McVoy C.W., Validity of agroecosystem models. A comparison of results of different models applied to the same data set, Ecol. Model. 81 (1995) 3–29.

[9] Driessen P.M., The water balance of soil, in: van Keulen H.,Wolf J. (Eds.), Modelling of agricultural production: weather, soils and crops, Pudoc, Wageningen, 1986, pp. 76–116.

[10] Ewert F., van Oijen M., Porter J.R., Simulation of growth and development processes of spring wheat in response to CO2 and ozone for different sites and years in Europe using mechanistic crop simulation models, Eur. J. Agron. 10 (1999) 231–247.

[11] Falloon P.D., Smith P., Coleman K., Marshall S., Estimating the size of the inert organic matter pool from total soil organic carbon content for use in the Rothamsted carbon model, Soil Biol. Biochem. 30 (1998) 1207–1211.

[12] Falloon P.D., Smith P., Smith J.U., Szabo J., Marshall S., Regional estimates of carbon sequestration potential: linking the

Rothamsted Carbon Turnover model to GIS databases, Biol. Fertil. Soils 27 (1998) 236–241.

[13] Foti S., Environmental studies on sweet and fibre sorghum, sunstainable crops for biomass and energy, 2nd annual report, EC contract FAIR CT96 – 1913, IACT, Università di Catania, Sicily, 1999.

[14] Gabrielle B., Modélisation des cycles des éléments eau-carbone-azote dans un système sol-plante, et application à l'estimation des bilans environnementaux des grandes cultures, Ph.D. dissertation, École Centrale, Paris, 1996.

[15] Gabrielle B., Angas P., Cosentino S., Mantineo M., Langensiepen M., Gosse G., Extrapolation of soil-crop models across Europe: is model structure still relevant compared to parameterization?, in: Donatelli M. et al. (Ed), Proc. 1st European Society For Agronomy Congress on Modelling cropping systems, 6/1999, Lleida, pp. 183–184.

[16] Gabrielle B., Menasseri S., Houot S., Analysis and field-evaluation of the CERES models' water balance component., Soil Sci. Soc. Am. J. 59 (1995) 1402–1411.

[17] Gosse G., Cellier P., Denoroy P., Gabrielle B., Laville P., Leviel B., Nicolardot B., Justes E., Mary B., Recous S., Germon J.C., Hénault C., Leech P.K., Water, carbon and nitrogen cycling in a rendzina soil cropped with winter oilseed rape: the Châlons Oilseed Rape Database, Agronomie 19 (1999) 119–124. (*http*: //www-egc.grignon.inra.fr/ecobilan/base/welcome.html, page viewed on 12 December 2001.)

[18] Hoogenboom G., Wilkens P.W., Tsuji G.Y., DSSAT v3, Volume 4, Univ. of Hawaï, Honolulu, Hawa, 1999.

[19] Houot S., Molina J. A.E., Chaussod R., Clapp C.E., Simulation by NCSOIL of net mineralization in soils from the Deherain 36 Parcelles plots at Grignon, Soil Sci. Soc. Am. J. 53 (1989) 451–455.

[20] Jamieson P.D., Porter J.R., Goudriaan J., Ritchie J.T., van Keulen H., van. Stol W., A comparison of the models Afrcwheat2, Ceres-Wheat, Sirius, Sucros2 and Swheat with measurements from wheat grown under drought, Field Crops Res. 55 (1998) 23–44.

[21] Johnsson H., Simulated nitrogen dynamics and losses in a layered agricultural soil, Agric. Ecosyst. Environ. 18 (1987) 333–356.

[22] Jones C.A., Kiniry, J.R. (Eds), CERESMaize: a simulation model of maize growth and development, Texas A&M University Press, College Station, Temple, TX, 1986.

[23] Justes E., Mary B., Meynard J.M., Machet J.M., Thelier-Huches L., Determination of a critical N dilution curve for winter wheat crops, Ann. Bot. 74 (1994) 397–407.

[24] Langensiepen M., Fuchs M., Bergamaschi H., Gräsle W., Scholberg J., Are crop models universally applicable?, in: Donatelli M. et al. (Eds), Proc. 1st European Society For Agronomy Congress on Modelling cropping systems, 6/1999, Lleida, pp. 209–210.

[25] Larocque M., Banton O., Determining parameter precision for modeling nitrate leaching: inorganic fertilization in nordic climates, Soil Sci. Soc. Am. J. 58 (1994) 396–400.

[26] Molina J.A.E., Clapp C.E., Shaffer M.J., Chichester F.W., Larson W.E.,. NCSOIL, a model of nitrogen and carbon transformation in soil: description, calibration and behavior, Soil Sci. Soc. Am. J. 47 (1983) 85–91.

[27] Mummey D.L., Smith J.L., Bluhm G., Assessment of alternative soil management practices on emissions from US agriculture, Agric. Ecosyst. Environ. 70 (1998) 79–97.

[28] Pang X.P., Gupta S.C., Moncrief J.F., Evaluation of nitrate leaching potential in minnesota glacial outwash soils using the CERES-Maize model, J. Environ. Qual. 27 (1998) 75–85.

[29] Quemada M., Cabrera M.L., CERES-N model predictions of N mineralized from cover crop residues, Soil Sci. Soc. Am. J. 59 (1995) 1059–1065.

[30] Rosenzweig C., Parry M.L., Potential impact of climate change on world food supply, Nature 367 (1994) 133–138.

[31] Saarikko R.A., Applying a site based crop model to estimate regional yields under current and changed climates, Ecol. Model. 131 (2000) 191–206.

[32] Sadler E.J., Gerwig B.K., Evans D.E., Busscher W.J., Bauer P.J., Site-specific modeling of corn yield in SE coastal plain, Agric. Syst. 64 (2000) 189–207.

[33] Sitompul S. M., Hairiah K., van Noordwijk M., Woomer P. L., Organic matter dynamics after conversion of forests to food crops or sugarcane: predictions of the CENTURY model, Agrivita 19 (1996) 198–206.

[34] Smith J.U., Smith P., Addiscott T.M., Quantitative methods to evaluate and compare Soil Organic Matter (SOM) models, in: Powlson D., Smith J.U., Smith P. (Eds), Evaluation of Soil Organic Matter Models, Springer-Verlag, Berlin Heidelberg, 1996, pp. 181–199.

[35] Smith P., Smith J.U., Powlson D.S., McGill W.B., Arah J.R.M., Chertov O.G., Coleman K., Franco U., Frolking S., Jenskinson D.S., Jensen L.S., Kelly R.H., Klein-Gunnewiek H., Komarov A.S., Li C., Molina J.A.E., Mueller T., Parton W.J., Thornley J.H.M., Whitmore A.P., A comparison of the performances of nine soil organic matter models using datasets from seven long-term experiments, Geoderma 81 (1997) 153–225.

[36] Smith W.N., Desjardins R.L., Pattey E., The net flux of carbon from agricultural soils in Canada 1970–2010, Global Change Biol. 6 (2000) 557–568.

[37] Suleiman A.A., Ritchie J.T., Estimating saturated hydraulic conductivity from drained upper limit water content and bulk density, Trans. Am. Soc. Agric. Eng. 44 (2001) 235–339.

[38] van Alphen B.J., Stoorvogel J.J., A functional approach to soil characterization in support of precision agriculture, Soil Sci. Soc. Am. J. 59 (2000) 1706–1713.

[39] Vold A., Breland T.A., Soreng J.S., Multiresponse estimation of parameter values in models of soil carbon and nitrogen dynamics, J. Agric. Biol. Environ. Stat. 4 (1999) 290–309.

[40] Wösten J.H.M., Schuren C.H.J.E., Bouma J., Stein A., Functionnal sensitivity analysis of four methods to generate soil hydraulic functions, Soil Sci. Soc. Am. J. 54 (1990) 827–832.

[41] Yiridoe E.K., Voroney R.P., Weersink A., Impact of alternative farm management practices on nitrogen pollution of groundwater: evaluation and application of CENTURY model, J. Environ. Qual. 26 (1997) 1255–1263.

APPENDIX

Table A. Soil and crop parameters involved in the site-specific calibration of CERES. Names follow the original CERES [22] and NCSOIL nomenclatures. The water balance parameters are supplied for each soil horizon, whereas those of the C-N turnover module pertain to the plough layer only.

Name	Definition	Unit
Water balance		
LL	Wilting point	$cm^3 \cdot cm^{-3}$
DUL	Field-capacity moisture content	$cm^3 \cdot cm^{-3}$
Turnover of carbon and N		
Pool I:	Microbial biomass	
— C(I)	Initial size of pool I	mg $C \cdot kg^{-1}$ sol
Pool II:	Actively-decomposing native organic matter (’humads’)	mg $C \cdot kg^{-1}$ sol
— C(II)	Initial size of pool II	g $C \cdot g^{-1}$ N
— C:N(II)	C:N ratio of pool II	day^{-1}
FOM	Fresh organic matter pool	
CF_{FOM}	Decomposition rate of FOM	
Crop phenology		
P1V	Sensitivity to cold s (wheat)	Unitless
Crop growth		
AWR	Specific leaf weight (wheat)	g dry matter$\cdot m^{-2}$
SMDFR	Moisture stress coefficient for root N uptake	Unitless
SWDF1	Moisture stress coefficient for net photosynthesis	Unitless
—	Moisture stress coefficient for the vertical penetration of roots	Unitless
—	Maximum root water extraction	cm water$\cdot cm^{-1}$ soil cm^{-1} root

Available online at www.sciencedirect.com
SCIENCE DIRECT
ELSEVIER
Agriculture, Ecosystems and Environment 110 (2005) 289–299
Agriculture Ecosystems & Environment
www.elsevier.com/locate/agee

Field-scale modelling of carbon and nitrogen dynamics in soils amended with urban waste composts

Benoît Gabrielle *, Jeanne Da-Silveira, Sabine Houot, Joël Michelin

Environment and Arable Crops Research Unit, Institut National de la Recherche Agronomique, 78850 Thiverval-Grignon, France

Received 13 December 2004; received in revised form 8 April 2005; accepted 21 April 2005
Available online 25 May 2005

Abstract

Composting has emerged as a valuable route for the disposal of urban waste, with the prospect of applying composts on arable fields as organic amendments. Proper management of urban waste composts (UWC) requires a capacity to predict their impacts on carbon and nitrogen dynamics in the field, an issue in which simulation models are expected to play a prominent role.

Here, we used a deterministic soil-crop model to simulate C–N dynamics in an arable field amended with three types of UWC (green waste and sludge, biodegradable waste, and solid waste), and a reference amendment (farmyard manure). The model is a version of CERES in which the soil C–N module was substituted with the NCSOIL model, whose microbiological parameters were determined from either laboratory incubation data or biochemical fractionation in a previous paper. CERES was tested against data from a field trial set up in 1998 in the Paris area, and managed as a maize (*Zea mays* L.)–wheat (*Triticum aestivum* L.) rotation. Comparison of observed and simulated data over the first 4 years of the field trial showed that CERES predicted the soil moisture and inorganic N dynamics reasonably well, as well as the variations in soil organic C. In particular, the parameterization of UWC organic matter from biochemical fractions achieved a similar fit as the parameterization based on incubation data. Wheat yields were also correctly predicted, but a systematic under-estimation of maize yields pointed at an under-estimation of spring and summer mineralization of N by CERES.

Simulated N fluxes showed that the organic amendments induced an additional leaching ranging from 1 to 8 kg N ha^{-1} yr^{-1}, which can be related to the initial mineral N content of the amendments. After 4 years, the composts had mineralized 3–8% of their initial organic N content, depending on their stability. Composts with slower N release had higher N availability for the crops. CERES could thus be used to aid in selecting the timing of compost application, in relation to its stability, based on both environmental and agronomical criteria.

Keywords: C–N dynamics; CERES; Urban waste compost; Modelling; Field experiment

1. Introduction

The management of urban waste has become a major issue worldwide, with steadily growing volumes to be disposed of and increased public awareness of

* Corresponding author. Tel.: +33 1 30 81 55 51; fax: +33 1 30 81 55 63.
E-mail address: benoit.gabrielle@grignon.inra.fr (B. Gabrielle).

0167-8809/$ – see front matter © 2005 Elsevier B.V. All rights reserved.
doi:10.1016/j.agee.2005.04.015

the resulting pressure on the environment. Amidst the range of waste treatments currently available, incineration and landfilling are the most frequent, and are commonly combined to meet the needs of local communities. However, both treatment routes raise a range of environmental problems, which have recently lead the French government to schedule a ban on most types of landfill disposal. Composting of urban waste has emerged as a valuable alternative because of the high proportion of organic matter in urban waste. The bio-degradable fraction (including food scraps, grass clippings and tree trimmings) is estimated at about 25% (fresh weight) in France, along with an additional 25% made up of paper and cardboard. Composts have long been used in agriculture, and urban waste composts (UWC) may be applied in arable fields as organic amendment to maintain soil organic matter as well as supply nutrients to crops (Stratton et al., 1995). Proper management of UWC requires a capacity to predict their impacts on C and N dynamics in the field.

Similar to other organic amendments, there exists a body of work on the effect of UWC on agricultural systems variables encompassing physical effects on soil structure and water balance (Agassi et al., 1998; Movahedi Naeini and Cook, 2000a), N availability to crop (Hadas and Portnoy, 1997; Sánchez et al., 1997), crop yield (Allievi et al., 1992; Movahedi Naeini and Cook, 2000b), and nitrate losses (Gerke et al., 1999; Mamo et al., 1999a). However, very few studies addressed the above items simultaneously, which is necessary to evaluate the environmental advantages and drawbacks of waste composting, as compared to other treatment routes (Mendes et al., 2003). Also, the environmental impacts of UWC use in agriculture are expected to vary widely according to crop management, climate and soil characteristics, together with the constituents and microbial load of the UWC material itself (Stratton et al., 1995).

Deterministic models of C–N dynamics in soil-crop systems provide a unique means of addressing these issues, as they simulate the major processes governing the impacts cited (Diekkrüger et al., 1995), and make it possible to single out soil, climate, and management factors through scenario analysis (Ramanarayanan et al., 1998). They may therefore help in issuing recommendations for UWC management in agriculture, regarding for instance the timing of UWC application in relation to the stability of their organic matter. Models can also approach long-term effects, which are particularly relevant to evaluate the effect of repeated applications of UWC on soil organic matter dynamics. For instance, a modelling study in Northern Germany spanning 30 years showed that nitrate leaching was much more sensitive to UWC applications in a sandy soil compared to a loamy one, and that an acceptable agronomical and environmental compromise could be struck by using mature UWC at moderate doses (Gerke et al., 1999).

However, there has been little work at the field level in comparison with laboratory-scale modelling (Hadas and Portnoy, 1997; Mamo et al., 1999b). Field-scale modelling poses the challenge of extrapolating microbiological parameters for UWC, generally obtained through laboratory incubations of disturbed soil samples, to actual field conditions where soil structure and organic matter placement affects C–N dynamics (Duxbury et al., 1989). Recent work showed that these microbiological parameters could also be approached by biochemical fractionation of UWC organic matter, thereby alleviating the need for time-consuming incubations in the laboratory (Gabrielle et al., 2004). However, it is still uncertain whether these proximate parameter values would give good results in the field.

In the framework of a long-term field experiment set up in the Paris area to evaluate the agronomic value and the environmental impacts of various types of UWC (Houot et al., 2002), we set out to predict the C and N balances of the UWC-amended plots with a deterministic simulation model. The model is based on CERES (Jones and Kiniry, 1986), as modified to suit French conditions (Gabrielle and Kengni, 1996). In particular, its soil C–N module was substituted with NCSOIL (Molina et al., 1983), a model that considers soil organic matter (OM) as being made up of a series of discrete pools with C and N flowing between the pools as a result of processing by soil microflora. In a previous paper (Gabrielle et al., 2004), NCSOIL was parameterized and tested against laboratory incubation data, using two parameterization methods: one based on laboratory incubation data, and the other based on a biochemical index. The first objective of this work was thus to evaluate the capacity of CERES to simulate UWC in the field, based on the two parameter sets obtained in the laboratory study. Such field test has not yet been conducted, to the best of our

knowledge. The second objective was to simulate the C–N balance from the various UWC-amended plots over the 4-year timeframe of the field experiment, with particular focus on soil organic C variations and soil N losses (leaching and gaseous).

2. Materials and methods

2.1. Experimental setup

The experiment was set up in 1998 at Feucherolles (48°90′N and 1°95′E; 50 km West of Paris, France), on a Typic Hapludalf, whose surface horizon had a silt loam texture (19% clay and 6% sand), a pH of 6.9, negligible $CaCO_3$ content, and an organic carbon content of 11.0 g C kg^{-1} dry soil. Three types of UWC were applied: (1) a bio-waste compost (BIO) resulting from the co-composting of green waste and the source separated organic fraction of municipal waste; (2) a co-compost obtained from a mix of 70% green waste and 30% sewage sludge, on a dry matter basis (GWS); and (3) a municipal solid waste compost (MSW). Cattle farmyard manure (FYM) served as a reference organic amendment. Readers may refer to Gabrielle et al. (2004) for more details on amendments' properties.

The four organic treatments were combined with two mineral fertilizer treatments: with or without additional mineral N, applied as a N solution containing 50% ammonium-nitrate and 50% urea. The total area of the field was 6 ha, and the lay-out followed a split-plot design with four blocks separated by a 25 m wide buffer strip to avoid contamination during spreading of the organic or mineral fertilizer. The blocks were divided into 10 plots (45 m × 10 m), separated by a 6 m wide strip. Plots located in the Eastern half of the field received additional mineral N, whereas those in the Western half did not. Treatments with additional mineral N will be noted +N.

The field was managed as a maize (*Zea mays* L.)–wheat (*Triticum aestivum* L.) rotation. Composts were spread once every 2 years on wheat stubble, and ploughed into the soil within a few days upon stubble clearing (see Table 1 for application rates). The controls received no organic fertilization. Maize was sown in May 1999 with a fertilization of 79 kg N ha^{-1} in the +N treatments, and harvested in November. Wheat was sown 1 week after maize harvest, and the +N section received two mineral fertilizations of 51 kg N ha^{-1} each, in February and April 2000, respectively. Wheat was harvested in August 2000, and the following maize was sown in May 2001 after a 68 kg N ha^{-1} fertilization on the +N treatments. The daily weather data required to run the CERES model were taken from a meteorological station located 5 km away from the field experiment.

Soil was sampled several times a year: before sowing, up to three times during the growing season, and after harvest. Three soil cores were taken from each replicate plot with an automatic auger (internal diameter: 2 cm). Cores were cut in 30 cm increments down to 90 cm, and pooled layer-wise. The composite samples were analyzed for gravimetric moisture content and mineral N using colorimetric methods. In autumn 2000 through autumn 2001, a bare soil plot was set up to monitor the mineralization of soil organic N in the absence of organic amendments.

Table 1
Characteristics of the organic amendments applied in 1998 and 2000

Amendment	Application rate (Mg DM[a] ha^{-1})	Organic C (Mg C ha^{-1})	Total N (kg N ha^{-1})	NO_3^--N (kg N ha^{-1})	NH_4^+-N (kg N ha^{-1})
FYM, 1998	13.1	3.8	313.0	3.0	74.0
BIO, 1998	16.2	2.6	265.0	0.0	20.0
GWS, 1998	10.7	2.9	303.0	0.0	34.0
MSW, 1998	10.0	3.0	202.0	0.0	22.0
FYM, 2000	9.6	3.7	186.2	1.3	0.7
BIO, 2000	25.0	4.4	297.5	6.2	0.7
GWS, 2000	18.8	3.6	347.6	0.1	21.7
MSW, 2000	16.9	5.3	348.5	0.4	12.5

MSW: municipal solid waste compost; BIO: bio-waste compost; GWS: green waste and sludge compost; FYM: farmyard manure.
[a] Dry matter.

During the growing seasons, individual plants samples were taken over replicate plots totaling 1 m^2 in area for the maize, and 0.5 m^2 for the wheat. Plants were brought to the laboratory for various analyses: plant density, leaf area index (LAI; measured by planimetry), dry matter and N contents of various plant compartments (leaf, stem, grain, ear or panicle).

2.2. The CERES model

CERES is a mechanistic model simulating the dynamics of water, carbon and nitrogen in soil-crop systems. It runs on a daily time step and is available for a large range of arable species (Jones and Kiniry, 1986). It runs from standard weather data including: solar radiation, rainfall, air temperature and potential evapo-transpiration. In the following, the term 'model simulation' will refer to a run of CERES with the input data detailed in Section 2.3, producing a set of outputs directly comparable with the field measurements.

CERES comprises three main sub-models. First, a physical module simulates the transfer of heat, water and nitrate down the soil profile, as well as soil evaporation, plant water uptake and transpiration in relation to climatic demand. Water infiltrates down the soil profile following a tipping-bucket approach, and may be redistributed upwards after evapo-transpiration has dried some soil layers. In both of these equations, we introduced the generalized Darcy's law in order to better simulate water dynamics in fine-textured soils (Gabrielle et al., 1995). Next, a microbiological module simulates the turnover of organic matter in the plough layer, involving both mineralization and immobilization of inorganic N. In our version, the NCSOIL model (Molina et al., 1983) was substituted for the original CERES module (Gabrielle and Kengni, 1996). NCSOIL comprises three endogenous soil OM pools: microbial biomass, active humus ('humads'), and passive humus. Active and passive humus differ in their turnover rates, set at 1 and 100 years, respectively (Gabrielle et al., 2004). The OM pools decompose according to first-order kinetics, and partly recycle into the microbial biomass. The third module simulates crop growth and development. Crop net photosynthesis is a linear function of intercepted radiation according to the Monteith approach, with interception depending on leaf area index based on Beer's law of diffusion in turbid media. Photosynthates are partitioned on a daily basis to currently growing organs (roots, leaves, stems, fruits) according to crop development stage. The latter is driven by the accumulation of growing degree days, as well as cold temperature and day-length for crops sensitive to vernalization and photoperiod. Crop N uptake is computed through a supply/demand scheme, with soil supply depending on soil nitrate and ammonium concentrations and root length density.

2.3. Model parameterization

CERES was parameterized by combining different methods according to available data. The soil physico-chemical properties indicated at the beginning of Section 2.1 were averaged across 43 samples taken in a field variability analysis at the onset of the field trial. Water retention parameters were measured in the laboratory on small clods collected in winter (Bruand and Tessier, 2000), while hydraulic conductivity was inferred from other properties using a pedo-transfer function (Gabrielle et al., 2002). The resulting values are listed in Table 2 for each soil layer.

Two sets of parameters were used for the soil C–N module of CERES, NCSOIL. The first set (referred to

Table 2
Physical parameters of the simulated soil layers

Horizon (cm)	Water content ($cm^3\ cm^{-3}$)			Saturated hydraulic conductivity ($cm\ d^{-1}$)
	Wilting point	Field capacity	Saturation	
0–30	0.100	0.310	0.420	5.0
30–60	0.131	0.306	0.398	5.0
60–90	0.131	0.300	0.403	5.0
90–120	0.131	0.315	0.417	5.0

The wilting point and saturation moisture contents were deducted from measurements under a suction of 16 and 0.01 MPa, respectively, while field capacity was inferred by pedo-transfer (Gabrielle et al., 2002).

as OPT) was obtained by fitting against laboratory incubation data, whereas the second set (BSI) was exclusively inferred from the biological stability index, a variable calculated from biochemical fractions of UWC organic matter (Linères and Djakovitch, 1993). The parameterization procedures are fully described in Gabrielle et al. (2004). Organic matter inputs from crop residues were partitioned into three fractions: carbohydrates, cellulose- and lignin-like, with decomposition rates of 0.1, 0.02 and 5×10^{-5} d^{-1}, respectively (Godwin and Jones, 1991).

3. Results and discussion

3.1. Extrapolation of laboratory-derived parameter sets to field conditions

Compared to the independent laboratory determinations, one parameter had to be adjusted to improve model fit against field data: the wilting point (WP) in the 60–120 cm soil layer. Using the laboratory-determined WP value of 0.131 cm^3 cm^{-3} for the subsoil resulted in a strong under-estimation of maize yields for both years (not shown). A better adjustment was obtained by setting this parameter to a lower value of 0.100 cm^3 cm^{-3}.

Regarding the transformations of exogenous organic matter in soil, two types of parameter sets were used: one based on laboratory incubation data (OPT), and the other based on a biochemical index (BSI). Fig. 1 shows that they resulted in a similar fit to observed nitrate dynamics in the topsoil. The simulation lines corresponding to the two parameterizations generally merged, or differed by 15 kg NO_3^--N ha^{-1} at most. The only notable deviations occurred in the year following the first compost application with the MSW and GWS composts, and in the year following the second application of MSW compost. A similar pattern appeared in the simulations done at the laboratory scale with NCSOIL (Gabrielle et al., 2004). The differences between the BSI and OPT parameterizations were most significant with the MSW compost in both years, and with the 2000 GWS compost.

Across the various treatments, the BSI simulation predicted lower nitrate concentrations than the OPT simulation after the first compost application, and higher concentrations after the second application (Fig. 1). The match of BSI with observed soil N data was not significantly better or poorer than that of OPT, and the same applied to other simulation variables (not shown). For instance, simulated final crop yields differed by 0.3 Mg grain dry matter ha^{-1} at most between the two parameterizations, which falls within the experimental error on the measurements. It can therefore be concluded that the BSI and OPT parameter sets achieved a similar performance. This confirms at the field level the laboratory finding by Gabrielle et al. (2004) that the biochemical index BSI could be used to parameterize soil C–N models such as CERES.

Fig. 1. Simulated (lines) and observed (symbols, ±1 S.D.) time course of topsoil (0–30 cm) nitrate content in the four amended plots that did not receive additional mineral N fertilizer. Simulations were run with two parameter sets for exogenous organic matter: one obtained from laboratory incubation data (OPT), and the other based on a biochemical index (BSI). Legend: MSW, municipal solid waste compost; BIO, bio-waste compost; GWS, green waste and sludge compost; FYM, farmyard manure.

3.2. Performance of CERES

3.2.1. Soil water balance

Along with soil temperature, which can be correctly predicted by CERES (Hoffmann et al., 1993), soil moisture is a major control of soil biological activity. Here, the CERES simulation of the soil moisture profile generally matched the observed data (Fig. 2a), with a slight tendency to over-estimate the latter in winter. This should be ascribed to the fact that the water table was shallow at this time of year, during which piezometric monitoring showed that it could rise to the topsoil layers. Since this contribution cannot be simulated within the CERES framework, it is likely to have participated in the above-mentioned discrepancy. In summer, there were unfortunately few moisture measurements, especially during the maize growing seasons. With its first parameter setting, as given in Table 2, CERES predicted serious water stress episodes that did not seem to have occurred in practice. This may also be explained by a contribution from the water table. We therefore adjusted the wilting point in the subsoil, as a proximate control for this phenomenon.

3.2.2. Soil mineral nitrogen

The model simulated the time course of nitrate content in the soil profile reasonably well, although it tended to over-estimate topsoil nitrate in the winter and spring periods following compost application (Fig. 2b). Despite the frequent applications of fertilizer N in the +N treatments, it was noticeable that the measured nitrate contents remained low throughout the profile, being less than 30 kg N ha^{-1} at all times.

Fig. 2. Simulated (lines) and observed (symbols, ±1 S.D.) time course of soil nitrate (a) and moisture content (b) in the treatment amended with the green waste and sludge compost and fertilizer N (GWS + N), over the 4-year simulation period.

This was especially surprising in the bare soil period between wheat harvest and maize planting, when favourable temperatures and moisture conditions could be expected to result in high mineralization fluxes and accumulation of inorganic N in the topsoil. During this period, soil nitrate was over-predicted by CERES as a result.

3.2.3. Soil carbon

Fig. 3a compares the simulated and observed variations in total carbon in the soil surface horizon over the 4-year period from September 1998 to September 2002. The predictions were especially good for the treatments without fertilizer N, with deviations ranging from 0 to 1.6 Mg C ha^{-1}. However, the model simulated an overwhelming effect of fertilizer N in the +N treatments, which was less pronounced in practice. This resulted in larger discrepancies between predicted and observed data. In principle, this effect of fertilizer N should result from the balance between two opposite factors. On the one hand, fertilizer N enhances microbial activity, since inorganic N is often a limiting factor in bio-degradation (Mary et al., 1996). On the other hand, N

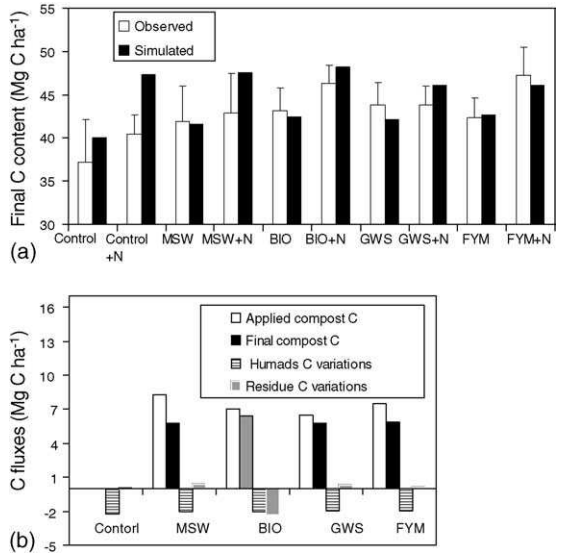

Fig. 3. Bar plots of simulated versus observed variations in C stocks in the top 30 cm of soil, from September 1998 to September 2002 (a). Simulated initial and final stocks of compost C, and variations in active humus C ('humads') and crop residues over the same period (b). Values are averaged across the two fertilizer N treatments in (b).

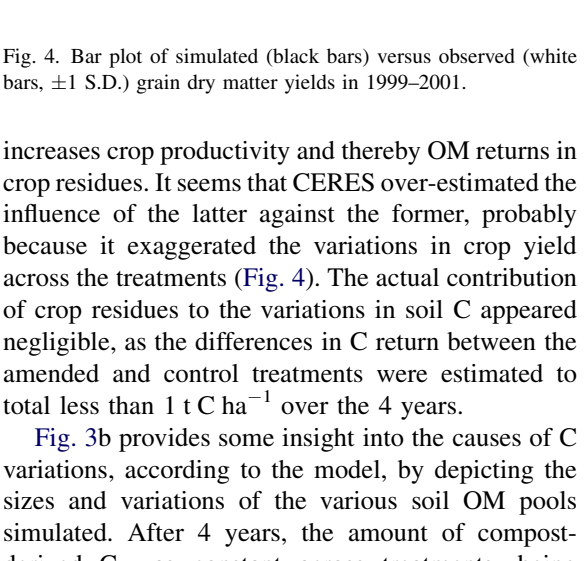

Fig. 4. Bar plot of simulated (black bars) versus observed (white bars, ±1 S.D.) grain dry matter yields in 1999–2001.

increases crop productivity and thereby OM returns in crop residues. It seems that CERES over-estimated the influence of the latter against the former, probably because it exaggerated the variations in crop yield across the treatments (Fig. 4). The actual contribution of crop residues to the variations in soil C appeared negligible, as the differences in C return between the amended and control treatments were estimated to total less than 1 t C ha^{-1} over the 4 years.

Fig. 3b provides some insight into the causes of C variations, according to the model, by depicting the sizes and variations of the various soil OM pools simulated. After 4 years, the amount of compost-derived C was constant across treatments, being around 6 Mg C ha^{-1}. Thus, differences in stability across amendments were accidentally compensated for by variations in the amounts of C applied. According to CERES, only 7–26% of applied organic

C (or 0.4–2.2 Mg C ha^{-1}) had degraded by September 2002. This percentage falls within the range of values reported for the potentially mineralizable C of UWC from laboratory incubations (Hadas and Portnoy, 1997; Bernal et al., 1998). On the other hand, crop residues C decomposed faster and only accounted for a marginal part of the soil C budget (Fig. 3b). Lastly, the organic amendments contributed only 0.4 t C ha^{-1} to the active humus pool (humads), which is a consequence of their low degradation rates. Thus, the amendments could not stop the decline in humads' C content, probably because this stable OM compartment would take longer than 4 years to replenish from exogenous organic matter.

3.2.4. Crop growth and yield

CERES provided relatively good predictions of final wheat yields in 2000, with the exception of the FYM + N treatment for which it produced a 25% over-estimation (Fig. 4). On the other hand, its simulation of maize yields raised significant errors in 1999, especially in the treatments without fertilizer N. CERES predicted a high N deficit, which resulted in simulated yields ranging from 4.9 to 6.6 Mg grain ha^{-1}, compared to the observed range of 8.1 to 8.5 Mg grain ha^{-1}. CERES also under-estimated shoot N uptake by 60 kg N ha^{-1} on average across the various treatments, as exemplified by Fig. 5. Since no soil mineral N measurements were taken during the maize growing seasons, we cannot conclude whether the model under-estimated soil N supply from organic matter, or under-estimated the capacity of maize plants to take up soil N via their rooting systems. The second hypothesis is supported by the fact that CERES was found to over-estimate the effect of soil dryness on limiting N inflow to plant roots, in Mediterranean environment (Gabrielle et al., 2002). Also, the same pattern appeared in 2001, but to a lower extent, with CERES under-estimating final maize yields by 1–2 Mg grain ha^{-1} (Fig. 4). Since the summer of 2001 was slightly wetter than that of 1999, this result is consistent with the hypothesis that the model under-estimates crop N uptake under dry conditions.

Regarding the first hypothesis, namely an under-estimation of soil N supply during the maize growing season, it implies that CERES failed to simulate the seasonal breakdown of compost N mineralization between the winter and summer seasons following compost application. A similar conclusion was reached with the DAISY soil-crop model, which anticipated the soil nitrate peaks observed in autumn after spring application of household and garden organic waste composts (Gerke et al., 1999). In our experiment, the bare control plot set up after compost application in 2000 showed that CERES over-estimated topsoil inorganic N in spring. It is thus likely that the two hypotheses contributed to the discrepancies noted on maize growth, so that corrections regarding both crop N uptake and soil N mineralization should be sought.

Fig. 5. Simulated (lines) and observed (symbols, ±1 S.D.) of crop N content in the treatment amended with the green waste and sludge compost (GWS). Crop components include grains (thick solid line and diamonds) and total aerial parts (thin lines and squares).

3.3. Nitrogen balances

Table 3 presents some N fluxes of agronomic and environmental relevance, as simulated by CERES in the various treatments. Bearing in mind some of the shortcomings with the simulations, some caution should obviously be exerted when discussing these figures. However, it can be expected that model errors will be considerably less when comparing treatments in a differential mode rather than when dealing with absolute values.

The first two items in Table 3 involve N losses (nitrate leaching and denitrification), whereas the next four approach the amendments' fertilizing value through the apparent crop recovery of applied organic N. Regarding nitrate losses, CERES predicted that all organic amendments induced increases in nitrate leaching, ranging from 2 to 11 kg N ha^{-1} yr^{-1}. Farmyard manure had the highest impact, despite its being moderately stable according to the biological stability index (Gabrielle et al., 2004). This was

Table 3
CERES-simulated N fluxes in the compost field trial

Flux type	Treatments									
	No additional N					Additional N applied				
	Control	MSW	BIO	GWS	FYM	Control	MSW	BIO	GWS	FYM
kg N ha^{-1} yr^{-1}										
Nitrate leaching	17.0	6.0	5.1	10.2	11.4	16.7	2.5	2.0	3.7	6.1
Denitrification	0.63	0.21	0.18	0.32	0.10	0.10	0.10	0.10	0.10	0.20
Net mineralization	82.1	17.9	15.2	24.3	27.6	80.3	12.6	10.8	18.4	22.1
Crop N uptake	86.4	20.3	16.5	27.2	34.5	171.1	18.5	12.2	27.9	34.7
Applied N[a]	8.5	137.7	140.5	162.7	124.7	79.2	137.7	140.5	162.7	124.7
% of applied N										
Apparent crop N recovery	0	14.7	11.7	16.7	27.7	106.9	13.4	8.6	17.1	27.8

Fluxes are annual averages over the period running from October 1998 to June 2002. The fluxes for the organic treatments (MSW, BIO, GWS and FYM) are expressed as a difference relative to the corresponding controls receiving no organic amendments. Crop apparent recovery of applied N is calculated as (treatment N uptake − control N uptake)/(applied N). MSW: municipal solid waste compost; BIO: bio-waste compost; GWS: green waste and sludge compost; FYM: farmyard manure.

[a] Organic and inorganic form.

probably due to its high initial ammonium content in 1998, corresponding to an application dose of 75 kg NH_4^+-N ha^{-1}. The ranking of the amendments in terms of nitrate losses directly reflected their initial mineral N content. Accordingly, the BIO compost lead to the smallest leaching increase because it contributed only 26 kg N ha^{-1} in mineral form over the two applications. This initial effect predominated over the differences in immobilization/mineralization dynamics among the various amendments. Based on organic matter stability, GWS could for instance be expected to result in less leaching compared to the other amendments since it immobilized N during the winter season following compost application. In practice, however, its high inorganic N content made it the second contributor to nitrate leaching (Table 3).

As far as gaseous losses are concerned, simulated denitrification was virtually nil in the controls (totaling less than 1 kg N ha^{-1} yr^{-1}), and was slightly enhanced by all organic amendments. These low denitrification rates are probably due to the fact that simulated water-filled pore space seldom reached the threshold level of 62% used to trigger denitrification in CERES (Hénault and Germon, 2000). Unfortunately, no measurements were carried out to verify these predictions.

It was surprising that the +N treatments should have had lower nitrate and denitrification losses than those receiving no additional mineral N fertilizers. The reason was that in the latter plots, plants experienced N stress early in the season, which hampered their capacity to take up the N made available through compost mineralization later on. Due to their reduced growth, these plants transpired less throughout the growing season, resulting in higher water drainage, nitrate leaching and denitrification, compared to the +N treatments.

Table 3 indicates the potential supply of compost-derived N to crops by comparing the amount of N mineralized in the amended and control treatments. Each compost application thus provided an additional amount of 11–28 kg N ha^{-1} yr^{-1} to the crops, which represented circa 3–8% of the organic N initially contained in the amendments. Interestingly, composts increased N uptake by slightly more than the amount of N they mineralized, because they also contained inorganic N. As a result, the apparent crop recovery of total compost N was in the 9–28% range, which is consistent with the 15–25% range reported from laboratory studies for UWC (Hadas and Portnoy, 1997; Sánchez et al., 1997; Bernal et al., 1998).

Similar to N losses, there was no direct relationship between amendment stability and fertilizing value. The stable BIO compost and less stable FYM were in the lower range, whereas the stable GWS compost and the less stable MSW lied in the upper range of values. The differences in crop recovery of compost-derived N also evidenced the issue of application timing. It

could indeed be expected that a fresher compost like MSW would mostly mineralize during the period between its application in autumn and the planting of maize in spring, therefore losing some of its N to leaching. More mature amendments such as BIO and GWS were on the other hand better suited to the timing used in this experiment.

4. Conclusion

Here, we tested the ability of a deterministic soil-crop model (CERES) to predict the impact of urban waste compost amendments on C–N dynamics in an arable field. A first issue involved the parameterization of its soil microbiological module, NCSOIL, for which two parameter sets were derived from previous laboratory studies (Gabrielle et al., 2004). Comparison with field data showed that both parameter sets yielded an acceptable fit, confirming that a simple biochemical index (BSI) could be used to predict the effect of UWC at the field-scale. CERES gave correct predictions of wheat yields, while it under-estimated the yields of maize. CERES was also able to reproduce the variations in soil organic carbon after 4 years, which were mostly attributed to compost organic matter. Regarding N balance, the modelled losses essentially occurred through leaching, as opposed to gaseous form, and were related to the initial mineral N content of the composts. Crop recovery of compost N was also dependent on composts' mineral N content, along with application timing.

We conclude that CERES could be used to further investigate the relationship between composts' biological properties, timing and rate of field application, and agronomical and environmental impacts. However, modelling efforts should be pursued to improve the simulation of N mineralization in the first few months following compost application.

Acknowledgements

The authors would like to thank J.-N. Rampon for invaluable help in the analysis of soil and compost samples, M. Lauransot for sampling of soil and crop material, and E. Personeni for her early contribution to the work. D. Clergeot and M. Le Villo-Poitreneaud (CREED, Véolia Environnement, France) are also acknowledged for technical and financial support. Additional support was provided by INRA through the AGREDE grant programme.

References

Agassi, A., Hadas, A., Benyamini, Y., Levy, G.J., Kautsky, L., Avrahamov, L., Zhevelev, H., 1998. Mulching effects of composted MSW on water percolation and compost degradation rate. Compost Sci. Util. 6, 34–41.

Allievi, L., Marchesini, A., Salardi, C., Piano, V., Ferrari, A., 1992. Plant quality and soil residual fertility six years after a compost treatment. Bioresour. Technol. 43, 85–89.

Bernal, M.P., Navarro, A.F., Sanchez-Monedero, M.A., Roig, A., Cegarra, J., 1998. Influence of sewage sludge compost stability and maturity on carbon and nitrogen mineralization in soil. Soil Biol. Biochem. 20, 305–313.

Bruand, A., Tessier, D., 2000. Water retention properties of the clay in soils developed on clayey sediments: significance of parent material and soil history. Eur. J. Soil Sci. 51, 679–688.

Diekkrüger, B., Söngerath, D., Kersebaum, K.C., McVoy, C.W., 1995. Validity of agroecosystem models. A comparison of results of different models applied to the same data set. Ecol. Model. 81, 3–29.

Duxbury, J.M., Smith, M.S., Doran, J.M., 1989. Soil organic matter as a source and sink of plant nutrients. In: Coleman, D.C., Oades, J.M., Uehara, G. (Eds.), Dynamics of Soil Organic Matter in Tropical Ecosystems. University of Hawaii Press, Honolulu, pp. 33–67.

Gabrielle, B., Menasseri, S., Houot, S., 1995. Analysis and field-evaluation of the CERES models' water balance component. Soil Sci. Soc. Am. J. 59, 1403–1412.

Gabrielle, B., Kengni, L., 1996. Analysis and field-evaluation of the CERES models' soil components: nitrogen transfer and transformation. Soil Sci. Soc. Am. J. 60, 142–149.

Gabrielle, B., Roche, R., Angas, P., Cantero-Martinez, C., Cosentino, L., Mantineo, M., Langensiepen, M., Hénault, C., Laville, P., Nicoullaud, B., Gosse, G., 2002. A priori parameterisation of the CERES soil-crop models and tests against several European data sets. Agronomie 22, 119–132.

Gabrielle, B., Da-Silveira, J., Houot, S., Francou, C., 2004. Simulating urban waste compost impact on C–N dynamics using a biochemical index. J. Environ. Qual. 33, 2333–2342.

Gerke, H.H., Arning, M., Stöppler-Zimmer, H., 1999. Modeling long-term compost application effects on nitrate leaching. Plant Soil 213, 75–92.

Godwin, D.C., Jones, C.A., 1991. Nitrogen dynamics in soil-plant systems. In: Hanks, R.J., Ritchie, J.T. (Eds.), Modeling Plant and Soil Systems, Agron. Monogr. 31. ASA, CSSA, and SSSA, Madison, WI, pp. 287–321.

Hadas, A., Portnoy, R., 1997. Rates of decomposition in soil and release of available nitrogen from cattle manure and municipal waste composts. Compost Sci. Util. 3, 48–54.

Hénault, C., Germon, J.C., 2000. NEMIS, a predictive model of denitrification on the field scale. Eur. J. Soil Sci. 51, 257–270.

Hoffmann, F., Beinhauer, R., Dadoun, F., 1993. Soil temperature model for CERES and similar crop models. J. Agron. Crop Sci. 170, 56–65.

Houot, S., Clergeot, D., Michelin, J., Francou, C., Bourgeois, S., Caria, G., Ciesielski, H., 2002. Agronomic value and environmental impacts of urban composts used in agriculture. In: Insam, H., Riddech, N., Klammer, S. (Eds.), Microbiology of Composting. Springer-Verlag, Berlin, pp. 457–472.

Jones, C.A., Kiniry, J.R., 1986. CERES-Maize, A Simulation of Maize Growth and Development. Texas A&M University Press, Temple.

Linères, M., Djakovitch, J.L., 1993. Caractérisation de la stabilité biologique des apports organiques par l'analyse biochimique. In: Decroux, J., Ignazi, J.C. (Eds.), Matières organiques et agricultures. Gemas-COMIFER, Paris, France, pp. 159–168.

Mamo, M., Rosen, C.J., Halbach, T.R., 1999a. Nitrogen availability and leaching from soil amended with municipal solid waste compost. J. Environ. Qual. 28, 1074–1082.

Mamo, M., Molina, J.A.E., Rosen, C.J., Halbach, T.R., 1999b. Nitrogen and carbon mineralization in soil amended with municipal solid waste compost. Can. J. Soil Sci. 79, 535–542.

Mary, B., Recous, S., Darwis, D., Robin, D., 1996. Interactions between decomposition of plant residues and N cycling in soil. Plant and Soil 181, 71–82.

Mendes, M.R., Aramaki, T., Hanaki, K., 2003. Assessment of the environmental impact of management measures for the biodegradable fraction of municipal solid waste in Sao Paulo City. Waste Manage. 23, 403–409.

Molina, J.A.E., Clapp, C.E., Schaffer, M.J., Chichester, F.W., Larson, W.E., 1983. NCSOIL, a model of nitrogen and carbon transformations in soil: description, calibration and behaviour. Soil Sci. Soc. Am. J. 57, 996–1001.

Movahedi Naeini, S.A.R., Cook, H.F., 2000a. Influence of municipal waste compost amendment on soil water and evaporation. Commun. Soil Plant Anal. 31, 3147–3161.

Movahedi Naeini, S.A.R., Cook, H.F., 2000b. Influence of municipal compost on temperature, nutrient status and the yield of a maize crop in a temperate soil. Soil Use Manage. 16, 215–221.

Ramanarayanan, T.S., Storm, D.E., Smolen, M.D., 1998. Analysis of nitrogen management strategies using EPIC. J. Am. Water Res. Assoc. 34, 1199–1211.

Sánchez, L., Díez, J.A., Polo, A., Román, R., 1997. Effect of timing of application of municipal solid waste compost on N availability for crops in central Spain. Biol. Fert. Soils 25, 136–141.

Stratton, M.L., Baker, A.V., Rechcigl, J.E., 1995. Compost. In: Rechcigl, J.E. (Ed.), Soil Amendments and Environmental Quality. Lewis, Boca Raton, pp. 249–309.